


Summer 2008

# Poly(ethylenedioxythiophene) based electronic devices for sensor applications

Jie Liu

*Louisiana Tech University*

Follow this and additional works at: <https://digitalcommons.latech.edu/dissertations>

 Part of the [Biomedical Engineering and Bioengineering Commons](#), [Electrical and Computer Engineering Commons](#), and the [Polymer Chemistry Commons](#)

---

## Recommended Citation

Liu, Jie, "" (2008). *Dissertation*. 465.

<https://digitalcommons.latech.edu/dissertations/465>

This Dissertation is brought to you for free and open access by the Graduate School at Louisiana Tech Digital Commons. It has been accepted for inclusion in Doctoral Dissertations by an authorized administrator of Louisiana Tech Digital Commons. For more information, please contact [digitalcommons@latech.edu](mailto:digitalcommons@latech.edu).

POLY(ETHYLENEDIOXYTHIOPHENE) BASED ELECTRONIC  
DEVICES FOR SENSOR APPLICATIONS

by

Jie Liu, M.S.

A Dissertation Presented in Partial Fulfillment of the  
Requirement for the Degree of  
Doctor of Philosophy in Engineering

COLLEGE OF ENGINEERING AND SCIENCE  
LOUISIANA TECH UNIVERSITY

August 2008

UMI Number: 3321331

## INFORMATION TO USERS

The quality of this reproduction is dependent upon the quality of the copy submitted. Broken or indistinct print, colored or poor quality illustrations and photographs, print bleed-through, substandard margins, and improper alignment can adversely affect reproduction.

In the unlikely event that the author did not send a complete manuscript and there are missing pages, these will be noted. Also, if unauthorized copyright material had to be removed, a note will indicate the deletion.

**UMI**<sup>®</sup>

---

UMI Microform 3321331

Copyright 2008 by ProQuest LLC.

All rights reserved. This microform edition is protected against unauthorized copying under Title 17, United States Code.

ProQuest LLC  
789 E. Eisenhower Parkway  
PO Box 1346  
Ann Arbor, MI 48106-1346

LOUISIANA TECH UNIVERSITY

THE GRADUATE SCHOOL

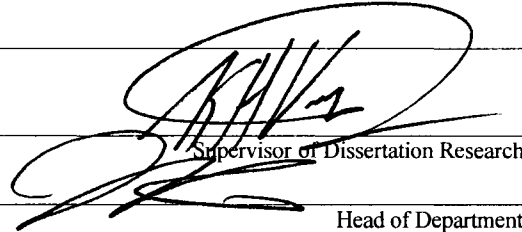
May 13, 2008

Date

We hereby recommend that the dissertation prepared under our supervision  
by Jie Liu

entitled POLY(ETHYLENEDIOXYTHIOPHENE) BASED ELECTRONIC DEVICES  
FOR SENSOR APPLICATIONS

be accepted in partial fulfillment of the requirements for the Degree of  
Doctor of Philosophy in Engineering



Supervisor of Dissertation Research

Head of Department

Engineering

Department

Recommendation concurred in:

Yuri Lvov

Chad O'Neal

Hafiz

Chad M

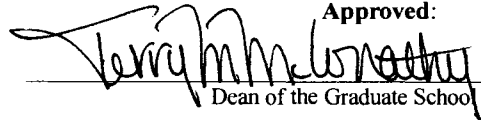
Advisory Committee

Approved:



Director of Graduate Studies

Approved:



Dean of the Graduate School

Stan Napp  
Dean of the College

## APPROVAL FOR SCHOLARLY DISSEMINATION

The author grants to the Prescott Memorial Library of Louisiana Tech University the right to reproduce, by appropriate methods, upon request, any or all portions of this Dissertation. It is understood that "proper request" consists of the agreement, on the part of the requesting party, that said reproduction is for his personal use and that subsequent reproduction will not occur without written approval of the author of this Dissertation. Further, any portions of the Dissertation used in books, papers, and other works must be appropriately referenced to this Dissertation.

Finally, the author of this Dissertation reserves the right to publish freely, in the literature, at any time, any or all portions of this Dissertation.

Author 

Date 08/11/08

## ABSTRACT

Organic electronic devices, based on Poly (3,4-ethylenedioxythiophene)-Poly (styrene sulfonic acid) (PEDOT-PSS) as the active layer for sensor applications, have been studied. Two sets of sensors have been developed. In one case, sensors consisting of PEDOT-PSS resistors have been realized and demonstrated for soil moisture monitoring. The resistor model for the soil moisture sensor enables the sensor device to be fabricated at low cost and easily tested with a simple structure. Unlike the large dimension device used in Time Domain Reflectometry (TDR), the sensors are small and are capable of capturing microscale behavior of moisture in soil which is useful for geological and geotechnical engineering applications.

The Field Effect Transistors (FETs) based on PEDOT-PSS and GOx have been developed for a glucose sensing application. The sensitivity of the developed FET-based sensors is enhanced by selecting the channel as the active sensing region as compared with the previously reported devices which use the gate as the active sensing region. This also allows the devices to be designed by a simple and cost-effective means, unlike other complex platform designs for polymer-based sensor devices.

PEDOT-PSS based sensors showed higher sensitivity and reversible electrical properties when compared to early versions of sensors fabricated using polymer electrolytes which showed irreversible change in the electrical properties when exposed to high moisture content. The output characteristics, which is the change in electrical sheet resistance of the PEDOT-PSS film versus the percentage change in relative

humidity (%RH), show that the conductivity of the film decreases when it is exposed to increasing levels of moisture content. The change in the output resistance of the developed PEDOT-PSS based sensor device was observed to be from 2.5 M $\Omega$  to 4.0 M $\Omega$  when exposed to soil samples (e.g. Buckshot Clay, CH) with 15 – 35 % change in gravimetric water content.

The FET-based glucose sensor using PEDOT-PSS and GOx as the channel materials, is designed and developed with the capability of precise, fast, and wide sensing range of measurement compared to that of traditional glucose sensors, which are costly and operate on a complex electrochemical based principle. The fabrication and characteristics testing steps of the present glucose sensor are also simpler in comparison to other glucose sensors, which use electrochemical cells for measurements. In the present device, GOx was immobilized on PEDOT-PSS conducting polymer film using a simple cost effective spin-coating technique. A linear increase in the FET drain current was observed, which was resulted from the increase in glucose concentration. The sensitivity of the glucose sensor was determined to be 0.3 Ampere per 1 mg/ml of glucose concentration. A linear range of response was found from 0.2 to 3 mg/ml of glucose, with a response time of 10 – 20 s. The results indicated that the reported FET-based glucose sensor retains the enzyme bioactivity and can be applied as a glucose biosensor. Moreover, the glucose sensor presented in this dissertation has displayed a reasonable level of sensitivity, repeatability, and stability. The evaluated range of glucose detection shows that the developed biosensor can be used to detect glucose concentration for normal and diabetic patients. This finding also opens a potential pathway for further development of novel biosensor devices.

## TABLE OF CONTENTS

LIST OF TABLES .....	vii
LIST OF FIGURES .....	viii
ACKNOWLEDGEMENTS .....	xii
CHAPTER ONE INTRODUCTION .....	1
1.1 Organic Electronics .....	2
1.1.1 Advantages and Disadvantages .....	3
1.1.2 Fabrication Techniques .....	6
1.1.3 Sensor Applications .....	7
1.2 Previous Work and Research Contribution .....	9
1.3 Dissertation Objectives .....	13
1.4 Organization of Dissertation .....	13
CHAPTER TWO ELECTROACTIVE POLYMER MATERIALS .....	15
2.1 Introduction .....	15
2.2 Conducting Polymer Structure .....	16
2.3 Conducting Polymer Electrical Characteristics .....	16
2.3.1 Energy Band Structure of Conducting Polymers .....	17
2.3.2 Doping Characterization of Conducting Polymers .....	19
2.4 Free Charge Carriers in Conjugated Polymers .....	25
2.5 PEDOT-PSS Structure and Electrical Characterization .....	30
CHAPTER THREE THEORETICAL BACKGROUND OF ORGANIC ELECTRONICS DEVICES .....	33
3.1 Overview .....	33
3.2 Operation of Organic Field Effect Transistors .....	34
3.2.1 Energy Band Diagrams .....	38
3.2.2 Charge Transport in Organic Field Effect Transistors .....	39
3.2.3 Carrier Mobility in Organic Field Effect Transistors .....	42
3.2.4 Contact Resistance Effects for Polymer Transistors .....	45
3.2.4.1 Ohmic Contact .....	45
3.2.4.2 Schottky Contact .....	47



CHAPTER FOUR MODELING AND SIMULATION.....	48
4.1 Technology Computer Assisted Design.....	48
4.2 Description of Models.....	49
4.3 Device Simulation Results.....	51
4.4 Summary .....	56
CHAPTER FIVE SOIL MOISTURE MONITORING SENSOR BASED ON PEDOT-PSS RESISTOR.....	57
5.1 Introduction.....	57
5.2 Experimental Details.....	59
5.3 Results and Discussion .....	62
5.4 Conclusions.....	70
CHAPTER SIX FIELD EFFECT TRANSISTOR BASED ON PEDOT-PSS.....	72
6.1 Introduction.....	72
6.2 Device Fabrication.....	73
6.3 Results and Discussion .....	74
6.4 Summary .....	79
CHAPTER SEVEN GLUCOSE SENSOR BASED ON PEDOT-PSS FIELD EFFECT TRANSISTOR.....	81
7.1 Introduction.....	81
7.2 Experiment Details.....	83
7.3 Results and Discussion .....	85
7.4 Summary .....	93
CHAPTER EIGHT CONCLUSIONS AND FUTURE WORK.....	95
8.1 Conclusions.....	95
8.2 Future Work.....	97
8.2.1 Glucose Sensors Based on Layer-by-Layer Self-Assembly .....	97
8.2.2 Heterostructure Organic Semiconductor Devices.....	99
8.3 General Considerations.....	102
APPENDIX A TAURUS-DEVICE INPUT SIMULATION COMMANDS.....	103
REFERENCES .....	111

## LIST OF TABLES

Table 4-1 Basic material parameters used in simulation .....	52
--	----

## LIST OF FIGURES

Figure 1-1 Organic light emitting is used in screens for mobile phones .....	3
Figure 1-2 PEDOT-PSS chemical structure .....	11
Figure 2-1 Polyaniline, Polypyrrole and Polythiophene chemical structures[88] .....	16
Figure 2-2 The overlapping of $2sp^2$ and $2p_z$ orbitals forms $\sigma$ and $\pi$ -bonds respectively[93] .....	18
Figure 2-3 Band formation in conducting polymers with increasing conjugation length [94] .....	19
Figure 2-4 Conductivity levels change of Polyacelene and PEDOT [97] .....	20
Figure 2-5 Generation of positive polaron and bipolaron in PEDOT. Energy levels of the neutral polymer, a polaron, a bipolaron and a polymer with bipolaron energy band are described above. ● denotes an electron not participating in a bond and □ denotes a hole [106] .....	23
Figure 2-6 Bonding arrangement change in PEDOT [ 107] .....	24
Figure 2-7 Generations of polaron and solitons in PEDOT. Energy levels of the neutral polymer, a polaron, solitons and a polymer with soliton energy band are described above [108] .....	25
Figure 2-8 Temperature dependence of the carrier mobility in doped and pristine amorphous organic materials [122] .....	29
Figure 3-1 FET structures (a) top-contact, (b) bottom-gate structures .....	35
Figure 3-2 Organic field effect transistor schematic structure .....	36
Figure 3-3 Energy gap diagrams of the OFET structure for a p-type semiconductor illustrating (a) flat band model, (b) accumulation model, and (c) depletion model .....	39
Figure 4-1 Schematic representation of the PEDOT-PSS OFET structure .....	51

Figure 4-2	Energy level diagram of the OFET ( $n^+$ -Si-SiO <sub>2</sub> -PEDOT-PSS) structure under thermal equilibrium. The cut line is chosen at the center of the device .....	53
Figure 4-3	Hole concentration profile in the channel along the direction normal to PEDOT-PSS/SiO <sub>2</sub> interface.....	54
Figure 4-4	Simulation output characteristics of OFET based on PEDOT-PSS.....	55
Figure 4-5	Simulation transfer characteristics of OFET based on PEDOT-PSS.....	56
Figure 5-1	Schematic illustration of the fabrication process steps for the sensors .....	59
Figure 5-2	Final packaged microsensor device to measure gravimetric water content in the soil samples .....	61
Figure 5-3	The soil sample testing setup system. ....	61
Figure 5-4	PEDOT-PSS surface measured using AFM.....	62
Figure 5-5	ATR-IR spectrum of PEDOT-PSS film without and with exposed to moisture content.....	64
Figure 5-6	The change in sheet resistance of PEDOT-PSS moisture sensor vs. change in relative humidity .....	65
Figure 5-7	The change in sheet resistance of PEDOT-PSS moisture sensor versus gravimetric water content in soil samples .....	67
Figure 5-8	Resistance versus water content in CH soil samples measured using unpackaged and packaged sensor device .....	68
Figure 5-9	Percentage change in resistance value of the two different packaged microsensors to the change in water content of the CH soil samples .....	69
Figure 5-10	Percentage change in resistance value of the two different packaged microsensors to the change in water content of the CH soil samples .....	70
Figure 6-1	The comparison between experimental and simulation output characteristics of OFETs based on PEDOT-PSS.....	75

Figure 6-2	The comparison of transfer characteristics of OFET based on PEDOT-PSS between simulation results and experimental .....	76
Figure 6-3	The comparison of transfer characteristics of OFET based on PEDOT-PSS without protective layer on three days .....	77
Figure 6-4	The comparison of transfer characteristics of OFET based on PEDOT-PSS with PVP protective layer on three days .....	78
Figure 6-5	The comparison of transfer characteristics of OFET based on PEDOT-PSS with cellulose acetate protective layer on three days .....	79
Figure 7-1	A schematic diagram of the device structure for the glucose sensor .....	84
Figure 7-2	The working mechanism of the PEDOT-PSS based glucose sensor .....	85
Figure 7-3	The drain current – gate voltage characteristic ( $I_D$ - $V_G$ ) of the OFET-based glucose sensor when exposed to 0 mg/ml (normal device), 1 mg/ml, and 3 mg/ml of glucose concentration solution.....	86
Figure 7-4	The output characteristic ( $I_D$ - $V_D$ ) of the OFET-based glucose sensor for 1mg/ml, and 3mg/ml of glucose concentration solution. Insert: $I_D$ - $V_D$ of the device in the absence of glucose solution .....	88
Figure 7-5	Drain current versus time, at $V_D=-1.5$ V and $V_G=0$ V, measured at different glucose concentration values .....	90
Figure 7-6	Drain current versus time, at $V_D=-1.5$ V and $V_G=0$ V, measured at different glucose concentration values, illustrating the effect of change in glucose concentration from 0.2mg/ml to adding DI water and subsequently adding 2mg/ml glucose solution .....	91
Figure 7-7	Drain current versus glucose concentration, at $V_D=-1.5$ V and $V_G=0$ V. The solid line is the linear fit of the displayed data points.....	92
Figure 7-8	Drain current $I_D$ of the OFET based on PEDOT-PSS as a function of PH. The gate voltage $V_G$ is set to 0 V and the drain voltage $V_D$ is set to 1.5V.....	93

Figure 8-1	A schematic cross section of Layer-by-Layer self-assembly PEDOT-PSS sensor .....	98
Figure 8-2	Drain current of the glucose sensor by LBL self-assembly technique versus glucose concentration, at $V_D=-1.5$ V and $V_G=0$ V. The solid line is the linear fit of the displayed data points.....	99
Figure 8-3	A schematic cross section of heterostructure sensor devices .....	100

## ACKNOWLEDGEMENTS

I am very grateful to my advisor, Dr. Kody Varahramyan, for his generous time and commitment. Throughout my doctoral work, he encouraged me to develop independent thinking and research skills. He continually stimulated my analytical thinking and greatly assisted me with scientific writing.

I am also very grateful for having an exceptional doctoral committee and wish to thank Dr. Yuri Lvov, Dr. Chester Wilson, Dr. Chad O'Neal, and Dr. Haifeng Ji for their advice and serving on my advisory committee for this dissertation.

I want to thank Dr. Mangilal Agarwal for his supervision and providing suggestions and advice on this research project and dissertation. I am also fortunate to have worked with a wonderful group of graduate students, and I would like to thank all of them for their mental and emotional support and helpful discussions and advice. They are Mercyma Dee Balachandran, Sudhir Shrestha, Raja Sekharam Mannam, Senaka Krishna Kanakamedala. I am also grateful to Mr. Abdul Khaliq and IfM staff members for the simulation and experimental work.

I would like to thank my family. My father and my mother have encouraged me with their love and passion which have given me a constant support for my life. I'm grateful to my brother for his care and thoughtfulness.

## CHAPTER ONE

### INTRODUCTION

Polymer electronic devices stimulate a steady development of new sensor types to interact with our physical world. Conducting polymers, such as poly(ethylenedioxythiophene), were utilized for sensor and transducer applications due to their electrically conducting characteristics. Sensors and transducers enable non-electrical signals from physical, biological and chemical domains to be converted into electrical quantities, such as voltage, current, resistance or capacitance. The discovery in 1977 that the conductivity of a polymer could be increased controllably by doping [1] opened a new era for organic electronic sensor applications. About a decade later, one of the most extensive applications, field effect transistors (FETs), using polymers as the active material, was developed [2]. The field effect transistor has been used in many sensor applications. For example, humidity sensors [3] and glucose sensors [4] have proven to be successful in this area.

In fact, microelectromechanical systems (MEMS) have produced high-density sensor arrays integrated with electronics circuit processing A/D signal. One of the advantages of field effect transistor sensors made from silicon is the possibility that the mechanical structure can be integrated with the read-out and signal-conditioning circuitry on the single chip. Although silicon, both as single-crystal and an amorphous film, is



successfully used for millions of sensors, there are applications where its use is disadvantageous, such as, the limitations caused by the mechanical properties of silicon. Therefore, there has been growing research in organic electronics to develop polymer applications with utilizing novel fabrication techniques. Due to the improvement in performance, polymer-based electronic devices have been demonstrated that use conducting polymer films [5,6] for sensing may provide unique technologies and generate new applications. Also some groups have embedded silicon sensing elements in polymer skins [7] or deposited active polymer layers on silicon substrates [8].

As for all commercial products, low cost is usually required. Therefore, low cost and easier ways to produce an electronic device are always welcome. Currently, conductive and semiconductive organic materials are utilized as substrate layers to build electronic integrated circuits. With novel polymer materials being produced, a new set of processing technologies is applied to thin films. These new techniques open a potential area for building organic electronic sensors with different properties and lower cost as compared to the traditional technologies. Investigation into these new materials and techniques is valuable for building new microsensor applications.

### 1.1 Organic Electronics

Due to their advantages over traditional inorganic semiconductor technologies, organic electronics have been the focus of a growing body of investigation and development for more than fifty years. The discovery of conductive property of organic solids was at the beginning of the 20<sup>th</sup> century. In 1941, Nobel Laureate Albert Szent-Györyi suggested that certain processes in biological system might be accounted for by the transfer of electrical charge carriers along molecular chains [9]. In addition to being

electrically conducting, organic materials were also capable of emitting visible light when excited optically or electrically. Since then, organic light emitting diodes (OLEDs), plastic solar cells and organic transistors have been developed in this area (Figure1-1). Alan Heeger, Hideki Shirakawa and Alan MacDiarmid established the foundation for the field of organic electronics with the discovery of the variation of electrical conductivity of polyacetylene [10]. With the early fundamental work done, many novel organic materials have been developed and investigated for fabricating electronics devices.



Figure 1-1 Organic light emitting is used in screens for mobile phones.

### 1.1.1 Advantages and Disadvantages

Unlike inorganic materials, organic material can be deposited by solution-processing, for example: spin-coating, spray-coating, ink-jet printing and self-assembling. This offers greater process throughput, lower fabrication costs and possibly a lower thermal budget as compared with inorganic materials.

Accordingly, organic electronic devices were fabricated and the performance improved with the ability to fabricate these devices over large areas on flexible substrates, such as plastic, paper, wood and glass. This capacity may provide unique technologies and generate new applications to address the growing needs for pervasive computing and enhanced connectivity [11]. Since the organic materials are assembled out of organic building blocks, they can be made bio-compatible [12]. Thus, they can be implanted and used in vivo without causing immune reactions. More electronic sensors based on polymer materials are likely to be developed in the near future for monitoring critical data, like local blood pressure or blood sugar concentration [13].

It is clear that innovative organic materials function either as conductors or insulators. As an insulator material, polymers are mainly used for the packaging of semiconductor chips which can provide protection from environment to ensure the reliability for the chips [14]. As an electrical conducting material, due to the low carrier concentration found in most organic materials [15], they can be used in many applications [16]. In addition, thin-film transistor based circuits and electronic integrated circuits incorporating several hundred devices on flexible substrates have been recently demonstrated [17, 18]. For example, radio frequency identification [RFID] tags have been developed from these levels of integration [19]. Organic transistors [20, 21, 22] have also been successfully integrated with display elements and used as image sensors.

Another promising advantage of organic materials is that the behavior of the material can be modified by evaluating parts of the molecular structure. Normally, the conductivity of organic materials can be changed by deliberate oxidative doping [23]. Eventual uses of organic molecules for electronic devices and circuits are to enlarge the

unique feature of individual molecules into a full material by synthetically controlling the structures and the intermolecular interactions [24]. For instance, alcohol soluble polypyrrole was composed using a functional doping agent di(2-ethylhexyl) sulfo succinate sodium salt ( NaDEHS) [25].

Since organic materials are still novel and in their development phase, there is one major drawback which might affect on performance of organic electronic device. They easily degrade from environment due to the effect of heat, light, fire, ionising radiation, biological agents, pollution and even combinations of these factors [26]. The mechanisms of degradation and stabilization procedures must be understood, if the manufacturing technology and devices of polymers continue to develop in advance. As part of the packaging processes, encapsulation technology plays an important function in protecting organic electronic devices and prints out circuits, and then a reasonable stability can be achieved for marketing [27].

The silicon industry has shown some decrease in integrated circuit feature size because of the demand for higher level performance and low cost manufacturing process. Moore's law predicted that the number of transistors on a chip doubles in every two years [28], which also showed cost level decrease per transistor. During this development process, there will be involved with several approaches including printing techniques for individual devices, thin film structures and semiconductor integrated circuits. Predictably, the organic electronics industry has already shown expansion on the compatibility of these fields due to low cost processing and has kept Moore's law on track [29]. Several important aspects that are related to the fabrication and operation of future organic electronic devices will be discussed in following sections.

### 1.1.2 Fabrication Techniques

The primary purpose of fabrication mechanisms for organic devices is to create promising structures with high speed, low cost, and easy manufacturing process. In order to achieve this goal, there is much fundamental research on fabrication techniques to be done.

Spin-coating is one of the basic and fundamental fabrication techniques. A typical spin coating process involves depositing a small amount of a fluid onto the center of a substrate, and then spinning the substrate at a speed that is determined speed by the viscosity of the fluid. Centrifugal acceleration will cause most of the fluid to spread off the edge of the substrate, leaving a thin film of fluid on the surface. Final film thickness and other properties depend upon the fluid viscosity, drying rate, percent solids, surface tension, and other parameters chosen for the spin coating process.

Another promising technique is layer-by-layer (LBL) self-assembly that has attracted a lot of attention in the manufacturing process of nanometer scale electronics [30]. This technique has been developed as a simple, practical and versatile method for creating nanometer scale films on large surfaces, microfibres and cores [31]. Stable film architectures can be formed during the fabrication process. These hierarchical structures can exhibit unique properties that might not occur on the individual components [32].

Since Cavendish Laboratory of the University of Cambridge developed a new approach to achieve higher resolution, which allowed all-polymer transistor circuits can be printed [33]. Ink-jet printing appears to the excellent features, such as low cost and printable organic electronics [34]. Recently, ink-jet printing has shown a success in organic applications, such as organic electronic transistors [35] and drug discovery [36].

Also, the ink-jet printing is one of the main techniques for the fabrication of flat screen displays, field emission [37] and organic light emitting diodes [38]. There are two mainly approaches utilized for ink-jet printing of materials for the manufacturing process. The first ink-jet printing technology is the “Continuous, Charge and Deflect” [39] that deflect drops up to 0.5 mm in diameter and appropriate for high-speed coverage of relatively large areas. The second is the “Drop-on-Demand” (DOD) technology which is suitable for smaller drops 20-100  $\mu\text{m}$  in diameter and the DOD technique produces drops that are near to the orifice diameter of droplet generator [40].

Lithography is considered as one of the manufacturing techniques since the most potential for the fabrication of organic electronic devices and circuits. The resolution has achieved to 10 nm since it was proposed by Chou, et al. in 1995 [41]. Direct printing processes are appropriate for submicron length scales, but might not be easy to get promising resolution in organic electronic devices [42]. Recently nano-imprint lithography (NIL) has been developed for the fabrication of gratings using conjugated materials, which is a preliminary step towards scattered feedback mirrors and waveguides, with promising results [43] and without degradation in devices electronic properties.

### 1.1.3 Sensor Applications

In order to develop the low-cost, large-area sensor applications, such as smart fabric systems, it is required that the simple, flexible, washable, and even disposable sensors design [44]. However, it is difficult that the silicon-based sensors design meets these requirements due to their being naturally brittle, size limitations and higher cost processes. Therefore, flexibility, low-cost fabrication techniques and nontoxic processes

make organic electronic devices, such as polymeric electrolytes or organic conducting polymers, to be investigated and developed for sensor applications.

One application of organic sensors is the response for controlling air pollution or for data storage. The chemical structure of the organic molecules is important for these applications. Like water vapor and gas sensing, conductivity of some materials show a variation when interacted with the change of vapor and gases, which provide the possibility to control the sensitivity to vapors by modifying their chemical structures [45]. For example, the detection of alcohols has been done by conducting polymer sensor arrays which consist of ten different conjugated polymer materials [46]. Another promising application is humidity sensors which are related to the formation of the cross-linked network structure in the sensing film and a change in the polymer chain if exposed to a humidity environment [47]. In addition, another application, biosensors [48] is developed with the technological and theoretical achievements on clinical, environmental and industrial analysis. Due to organic materials flexibility to build different electronic devices and the successful design of tactile sensitive skin, biological tactile sensors [49], which can be found in the skin of a human finger, were developed and investigated to detect hardness, temperature, thermal conductivity and surface roughness [50].

Integration into microelectromechanical systems (MEMS) is one novel trend in the development and implementation of organic sensors. The approach for devices based on the same platform technology has been successfully proven in the field of organic MEMS integrated sensors [51].

## 1.2 Previous Work and Research Contribution

As discussed above, there has been a rapid growth in the development of organic sensor applications based on organic electronic materials addressed primarily in the medical and gas fields to monitor various parameters, such as temperature, relative humidity, and chemical gases. One important characteristic of organic polymer materials widely used is that both ions and electrons can be acted as charge carriers [52], which are very important for medical and humidity sensor application. In the past, humidity sensors have been developed by using different types of materials, such as electrolytes [53], organic polymers [54] and porous ceramics [55]. Humidity sensors based on alkali salts of poly(2-acrylamido-2-methylpropane sulfonic acid) (AMPS) and made of an organic electrochemical resistor type have been reported by Sakai, et al.[56]. Conducting conjugate polymers show significant change in their electrical properties when exposed to humidity. Different fabrication techniques, such as electrochemical polymerization, chemical and electrochemical deposition, and spin coating have been applied to the manufacturing process of polymer humidity sensors [57]. These sensors detect either the absolute value of a physical quantity or a change in the value of an electrical quantity, and convert the measurement into useful input signals for an indicating or recording instrument. In the early stages of humidity sensor development, commercially available polymer electrolytes were directly used as an active sensing material. However, these polymers have the serious drawback of an irreversible change in the electrical properties when exposed to high humidity [58]. On the other hand, conducting polymers, like Poly (3,4-ethylenedioxythiophene)-Poly (styrene-sulfonate) (PEDOT-PSS) [59], show high sensitivity and reversible electrical properties when exposed to a humidity environment.



The electronic properties of PEDOT-PSS film was controlled by its polymer chain structure which interconnected conductive PEDOT with PSS matrix [59], which is shown in Figure 1-2. The use of PEDOT-PSS polymer material for humidity sensing applications using transistor applications was first reported by Nilsson, et al [60]. Polyamide fibers coated with PEDOT-PSS polymer material were also studied for humidity and temperature sensor applications [61]. Since monitoring moisture content in soil has become a pre-requisite for a variety of processes, such as agriculture, areas prone to landslides and laboratory testing. So far, measurement of moisture content has been guided by the agricultural industry resulting in development of time Domain Reflectometry Devices (TDR) [62] whose dimensions are far too large for capturing microscale behavior for geological and geotechnical engineering applications. For this work, the new microsensors was developed, based on the PEDOT-PSS polymer material, for detecting gravimetric water content in soil samples and which present promising features, such as simple structure and small size. Those features result in the presented sensor device, compared to TDR devices; to enable the gravimetric moisture content to be measured when capturing its microscale behavior in the soil samples. The change in the resistance of the polymer film is monitored when it is exposed to different soil samples to compute the gravimetric water content present in the samples. Moreover, when compared to the PEDOT-PSS humidity sensors developed based on a transistor structure, the sensors based on a resistive structure show the simplest structural design without intricate fabrication processes and use easier testing techniques. The simplicity and size of the developed sensor devices compared to other reported devices enabled the measurement of the gravimetric water content present in the soil samples.

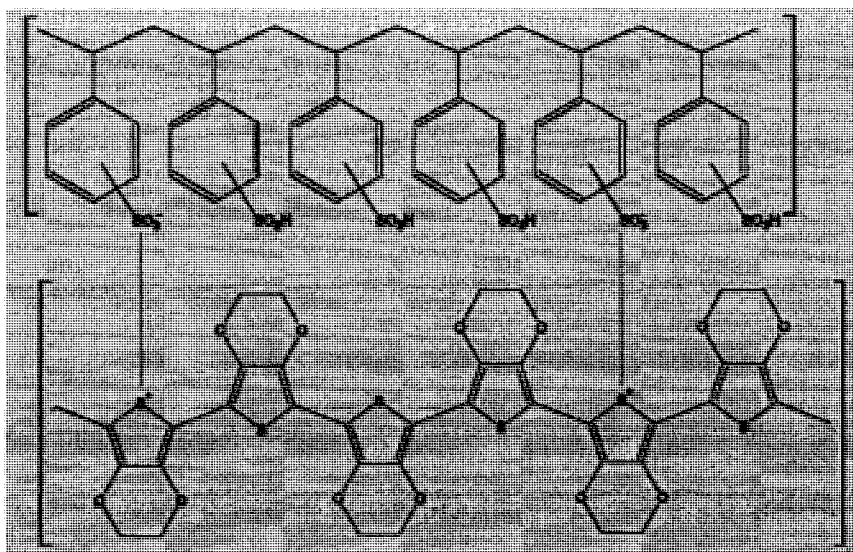


Figure 1-2 PEDOT-PSS chemical structure [60]

As introduced earlier, OFET and FET offer much promising results for chemical and biological sensing applications [63, 64]. OFETs have a number of advantages over biosensors based on other type of electrical models since the organic sensing materials can be fabricated into sensor devices using low-temperature processes and low-cost substrates. Moreover, as OFETs are based on organic semiconductors, the molecular structure and morphology of these materials can be more easily modified to enhance the sensitivity and selectivity of the resulting biosensors [65].

In recent years, conducting polymer materials as potential candidates, such as polypyrrole (PPy) and polyaniline, have showed the promising properties for biosensor applications [66, 67]. Researchers have used these polymers and their composites as the charge-transfer reaction layer between an enzyme and electrode in OFETs, via a conducting polymer matrix network [68]. Traditional  $\text{GO}_x$ -based biosensors, which rely on anodic peroxide detection, use  $\text{H}_2\text{O}_2$  permselective membranes. However, conducting polymer-based glucose sensors use a  $\text{GO}_x$  membrane and are capable of precise and fast

measurement, with sensing range extending to 30 mM, as compared to that of traditional glucose sensors (~2 mM) [69].

Recently, there has been an increased interest in the application of PEDOT-PSS as a suitable matrix system for enzyme entrapment and charge-transfer media in glucose sensors. PEDOT-PSS also displays excellent electrochemical stability, reliability, and interesting redox properties, as compared to that of PPy [70]. The redox properties of PEDOT-PSS make a different oxidation state and conductivity switched by changing the applied potential or pH. For instance, during the operation of OFETs based on PEDOT-PSS, the applied gate voltage allows this material to switch between different redox states [71]. Within a potential range, the redox states can affect enzyme interactions with conducting polymers [71]. Therefore,  $GO_x$  enzyme can interact directly with the conducting polymer (PEDOT-PSS) to form a biosensor. Since then, some biosensors based on PEDOT-PSS have been developed and their mechanisms of operations were fundamentally based on traditional potentiometric and amperometric devices. An OFET-based glucose sensor, with PEDOT-PSS and  $GO_x$  as the channel materials to detect different levels of glucose concentration, is investigated and presented in the dissertation. The mechanism of operation of this biosensor device is fundamentally different from that of traditional PEDOT-PSS based biosensors, where the conducting polymer is used as an electrode. The fabrication and characteristics testing steps of the present glucose sensor are also simple. Moreover, the glucose sensor presented in this paper has displayed a reasonable level of sensitivity, repeatability, and stability. The evaluated range of glucose detection shows that the developed biosensor can be used to detect glucose concentration between normal and diabetic patients.

### 1.3 Dissertation Objectives

The aim of this dissertation research is to investigate low cost methods to manufacture flexible polymer electronic devices. First, PEDOT-PSS based humidity sensors and glucose sensors are fabricated and characterized with a solution process. After several optimizing steps, the humidity sensors and glucose sensors, based on PEDOT-PSS electronic devices, present promising performance and improved quality. Also, TCAD simulation was applied to gain a better understanding of the devices (field effect transistors) and to identify the key factors that could limit device performance.

### 1.4 Organization of Dissertation

Chapter One introduces the investigation and development of organic electronic devices which are mainly assembled with three components, namely, conductor, semiconductor and insulator. Related work that has been done and the special requirements for these three components are briefly addressed in order to highlight the issues that could lead to high-performance OFETs. By comparing to previous work, the improvements of organic electronic sensors are presented.

Chapter Two covers the knowledge of conducting polymers. The conducting mechanisms of the conjugated polymer are introduced, followed by properties and operation principle of the special polymer material, such as PEDOT-PSS, as the channel material of the OFETs.

The theoretical background that has been applied in this work will be presented in Chapter Three. In the operating principles of the OFETs, the energy band diagrams,

electric characteristics, contact resistance effects, trapping effects and field effect mobility have been displayed.

Chapter Four will discuss the modeling and simulation of electronics polymer devices. Technology Computer Aided Design (TCAD) is introduced, highlighting the importance of the numerical simulation on the design and understanding of the semiconductor devices.

Fabrication and analysis of PEDOT-PSS based humidity sensors are given in Chapter Five. Device characteristics are investigated by considering moisture effects and the dependence of sensitivity on the environment.

Organic field effect transistors (OFETs) based on PEDOT-PSS, which is used as the active channel, will be presented in Chapter Six. Fabrication process and device electrical characteristics are investigated considering the PEDOT-PSS material degradation phenomena and protective films for the active channel are evaluated for the degradation problem.

In Chapter Seven, a glucose sensor based on an organic thin film transistor using glucose oxidase and conducting polymer has been investigated and developed. The use of a cellulose acetate membrane in glucose sensor devices to prevent dissolution of GOx and PEDOT-PSS in water has been shown. The sensitivity of the developed glucose sensor was determined by measuring different glucose concentration.

The conclusion and future work will be presented in Chapter Eight. The contribution of the work and some topics for future work will be highlighted.

## CHAPTER TWO

### ELECTROACTIVE POLYMER MATERIALS

#### 2.1 Introduction

It is known that organic electronic technology has been developed since the organic materials were investigated. Generally, there are three main groups for organic materials, the first is organic dielectric, the second is organic semiconductors and the third is organic metals. Comparing these three types material, organic semiconductors, such as polymer materials, offer significant advantages, such as being more robust than molecular crystals, low cost and simple fabrication techniques [72]. Another important feature is that polymers can be soluble in common solvents. Moreover, polymer materials have been used in a wide range of applications as coatings, adhesives, structural materials and for flexible organic electronics and circuits. Currently, an increasing demand for highly specialized materials for use in optical and electronic applications has found that the polymers provide a particular potential in this case [73]. “There is considerable interest in the development of polymers with targeted optical properties, such as second-order optical nonlinearity [74], and conducting polymers as electrode materials [75] and as electroluminescent materials” [76].

## 2.2 Conducting Polymer Structure

A polymeric solid is made of many repeating chemical units or molecules called monomers. An important feature of a conducting polymer is the conjugation of  $\pi$ -electrons extending over the length of the polymer backbone. The chemical structures of some common conducting polymers, for example, polyaniline(Pan), polypyrrole(PPy) and polythiophene(PTh), are presented in Figure 2-1. Normally, they incorporate aromatic compounds, thiophenes and pyrroles. Within the backbone of the molecular chain there are alternative single and double carbon bonds along their polymer chains. Benzene rings with six carbon atoms are building blocks for aromatic compounds. In thiophenes, four carbon atoms and one sulfur atom form a ring while the sulfur is replaced by a nitrogen atom in pyrroles.

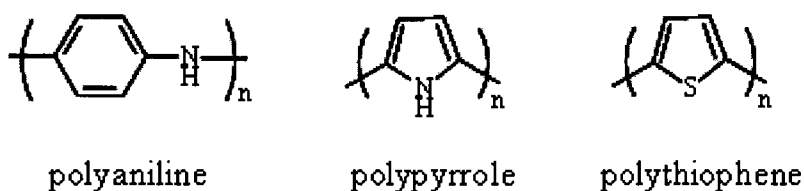


Figure 2-1 Polyaniline, Polypyrrole and Polythiophene chemical structures [77]

## 2.3 Conducting Polymer Electrical Characteristics

Conjugated polymers show various mechanical, electrical and optical properties depending on the synthesis conditions and variation chemical properties of the polymer chain. The electrical conductivity of insulating polymers is about  $10^{-18}$  S/m, whereas that of doped conducting polymers can reach  $10^7$  S/m [78]. Some polymers are sensitive to high-energy radiation and when those polymers are exposed to ultraviolet light, the

chemical properties, such as solubility, will change [79]. For example, photolithography, which is a very well known process in micro-electronics, accords to this principle.

The basis of conjugated polymer electronic properties is due to every repeating unit forming a separate molecule having molecular orbitals in a certain electronic state [80]. Since then, the number of repeat units determines the electronic properties of the polymer. The possibility of transport charge (holes and electrons), due to the  $\pi$ -orbital overlap of neighboring molecules, allows the conjugated polymers to emit light, conduct current and act as semiconductors. The electrical conductivity of the conjugated polymers can be tuned by doping an oxidizing or a reducing agent.

### 2.3.1 Energy Band Structure of Conducting Polymers

Semiconducting properties of conducting polymers come from delocalized  $\pi$ -electron bonding along the polymer chain [81]. Molecular orbitals of the repeated units overlap in space and form a series of energy bands:  $\pi$ -bond and  $\sigma$ -bond [82]. In these compounds, electrons are delocalized from their parent atoms and form two molecular orbitals of different energies, which act as the highest occupied molecular orbital, defined as HOMO (valance band), and the lowest unoccupied molecular orbital, defined as LUMO (conduction band), of a conjugated polymer. “Carbon-carbon double bonds are formed when two of the three 2p orbitals on each carbon atom combine with the 2s orbital to form three  $2sp^2$  hybrid orbitals. These lie in a plane directed at  $120^\circ$  to each other, and form  $\sigma$ -orbitals with neighboring atoms. If the hybrid orbitals are formed from one 2s and two 2p orbitals, a planar  $\sigma$ -bond structure occurs. The third  $p_z$  orbital on the carbon atom, the  $2p_z$ , points perpendicularly to this plane, and overlaps with a  $2p_z$  orbital on a neighbouring carbon atom, to form two pairs of  $\pi$ -orbitals” [82] (Figure 2-2). The



resulting  $\pi$ -bond will form parallel to the underlying  $\sigma$ -bond. As equivalent  $\pi$  orbitals are formed between nearby atoms along the chain, the wave-functions overlap, resulting in a delocalisation over the polymer chain. The electrons in the  $\pi$ -bond are less strongly bound than the electrons in the  $\sigma$ -bond. Thus the electrons in the  $\pi$ -bond can be more easily removed as compared to electrons from the  $\sigma$ -bond. The weaker binding of the  $\pi$ -bond also means that polymer materials have the potential to display either semiconductor or metallic behaviour, due to the unstable of  $\pi$ -bond.

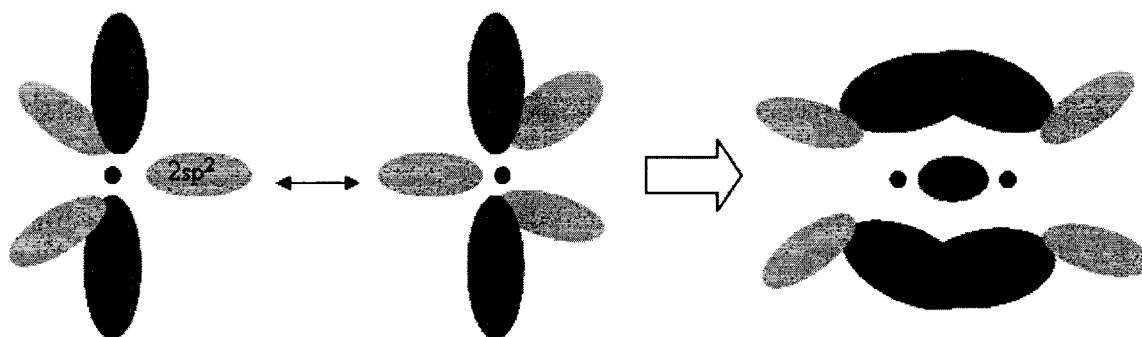


Figure 2-2 The overlapping of  $2sp^2$  and  $2p_z$  orbitals forms  $\sigma$  and  $\pi$ -bonds respectively [82].

The difference in energy between the highest occupied molecular orbital (HOMO) in the valence band and the lowest unoccupied molecular orbital (LUMO) in the conduction band gives the energy gap  $E_{gap}$ . In Figure 2-3, the energy gap decreases with an increase in the conjugation length, which also corresponds to an increase in the number of energy levels [83]. The energy gap determines the electronic and electric properties of the conducting polymers. Therefore, control of the HOMO-LUMO energy differences in molecules and, specifically, the design of low band gap polymers have currently gained importance.

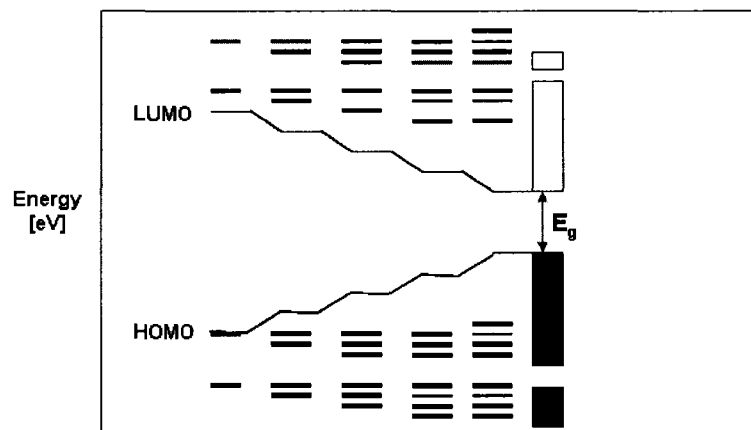


Figure 2-3 Band formation in conducting polymers with increasing conjugation length [83]

To design a low band gap conjugated polymer, it is desirable to start with monomer units with small excitation energies [84]. One way to obtain excitation energies is to calculate the energy of the ground and excited state explicitly and to take the energy difference.

### 2.3.2 Doping Characterization of Conducting Polymers

Doping refers to the process of intentionally introducing impurities into an extremely pure (intrinsic) semiconductor in order to change its electrical properties. On conjugated polymers, the doping level determines the transport mechanisms [85]. By adjusting the level of doping in the chemical process, the conductivity of the polymer can be varied. For example, PEDOT and polyacetylene, which have intrinsic conductivities much lower than  $10^{-5} (\Omega.cm)^{-1}$ , could be made highly conducting,  $\sim 10^6$  and  $\sim 10^5 (\Omega.cm)^{-1}$  respectively [86] (shown in Figure 2-4).

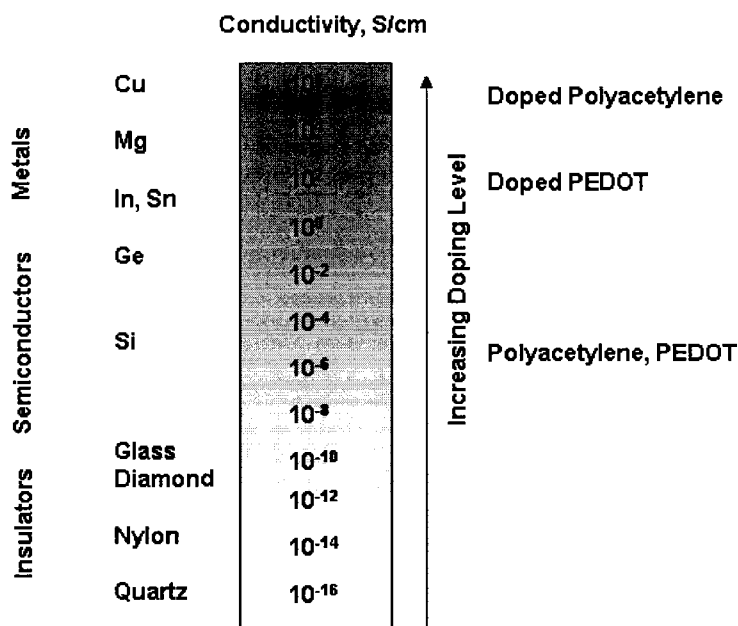
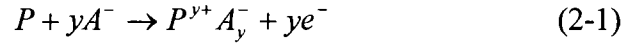


Figure 2-4 Conductivity levels change of Polyacelene and PEDOT [86]

Generally, charge transport mechanisms are based on the motion of radical cations or anions [87], which are created by oxidation or reduction along the polymer chain. A redox process, oxidation or reduction, causes a change in the electronic structure. Impurity or dopant atoms in the polymer backbone can be thought of as interstitial defects that take up positions between the chains.

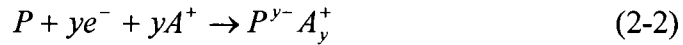
There are several doping methods for polymers: chemical doping, electrochemical doping, photo-doping and charge-injection doping [88]. Chemical and electrochemical doping are the most common approaches. Conjugated polymers can be both p-type and n-type doped. P-type doped is the partial oxidation of the polymer by chemical oxidant or an electrode and causes depopulation of the bonding p orbital (HOMO) with the injection of holes (excess acceptors) [89]. The process involved in p-doping is equivalent to taking electrons from the  $\pi$ -system of the polymer backbone. Oxidation doping of conducting

polymers results in the polymer backbone being changed from a neutral polymeric chain into a polymeric cation [90]:



$P$  means the polymer chain,  $A$  denotes the charge-compensating counter-ion,  $e^-$  is the electron and  $y$  is the number of counter-ions.

N-type doped, which refers to the partial reduction of the polymer by a chemical reducing agent or electrode with the injection of electrons (excess donors) in the anti-bonding p system (LUMO) and the chain is instead reduced compared to its neutral state. During the n-doping process, electrons are introduced into the  $\pi$ -system of the polymer chain to form a negatively charged unit in the conjugated system [90]:



As described above, charge carriers can be created through oxidative or reductive doping. The charge carriers can either be solitons, polarons or bipolarons, which are not real physical particles, but rather quasi-particles [91]. “When two chain segments of conjugated polymer interact, with different bond order, a defect in the form of an unpaired electron is created, which is named a neutral soliton” [92]. This unpaired electron will end up at a new energy level inside the band gap. However, most conductive polymers result from acceptor doping and the formation of positive polarons, since the negatively charged counterparts are chemically unstable. These polarons, or radical-cations, have conventional charge-spin relationships. It is also possible to form bipolarons, or dications, in which the Coulomb repulsion of two positively charged polarons can stabilize a short length of the higher energy polymer structure [93]. For such polymers, heavy doping can be viewed as producing polarons and bipolarons that interact

to form bands that eventually fill the whole intrinsic band gap which leads to a metallic state.

Within this framework, two types of conductive polymer exist: those with a degenerate ground state (ie. polyacetylene) and those with a non-degenerate ground state (ie. PEDOT and PPy)[94]. With degenerate ground states, the initial charge forms a polaron, and another polaron will be created by the subsequent charge. The two polarons, will degenerate to form two charged solitons. However, for non-degenerate polymers, solitons are not formed with two charges, but a pair of defects is created called bipolarons.

As described above, in non-degenerate ground state systems, the combination of the charges and the structural deformation create polarons or bipolarons. Figure 2-5 shows the energy band structure change during the doping process for PEDOT [95]. By oxidising the polymer, an electron is removed and the associated positive polaron occupies an energy level in the energy band gap. By withdrawing an electron from a polymer chain with a non-degenerate ground state, a cation-radical pair is formed, which can be observed in Figure 2-5. In between the cation and the radical, a change in the polymer structure is created. “In thiophenes, the structural deformation of the benzene ring to change from a benzenoid to a quinoidal form upon creating a polaron, is presented in Figure 2-6” [96]. The quinoid structure is a higher energy state compared to the benzenoid form. In contrast to solitons, polarons must overcome an energy activation barrier related to the benzenoid-quinoid transformation while moving. A polaron occupies up to approximately five monomer units along the polymer chain. If two electrons are withdrawn from the conjugated polymer, a positive bipolaron, with two

positive charges, is created. If the polymer is oxidised even further, bipolaron energy bands are generated in the band gap.

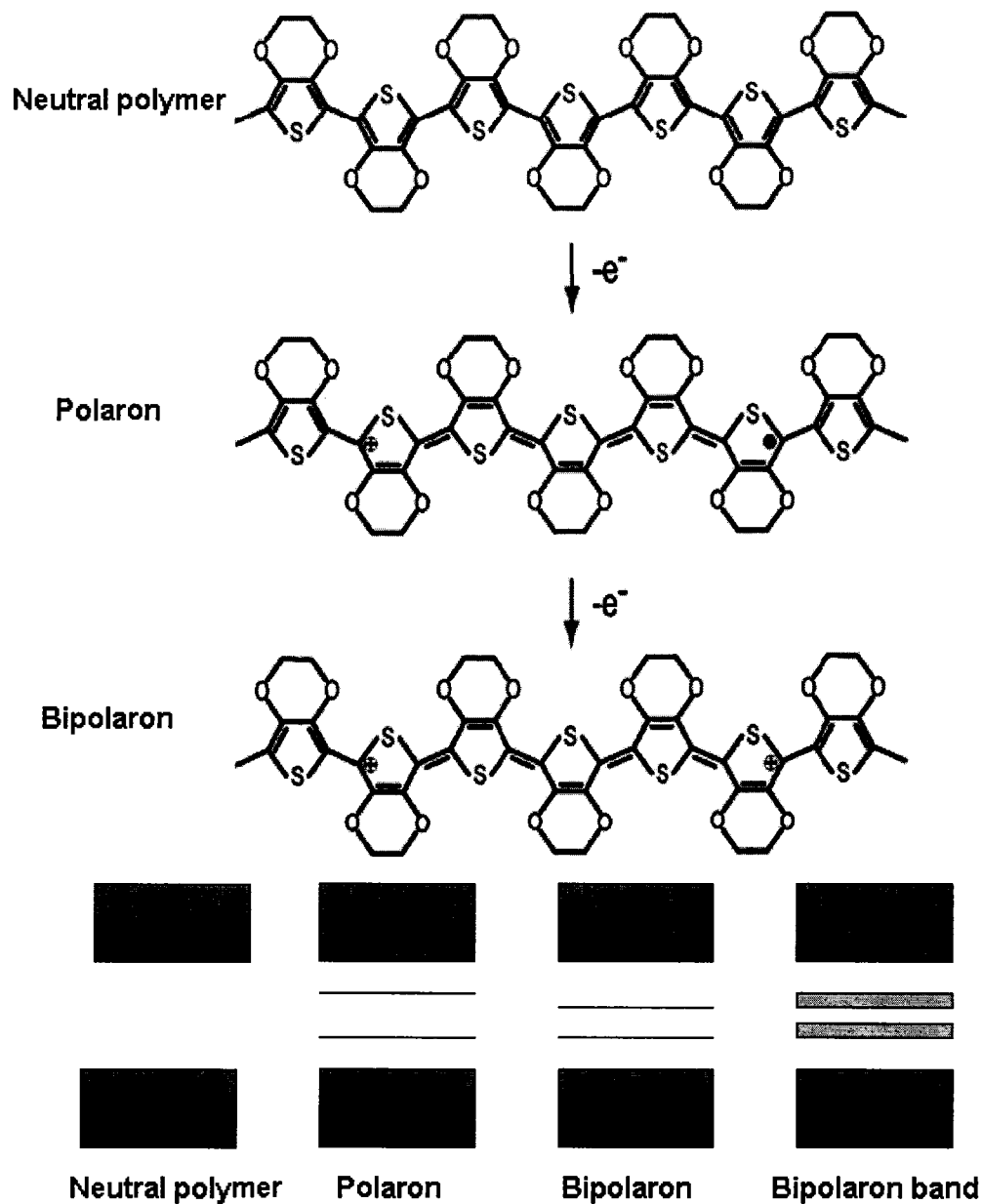


Figure 2-5 Generation of positive polaron and bipolaron in PEDOT. Energy levels of the neutral polymer, a polaron, a bipolaron and a polymer with bipolaron energy band are described above.  $\bullet$  denotes an electron not participating in a bond,  $\oplus$  denotes a hole [95].

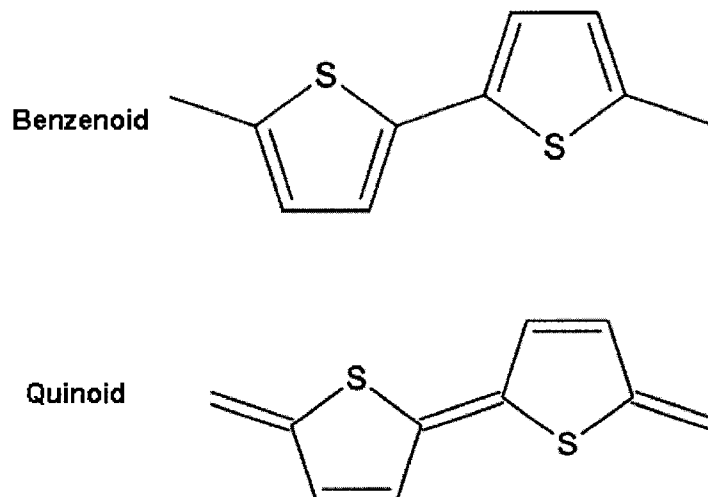


Figure 2-6 Bonding arrangement change in PEDOT [96].

The evolution of the doping properties in a polymer with a degenerate ground state, for example, polyacetylene, is similar to that in PEDOT except considering charged solitons rather than bipolarons. As the ground state structure of those polymers are twofold degenerate, the charged cations are not bonded to each other by a higher energy bonding configuration and can be separated along the chain. Thus, “the charged defects are independent of one another and can form domain walls that separate two phases of opposite orientation and identical energy” [97]. At the lower doping levels, the recombination among polarons or existing neutral solitons creates charged solitons which are shown in Figure 2-7. With the doping level increasing, soliton energy states at midgap become overlapping to form a soliton band. These soliton bands result in the creation of new localized electronic states that are present in the middle of the energy gap. “With the doping concentration increased, the charged solitons interact with each other to form a soliton band which can merge with the edges of the valence band and conduction band to produce true metallic conductivity” [98].

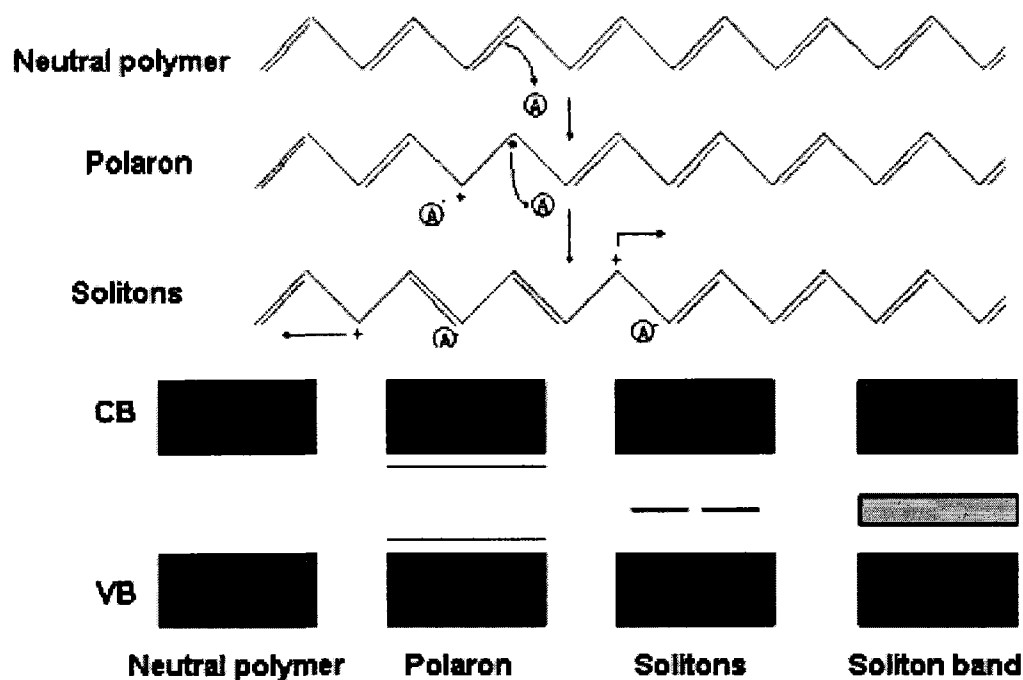


Figure 2-7 Generations of polaron and solitons in PEDOT. Energy levels of the neutral polymer, a polaron, solitons and a polymer with soliton energy band are described above [97].

#### 2.4 Free Charge Carriers in Conjugated Polymers

Conjugated polymers consist of long carbon molecular chains with alternating single and double bonds and  $\pi$ -electrons are delocalized along the whole backbone. In order to reach electrical conduction in a conjugated polymer, there should be some free charges in the polymer chain. As described earlier, the doping and de-doping processes can create the charge carriers which are transported through the  $\pi$ -bonded polymer chain. Electrons of the conjugated structure are attracted from the positive charge of the carbon atom that donated the electron. Thus, the charge becomes delocalized and can hop along the chain.

The working mechanism of charge transport along conjugated polymers was originally proposed by Conswell [99] and Mott and co-workers [100,101]. The process to



describe this charge transfer is named intermolecular hopping and is a thermally assisted tunneling effect [102]. The transition rates for this tunneling are given by Miller and Abraham [103]. Due to the disorder introduced from the end-groups of conjugated polymer chains and defects in form of kinks, cross-links and impurities, the charge hopping between conjugated parts of the polymer becomes the most important factor for conduction in the materials [104]. The degree of disorder with the wide range of charge species is the main reason affecting the charge transport in conjugated polymers.

In the case of hopping transport, lower mobility values, such as  $\sim 10^{-3} \text{ cm}^2/\text{Vs}$ , in many cases even much lower values, will be resulted due to the disorder of the polymer chain and weak intermolecular interaction [105]. In order to achieve high conductivity, higher concentration of charge carriers is required. Thus, the doping of an energetically disordered hopping transport system produces free charge carriers and also creates localized states in addition to the intrinsic density of state (DOS) distribution [106]. In equilibrium condition, charge carriers mostly occupy positions in the deep tail of the DOS while charge carrier hopping will occur generally via much shallower states that belong to the effective transport level [107]. The charge carrier density increasing strongly increases the mobility at low to moderate doping levels [108]. According to the doping process principle, the Fermi energy shifts to the center of the DOS distribution at high doping levels. Therefore the high concentration of dopant will lead to decreasing carrier mobility.

Hopping of either electrons within a manifold of lowest unoccupied molecular orbitals (LUMO) or holes within a set of highest occupied molecular orbitals (HOMO) in disordered conjugated polymers magnify conductivity of the materials [109]. Both

LUMO and HOMO manifolds are characterized by random positions and relatively broad (Gaussian) energy distributions of hopping sites [110]. Being embedded into a random medium, dopant atoms or molecules are also inevitably subjected to positional and energy disorder. Since the HOMO level in most organic solids is deep and the gap separating LUMO and HOMO states is wide, energies of donor and acceptor molecules are normally well below LUMO and above HOMO, respectively. Therefore, a double peak Gaussian function should be a realistic model for the DOS distribution in a doped polymer [111]:

$$g(E) = \frac{N_i}{\sqrt{2\pi}\sigma_i} \exp\left(-\frac{E^2}{2\sigma_i^2}\right) + \frac{N_d}{\sqrt{2\pi}\sigma_d} \exp\left(-\frac{(E + E_d)^2}{2\sigma_d^2}\right) \quad (2-3)$$

in which  $N_i$  and  $N_d$  are the densities of intrinsic states and dopants,  $\sigma_i$  and  $\sigma_d$  the Gaussian widths of the intrinsic and dopant,  $E$  is the energy of charge carrier and  $E_d$  is the energy shift between these distributions. The equilibrium distribution of charge carriers,  $\rho_{eq}(E)$ , is directed by the Fermi–Dirac distribution  $f_{eq}(E)$ [111]:

$$\rho_{eq}(E) = g(E)f_{eq}(E) = \frac{g(E)}{1 + \exp[(E - E_F)/kT]} \quad (2-4)$$

with the Fermi energy  $E_F$  determined by the condition that the total density of charge carriers must be equal to the density of dopants  $N_d$  as [111]:

$$N_d = \int_{-\infty}^{\infty} dE \rho_{eq}(E) = \int_{-\infty}^{\infty} \frac{dE g(E)}{1 + \exp[(E - E_F)/kT]} \quad (2-5)$$

According to the Miller–Abrahams equation [112], the rate of carrier jump strongly reduces with increasing of the distance and energy difference between starting and target sites. The distance and energy variation, which provide the highest hopping rate, is determined by the temperature, the carrier localization radius  $1/\gamma$ , and the shape of

the DOS distribution [113]. The research results have shown that a carrier will most probably jump from a currently occupied state to a hopping site which belongs to the effective transport level of the energy,  $E_{tr}$ . If there are carriers partially filling in a DOS distribution, the equation for the effective transport energy is [109],

$$\int_{-\infty}^{E_{tr}} dE \frac{g(E)(E_{tr} - E)^3}{1 + \exp[-(E - E_F)/kT]} = \frac{6}{\pi} (\gamma kT)^3 \quad (2-6)$$

The occurrence of the effective transport energy reduces the problem of variable-range hopping in the trap controlled transport model with a broad distribution of localized states.

The weak-field equilibrium mobility  $\mu$  can be estimated from the Einstein relation as  $\mu = eD/kT$ , with  $e$  being the elementary charge and  $D$  the diffusion coefficient.

$$D \text{ can be used as } \langle v \rangle r_j^2$$

where  $r_j$  is the typical jump distance and  $\langle v \rangle$  the average jump rate. By calculating  $r_j$  as

$$r_j = \left[ \int_{-\infty}^{E_{tr}} dE g(E) \right]^{-1/3} \quad (2-7)$$

and averaging the jump rate one obtains the following expression for the equilibrium mobility [114],

$$\mu = \frac{ev_0}{kTn} \left[ \int_{-\infty}^{E_{tr}} dE g(E) \right]^{-2/3} \int_{-\infty}^{E_{tr}} \frac{dE g(E)}{1 + \exp[(E - E_F)/kT]} \exp\left(\frac{E - E_{tr}}{kT}\right) \quad (2-8)$$

where  $v_0$  is the attempt-to-jump frequency.

From Figure 2-8 [111], it is observed that the doping efficiency increases with decreasing temperature although the material is doped by very deep traps. It can be explained that the activation energy of the equilibrium mobility of extrinsic charge carriers strongly increases with decreasing temperature. However, in a doped material, this energy cannot be larger than the energy difference between the energy of dopants and

the maximum of the intrinsic DOS. Thus, the mobility remains basically constant at low carrier densities; it strongly increases at higher carrier concentrations. This limits the maximum activation energy of the mobility in a doped material and does not allow the mobility to decrease as steeply as it decreases for a low density of extrinsic carriers [111].

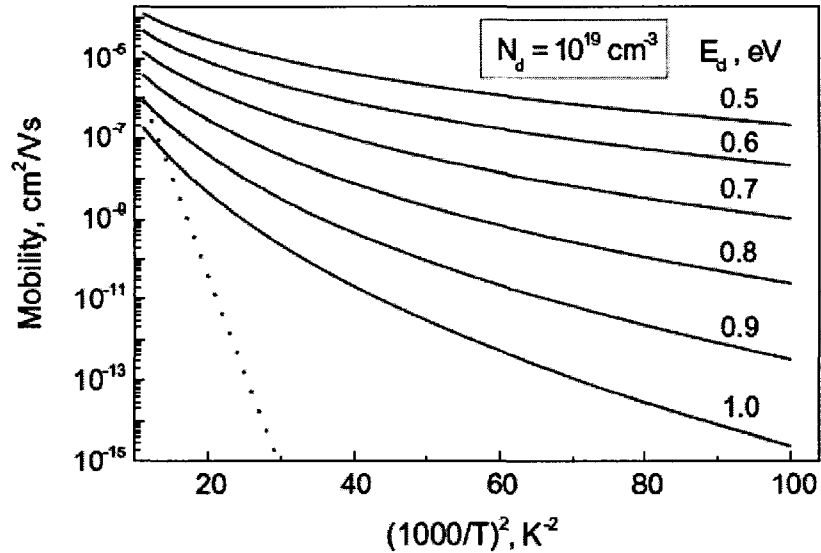


Figure 2-8 Temperature dependence of the carrier mobility in doped and pristine amorphous organic materials [111]

Instead of a power law, the temperature dependence shows an activated behavior and the mobility also depends on the applied electric field [115].

$$\mu(E, T) \propto \exp(-\Delta E / kT) \cdot \exp(\beta\sqrt{E} / kT) \quad (2-9)$$

On a macroscopic level, the current density,  $J$ , through a material is given by the charge carrier density  $n$  and the carrier drift velocity  $v$ , where the latter can be expressed by the mobility  $\mu$  and the electric field  $E$ :

$$J = qnv = qn\mu E \quad (2-10)$$

Due to the carrier density and mobility both depending on the applied electric field, the relationship between  $J$  and  $E$  is not linear for the disordered organic polymer

materials. From Equation (2-10), apart from the field, the current is determined by another two parameters,  $n$  and  $\mu$ . As discussed above, the mobility strongly depends on the degree of order and doping level of the disordered organic polymers. The density of charge carriers is equal to the density of dopants  $N_d$ , as shown in Equation (2-4).

Furthermore, space-charge and trapping effects, as well as details of the charge carrier injection mechanism, are considered for the charge carrier transport in conjugated polymers [116].

### 2.5 PEDOT-PSS Structure and Electrical Characterization

“Poly(3,4-ethylenedioxythiophene) (PEDOT) belongs to a novel class of polythiophenes with very high electrochemical stability in oxidized states and a moderate band-gap with good stability in the doped state” [117]. Another promising feature is that high conductivity if the material is in its oxidized form, which is due to a planar structure and delocalization of  $\pi$  electrons in polymer chain. And also PEDOT gives promising optical transparency in the visible region [117]. However, PEDOT formed by using oxidative chemical or electrochemical polymerization due to its insoluble property. Recently, this problem was solved with the “combination of poly(4-styrenesulfonate) (PSS) as a water soluble polyelectrolyte and charge-compensating counter-ion” [117] to form PEDOT-PSS. Each styrene ring of the monomer has one acidic  $\text{SO}_3\text{H}$  group. Part of the sulfonyl groups are deprotonated and carry a negative charge and the other component PEDOT carries positive charges. This chemical structure makes PEDOT-PSS form a high regiochemically defined material [118]. Therefore, the polymer requires the easy fabrication and then can form well films which retaining promising optical transparency, high chemical stability and good conductivity. According to the promising

features of the polymer, the PEDOT-PSS originally was used as an antistatic coating for photographic films and plastic components [119]. Its uses can also be developed for conducting electrodes in capacitors and FETs [120]. Because of its planar structure, which leads to “high electron delocalization along the chain, then the relative high conductivity [121] and good transparency can make PEDOT-PSS usable for LEDs [122], due to its high work function, and, as mentioned previously, as a charge injecting layer in PLEDs” [123]. Finally, it is a promising electrode material for organic photovoltaic cells because of the low current densities [124].

The conductivity of PEDOT-PSS can be varied widely due to the different doping level in the polymer. For example, the original PEDOT-PSS has a conductivity of about 10 S/cm. However, after the doping process, like redox, the conductivity of PEDOT-PSS can be improved up to several hundred S/cm. The principle of PEDOT doping is depicted in Figure 2-5.

Except for getting high conductivity PEDOT-PSS, the lower conductivity also can be achieved by changing the particle size and by increasing of the PSS content [125]. “Normally, the material with conductivity of around  $10^{-3}$  (1:6 PEDOT: PSS by weight) or  $10^{-5}$  (1:20 PEDOT: PSS by weight)” [126] used in PLEDs is this type.

Recently, spectroscopic methods, such as Raman, infrared (IR), X-ray (XPS) and ultraviolet photoelectron spectroscopy (UPS) are applied to the investigation of the electronic structure and characterization of PEDOT-PSS film. The sulfate doping level can be determined by analysis from spectroscopic measurement [127]. The key role of PSS in making PEDOT-PSS an effective hole-injection material was established and the work function of this polymer material changes with PSS quality [128]. Thus, flexible

conductivity PEDOT-PSS films can be formed. This is a potential application of PEDOT-PSS to future organic electronics and displays.

## CHAPTER THREE

# THEORETICAL BACKGROUND OF ORGANIC ELECTRONIC DEVICES

### 3.1 Overview

“Organic electronics is attracting more and more attention from theoreticians and computational physicists both for its potential applications and for the interesting fundamental theory” [129]. The availability of organic semiconductor electronics devices may open the new way to completely new set-ups, fabrication processes, and applications. Then the processing of organic material by printing and lithography can be visualized and then large volume, low cost production of field-effect transistors based on polymers using thin film technologies can be realized [129]. As mentioned earlier, organic field-effect transistors (OFETs) can be manufactured by using organic materials. The insulating polymer material, such as, polyester, polyethylene and polyimide can be chosen as the dielectric layer of OFETs, and the conducting channel material can be a conjugated polymer which provides the reasonable conductivity and mobility for devices.



### 3.2 Operation Models of Organic Field Effect Transistors

Organic Field Effect Transistors (OFETs) have been developed due to their good compatibility with different substrates and opportunities for structural tailoring. The trend towards competing with conventional semiconductor technologies is growing because of the advantages of organic electronic devices, like inexpensive, large-area, flexible devices processed with lower temperatures and lower cost fabrication techniques.

The most common OFET device structure diagram is based on the traditional metal oxide semiconductor field effect transistor (MOSFET) configuration. A thin film of organic semiconductor material is deposited on top of a dielectric with an underlying gate electrode, which is shown in Figure 3-1. The source-drain electrodes providing the contacts are defined either on top of the organic film or on the surface of the FET substrate prior to deposition of the semiconductor film. There are two different device structures in Figure 3-1, (a) is top-contact, bottom-gate; (b) is bottom-contact, bottom-gate [130]. In both cases, an organic semiconductor film is deposited on a gate/insulator substrate and is contacted with metallic source and drain electrodes. Each of these structures has its advantages and drawbacks. For bottom contact architecture, contacts are deposited on the insulator layer and the electrode contacts can be patterned or printed by means of microlithography and metallization techniques. However, in the top contact structure, a shadow mask is used for the deposition of contacts. The organic semiconductor film can be coated from the vapor phase or from solution. The metal source and drain electrodes are e-beam deposited or metal evaporation through a shadow mask. The comparison between top-contact and bottom contact devices shows that the two structures have similar channel characteristics but differ in the formation of the

contact-polymer interface [130]. “The interface between the contact electrode and the polymer film is much more uniform for top-contact devices than for bottom contact devices which results in a reduction of the contact resistance effect” [131]. Therefore, in this research work we developed the OFET based on the top contact structures.

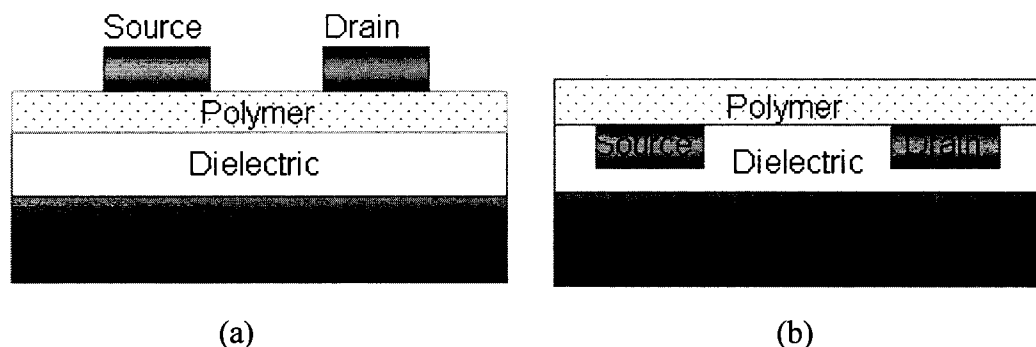


Figure 3-1 FET structures (a) top-contact, (b) bottom-gate structures

“The basic principle of operation of an OFET is that the density of charge carriers between the source and drain is modulated via capacitive coupling between the gate contact and the transistor channel” [132]. The capacitor consists of the gate contact, the dielectric medium, and the semiconducting polymer channel as the other electrode. The voltage applied between the source and drain is called the source-drain voltage,  $V_{DS}$ . Under a given  $V_{DS}$ , the current flow which is across the channel film from source to drain, depends on the voltage  $V_{GS}$  applied to the gate electrode. The channel film and gate electrode are coupled such that application of a bias on the gate induces charge in the semiconductor film, as shown schematically in Figure 3-2. Much of this charge carrier moves in response to the  $V_D$ . Ideally, when no gate voltage is applied on the device, the conductance of the semiconductor film is extremely low because there are no mobile charge carriers, and the device is switched off. When there is voltage applied, mobile charges are induced, and the device is turned on. At low drain-source voltages, the drain-

source current ( $I_D$ ) has a linear relationship with  $V_D$  and the characterization of the device behaves as a resistor. As the  $V_{DS}$  is increased to saturation, the thickness of the highly conductive channel is reduced to zero, which results in pinch off. Beyond  $V_{DS}$ ,  $I_D$  remains essentially constant and, therefore, the transistor acts as a current generator.

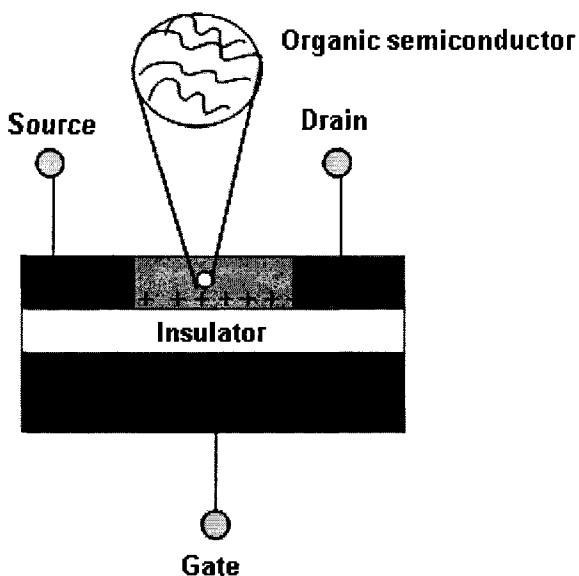


Figure 3-2 Organic field effect transistor schematic structure

Now consider an organic FET as shown in Figure 3-2 with channel length and width  $L$  and  $w$ , respectively. The active layer channel is assumed to be p-doped and has a p-accumulation channel with hole mobility ( $\mu$ ). These defined OFET characteristics are similar to those of the MOS field effect transistor (MOSFET) at gate bias voltage ( $V_{GS}$ ) higher than the threshold voltage  $V_T$ , as illustrated in [132] and in our research. At low drain-source voltages ( $V_{DS} \ll V_{GS}$ ), there is a linear (ohmic) area in which the drain current ( $I_D$ ) is independent of gate voltage ( $V_G$ ), but dependent on the drain-source voltage ( $V_{DS}$ ). With an increase of  $V_{DS}$ , a saturation of  $I_D$  occurs. The relationship of the

drain current of the transistor dependent on drain-source voltages and gate-source voltage  $V_{DS}$  and  $V_{GS}$ , respectively, can be evaluated as:

$$I_D = \frac{W}{L} \mu \cdot C_i \left( V_{GS} - V_T - \frac{V_{DS}}{2} \right) V_{DS} \quad (3-1)$$

For linear mode, where  $V_{DS} < V_{GS} - V_T$

$$I_D = \frac{W}{L} \frac{\mu \cdot C_i}{2} (V_{GS} - V_T)^2 \quad (3-2)$$

For saturation mode, where  $V_{DS} > V_{GS} - V_T$

Here  $C_i$  is the gate-insulator capacitance per unit area and  $V_T$  is the threshold voltage.

Furthermore, it was observed that the behaviour of the I-V characteristics in a OFET at low gate biases ( $V_{GS} < V_T$ ) is also similar to that in MOS transistors because  $I_D$  is an exponential function of  $V_{GS}$  [133]. According to the MOS model for the sub-threshold regime, the exponential dependence can be written as

$$I_D = I_0 \cdot \exp\left(\frac{V_{GS}}{\phi_1}\right) \cdot \left[ 1 - \exp\left(-\frac{V_{DS}}{\phi_2}\right) \right] \quad (3-3)$$

For the sub-threshold mode, where  $V_{GS} < V_T$ .

To summarize, the shape of the I-V characteristics in an OFET is similar to those in a crystalline field-effect transistor. From Equations (3-1) and (3-2) the estimated values for the mobility ( $\mu$ ) in OFETs are low, and have a very wide range  $\sim 10^{-5}$ -  $10^{-1}$   $\text{cm}^2/\text{Vs}$  [134]. The low mobility in OFETs is an important issue because it limits the applications for the device. Thus, much effort is devoted to develop polymers and processing technologies in which the effective mobility is improved to higher values.

### 3.2.1 Energy Band Diagrams

“The highest occupied and lowest unoccupied molecular orbital (HOMO/LUMO) energies are the origin of gate-induced charge (field effect) and determine the acceptable performance of the organic FET” [135]. Figure 3-3 shows the position change of the HOMOs and LUMOs of the organic semiconductor relative to the Fermi levels with different gate bias. Due to the work function potential difference between the semiconductor and the metal, a gate voltage is applied so that the Fermi levels of metal and semiconductor align. Then no band bending will occur in the semiconductor [136], as shown in Figure 3-3a. This gate voltage is called the flat band voltage ( $V_{FB}$ )

$$V_{FB} = \phi_{ms} = \phi_m - \left( \chi + \frac{E_g}{2q} + \phi_b \right) \quad (3-4)$$

Here,  $\phi_{ms}$  is the work function difference between metal and semiconductor,  $\phi_m$  is the metal work function,  $\chi$  the electron affinity,  $E_g$  the semiconductor bandgap,  $q$  the electron charge, and  $\phi_b$  the potential between the Fermi level and the intrinsic Fermi level  $E_i$ . When the work function of metal is similar to the Fermi level of the semiconductor, the flat band voltage will be close to zero. Here we are not considering the interface charges that also affect the flat band voltage. Applying a negative gate voltage will induce charges at the semiconductor-insulator interface. This results in the energy-band bending-up and the accumulation of holes at the interface which are shown in Figure 3-3b. Under this condition, the p-channel transistor is turned on. If a positive gate voltage is applied, the mobile holes are depleted from the semiconductor-insulator interface due to the electric field, causing bending down of the energy-band in the p-type semiconductor as illustrated by Figure 3-3c.

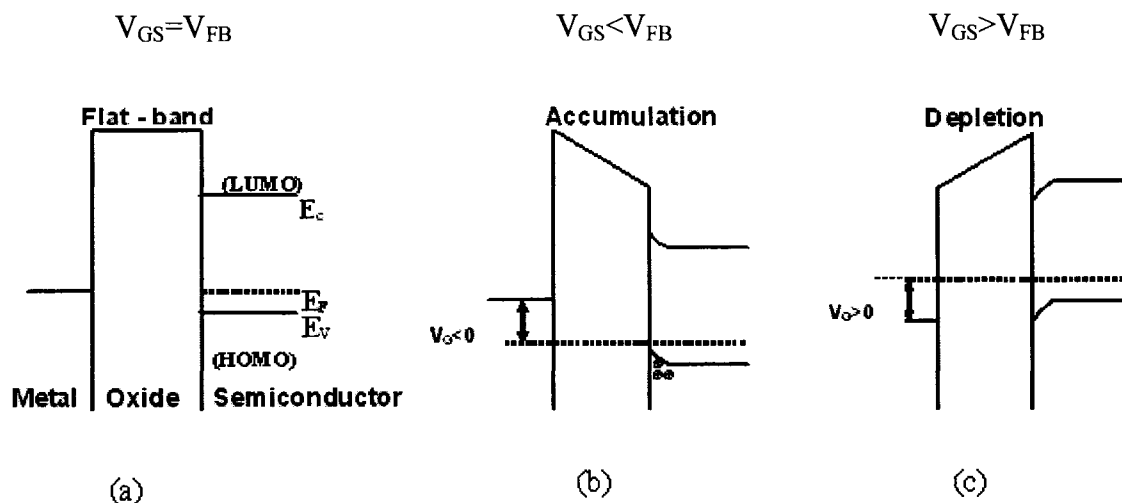


Figure 3-3 Energy band diagrams of the OFET structure for a p-type semiconductor illustrating (a) flat band model, (b) accumulation model, and (c) depletion model

### 3.2.2 Charge Transport in Organic Field Effect Transistors

Electronic properties of various organic semiconducting materials are discussed in Chapter Two. For OFETs, the charge carrier mobility and on-off current ratio are two important parameters. In order to improve these parameters, the mechanism of charge transport should be studied. As discussed in Chapter Two, the transport of carriers within the organic semiconductor is governed by the hopping between localized states [137]. It is useful to know that the charge carrier density is not uniformly distributed in the accumulation channel and it is also very helpful for understanding the transfer characteristics of disordered OFETs. In OFETs, the mobility is dependent on the charge carrier density deduced from the hopping model. Consequently, the charge carrier mobility does not obtain a constant value under a certain gate voltage [138], but a distribution of charge carrier mobilities is achieved in the disordered OFETs.

For OFETs at a given drain-source bias voltage ( $V_D$ ), the drain-source ( $I_D$ ) is a function of the conductivity of the polymer film [139]. This conductivity has to be

controlled by the gate-source bias voltage ( $V_G$ ). In order to prevent current leakage due to gate electric field, a charge enhancement in the polymer film has to be produced. As discussed above, since the gate is isolated from the S/D contacts and the organic polymer film, MOS theory can be applied to explain charge transport in OFETs. Even with the complications of applying MOS transistor theory to OFETs, much effort was devoted to finding appropriate organic or polymer materials and electrode insulator configurations for improved electrical performance. However, some issues stay unresolved for the explanation of charge transport in OFETs. The first issue is that the characteristic of charge transport in polymers and crystals is different. In crystals, charge carriers move at the thermal velocity in the conduction or valence band and the mobility is controlled by scattering [140]. However, in polymers, the charge carriers are localized in the energy states of the films. “At cryogenic temperatures, delocalized conduction with high mobility is possible in organic films ( $\mu \sim 3\text{-}300 \text{ cm}^2 / \text{Vs}$  and even higher), but above 30K, the delocalized conduction degrades quickly, and above 100K, the localized conduction (charge hopping) takes over. Then at room temperature, the mobility of the charge hopping is low ( $\mu < 1 \text{ cm}^2 / \text{Vs}$ )” [140]. Charge hopping between energetically and spatially distributed states is the conduction mechanism in polymer films [110]. Since we know that the definition for HOMO and LUMO to be continuous valence and conduction bands in the polymer film is rough due to the HOMO and LUMO states which are spatially distributed in the polymer chain, and there is a distance and barrier between neighboring states which leads to the localization of the charge carriers. However, the source and drain contact material plays an important function in the performance and mobility of the OFET [141]. It has been shown that for the same polymer films, the

voltage drop at the source electrode is a significant portion of  $V_{DS}$  for Ni and Pd electrodes, whereas for Pt, it is low [142].

According to the above discussion, dependence of OFET performance on the source-polymer contact cannot be explained only in terms of the MOS model for carrier enhancement in a polymer film owing to the gate bias and that the contact effects are not negligible. In the case of MOSFET theory (Equation (3-2)), at low  $V_D$  and at the same gate biasing voltage ( $V_{GS}$ ), the current is inversely proportional to the channel length ( $L$ ). This indicates that the “charge injection from the source electrode to the polymer film can explain the behavior of short-channel OFETs by assuming a superposition of the electric fields produced by the gate and drain bias voltages” [143]. Therefore, the charge enhancement in the polymer film of an OFET can also be due to injection of carriers through the source-polymer barrier, rather than only due to the charge induction caused by a potential bending in the polymer.

Furthermore, for the injection process in OFET, there are two phenomena which are important for the metal-polymer interface. The first is a reduced charge enhancement in a narrow region in the vicinity of the interface and it applies for both the charge injection and charge extraction processes at the metal-polymer interface. The second phenomenon is the metal-polymer charge injection itself. For the source-polymer contact, this is very important only for the injection electrode, not for the charge extraction due to the fact that the voltage drop  $\Delta V_S$  at the source electrode is always larger than the voltage drop  $\Delta V_D$  at the drain electrode [143]. The difference,  $V_J = \Delta V_S - \Delta V_D$ , is associated with charge injection and the injection resistance,  $R_J = V_J/I_D$ .  $R_J$  decreases when increasing the charge enhancement owing to gate biasing, that is,  $R_J$  is lower at higher  $|V_{GS} - V_T|$  and  $I_D$ .



Therefore, it should be realized that the contact effects are significant for OFETs, and that these effects can be dominant in the charge transport in OFETs with short channels ( $L < 1 \mu\text{m}$ ). Thus, the charge injection has to be included in the charge transport models for the polymer FET, and the injection mechanisms needs to be explored further in order to obtain agreement between the many explanations proposed over the last two years.

The third issue is about non-stationary effects in OFETs, for example, hysteresis in I-V curves, non-monotonic variation of the drain current with time at constant biasing, and threshold voltage shift towards the gate bias. The slow variations do not coincide with the assumption of quasi-equilibrium in the treatment of charge trapping in terms of energy band bending, as adopted from MOSFET theory [144].

Overall, it should be realized that none of these three issues is negligible for the physical explanation of the charge transport in OFETs. These phenomena are the carrier injection from the source electrode into the polymer material, the drift of the injected carriers in the charge-enhanced polymer material or at the interfacial layers. The injection-drift limited model (IDLM) of charge transport in OFETs [145] has been introduced since the charge injection from the source electrode limits the number of carriers and the effective mobility of charge hopping in the polymer determines the drift of the carriers toward the drain electrode.

### 3.2.3 Carrier Mobility in Organic Field Effect Transistors

Charge carrier mobility ( $\mu$ ) is the central transport parameter in determining device performance in electronics applications. Most of the work related to the mobility is on the temperature and electric field dependence [146] described in Equation (2-14). Due to the research on the polymer field effect transistor, it has been recently found that

the carrier concentration also plays an important role for the mobility. Generally, for OFETs, the thin film is disordered. Thus, for these transistors, parameters such as mobility ( $\mu$ ) are primarily determined by disorder and grain size in the semiconductor [147], which in turn are strongly influenced by fabrication techniques and associated process conditions. In hydrogenated amorphous silicon, the disorder in the bond lengths and angles leads to a high density of localized states. These states trap most of charge carriers and low conductivity can be observed due to the small portion of charge carriers excited to the extended states [148]. In the organic semiconductor, disorder in the molecular arrangement and the presence of grain boundaries lead to a high density of localized states. Hopping of charge carriers between these density states constitutes the means for conduction.

The carrier concentration also affects the mobility ( $\mu$ ) in the Arrhenius behavior of mobility in the temperature dependence measurements of OFETs [149]. The mobility ( $\mu$ ) usually shows Arrhenius behavior with activation energy ( $E_a$ ), which decreases with increasing gate bias, as reported in literature [150]. The dependence of ( $E_a$ ) on gate bias is because of the effect of carrier concentration on mobility ( $\mu$ ).

According to the traditional crystalline semiconductor transistor, mobility is scattering limited and its parasitic bias dependence is only due to surface or impurity scattering. Neglecting electron-electron interactions, carriers in organic material contribute to conduction in which the conductivity ( $\sigma$ ) is linearly dependent on the carrier density ( $n$ ).

$$\sigma = q\mu_{FE}n \quad (3-5)$$

In this equation,  $q$  is the elementary charge,  $\mu_{FE}$  is the mobility of the FET and  $n$  is the charge carrier concentration. Also, this equation can be applied to OFETs. Following the conventional linear field-effect mobility definition for a transistor, the mobility of the field effect transistor can be calculated by Equation (3-1) as:

$$\mu_{FE} = \frac{L}{WC_i V_{DS}} \frac{\partial I_{DS,lin}}{\partial V_{GS}} \quad (3-6)$$

$W$  and  $L$  are the channel width and length, respectively and  $I_{DS,lin}$  is the drain current in the linear region. When this equation is applied to polymer semiconductor FETs, there are more complexities for analysis. In Equation (3-6), namely the uniform mobility transconductance method (UT), the mobility derivative was neglected and a uniform mobility across the channel was assumed. In the saturation region of operation, the field-effect mobility is calculated by Equation (3-2):

$$\mu_{FE} = \frac{2L}{WC_i} \left( \frac{\partial \sqrt{I_{DS}}}{\partial V_{GS}} \right)^2 \quad (3-7)$$

In the disordered material,  $\sigma$  is proportional to the density of carriers that contribute to the conduction band, which is referred to as transport band carriers. However, most of the carriers are trapped and contribute in conduction only excitation to the transport band. For a transistor device, the conductance ( $g$ ) as described in Equation (3-8) is averaged over the semiconducting film and can be spatially related to the conductivity ( $\sigma$ ) by

$$g^{-1} = \int \frac{dl}{\int_A \sigma da} \quad (3-8)$$

Where  $A$  is the cross section area and  $L$  the length of the semiconducting film.

For polymers used in field-effect devices, mobility ( $\mu$ ) is lower than  $1 \text{ cm}^2/\text{Vs}$ , and typically has a very wide range of  $\sim 10^{-5}$ -  $10^{-1} \text{ cm}^2/\text{Vs}$  [137]. This means that one has, in any case, some kind of hopping transport. It should be noted that the mobilities determining the transport in the device are defined only as averages. The exact values can be regarded as to be determined from fitting e.g. current characteristics; however, this mobility is not directly achievable from experiments. Further, field dependence of the mobilities can be taken into account. But it is worth while to check whether the electrical field in the transistor becomes really large enough for this effect to become important. At present, there is little information available on the possible dependence of the mobilities on the carrier concentration for a given doping, which, in principle depends on the type of hopping transport.

#### 3.2.4 Contact Resistance Effects for Polymer Transistors

With the polymer applied as the channel material and the charge-carrier mobility improved, the limitation by contact resistance is becoming increasingly critical and finding ways to reduce these limitations has become a key issue. Mainly, there are two different contacts which can behave as an ohmic contact or as a Schottky barrier and which are dependent on the characteristics of the interface.

##### 3.2.4.1 Ohmic Contact

Ohmic contact means that between the metal and semiconductor there is no potential barrier and the potential drop across these junctions is negligible under both forward and reverse bias. Equal currents will also flow with forward and reverse bias. In ohmic contact, the current produced by the device is determined by the polymer film conductivity rather than the properties of the contact. Carriers can flow freely in or out of

the device and this condition leads to minimal resistance across the contact. When the polymer is heavily doped, the Schottky barrier depletion region becomes very thin [151, 152, 153]. At very high doping levels, a thin depletion layer becomes quite transparent for electron tunneling. Thus, in order to obtain a reliable ohmic contact, the polymer contact with the metal should be heavily doped.

The image most commonly used to describe source and drain contacts is that of a metal-semiconductor junction. The contacts are expected to be ohmic when the work function of the metal is close to the HOMO and LUMO level of the semiconductor, depending on whether the semiconductor is p or n-type. If the reverse situation prevails, an energy barrier forms at the metal-semiconductor interface, leading to poor charge injection. From this standpoint, the Au/PEDOT-PSS interface would be a good candidate as a low-resistance contact. In practice, the real resistance is rather high. The mechanism of barrier formation at metal-organic semiconductor interfaces has been studied in great detail for organic light-emitting diodes (OLEDs), where contact resistance is also a crucial issue. UV Photoelectron Spectroscopy (UPS) has been used for the precise determination of the energy levels at both sides of the interface [154, 155]. A typical result for the Au/PEDOT-PSS interface is shown in Figure 3-10 [156], which clearly shows that the actual interface strongly deviates from the MOS model. Instead, the interface has an additional “dipole” barrier ( $\Delta$ ), which shifts the HOMO level downward by more than 1eV, hence increasing the barrier height by the same amount. The reason for this rather large interface dipole is that the electron density at a metal surface presents a tail that extends from the metal-free surface into vacuum, thus forming a dipole

pointing at the metal bulk [157,158]. Molecules deposited on the metal tend to push back this tail, thus reducing the surface dipole and reducing the work function of the metal.

#### 3.2.4.2 Schottky Contact

In many devices, the contact between a metal and polymer material is rectifying and then becomes a Schottky contact. When current goes through the junction in one direction, there is a minimum potential drop across it, but in the opposite direction there exists a large potential drop [159]. Theoretically, the energy band diagrams can predict the behaviour and characteristic of the contact.

If contacts do behave as Schottky barriers, one would expect the voltage drop at the source to be substantially higher than that at the drain. This is what is indeed observed with a “bad” contact. For “good” contacts, however, a comparable voltage drop is observed at both electrodes. A possible origin of this behavior has recently been suggested. The model assumes that the region immediately adjacent to the electrodes is made of organic material of quality different from that of the rest of the conducting channel and with very low mobility.

It is worth noting that the contact resistance of the top contacts is normally smaller than that of bottom contacts [160]. The asymmetry of the organic-metal contact, depending on whether the organic film is deposited on the metal or the metal on the organic layer, has been studied theoretically and experimentally [161].

## CHAPTER FOUR

### MODELING AND SIMULATION

#### 4.1 Technology Computer Assisted Design

Technology Computer Aided Design, or TCAD [162], is used to describe a computer-aided design and engineering method used in a broad range of modeling and analysis activities. The TCAD process consists of semiconductor device design, fabrication process design, and technology characterization for integrated-circuit (IC) lithographic processes [163]. The essence of this concept is for the successful design of today's devices and circuits because of their increasing complexity and the high cost and delay associated with experimental design iterations. Simulation tools are increasingly integrated into TCAD systems which provide a controlled and repeatable numerical experiment. For these tools to be useful in a practical environment, they must be physically accurate, computationally robust, and usable by users other than the software developers. Depending on the users technical background and needs, different demands on such system will arise.

Simulation of fabrication and operation of the field effect transistor (FET), bipolar, or CMOS structures is routinely conducted in two-dimensional space and is widely used [164]. TCAD software requires an investment both in the development of new capabilities and training in the use of the software. We have used TCAD software to

shorten our device development cycle. Numerical experiments are much faster than physical experiments, provided that the models are accurate. TCAD simulation can also provide a better understanding of the device and a better design and performance improvement by simulating the effects that cannot be measured or visualized, such as leakage paths, locations of depletion regions and a complete description within the device of the parameters of interest. Without the device-to-device variations that occur in the real environment, TCAD software analyzes sensitivities and tradeoffs in a controlled situation, which has allowed a much more robust design to be developed.

#### 4.2 Description of Models

These numerical simulations were typically based on the drift-diffusion (DD) model, which does not depend on the type of the microscopic transport mechanism, and therefore, can also be valid for the case of hopping transport in organic material systems [165]. Regarding the modeling of the electrostatics, most of the work has been based on solving the two-dimensional current continuity equation involving drift and diffusion currents together with Poisson's equation self-consistently.

The electrostatic potential across the device is determined by the doping profile and mobile charges, as directed by the Poisson equation.

$$\epsilon \nabla^2 \psi = -q(p - n + N_D^+ - N_A^-) - \rho_s \quad (4-1)$$

where  $\epsilon$  is the permittivity of the medium,  $\psi$  is the potential,  $q$  is the elementary charge,  $p$  and  $n$  are hole and electron density, respectively,  $N_D^+$  and  $N_A^-$  are ionized donor and acceptor concentrations, respectively, and  $\rho_s$  is the surface charge density. For the concentrations, the corresponding expression for holes density and electrons density in the quasi-equilibrium contact regions in terms of the local Fermi level,



$$p = n_i \exp\left\{\left(\varphi_{Fp} - \varphi\right)/V_T\right\} \quad (4-2)$$

$$n = n_i \exp\left\{\left(\varphi - \varphi_{Fn}\right)/V_T\right\} \quad (4-3)$$

$$n_i = \sqrt{N_V N_C} \exp\left\{-\frac{\varepsilon_g}{2eV_T}\right\} \quad (4-4)$$

The intrinsic density ( $n_i$ ) is connected with the gap energy ( $\varepsilon_g$ ) and  $N_V$  and  $N_C$ .  $V_T = k_B T/e$  is the thermal voltage. The electron and hole continuity equations are:

$$\frac{\partial n}{\partial t} = \frac{1}{q} \bar{\nabla} \cdot J_n - U_n \quad (4-5)$$

$$\frac{\partial p}{\partial t} = -\frac{1}{q} \bar{\nabla} \cdot J_p - U_p \quad (4-6)$$

where  $U_n$  and  $U_p$  are net electron and hole recombination, respectively.  $J_n$  and  $J_p$  are electron and hole current density, respectively. Drift and diffusion current can be calculated as:

$$\bar{J}_n = -qn\mu_n \bar{\nabla} \varphi_{Fn} + qD_n \bar{\nabla} n = qn\mu_n \bar{E}_n + qD_n \bar{\nabla} n \quad (4-7)$$

$$\bar{J}_p = -qp\mu_p \bar{\nabla} \varphi_{Fp} - qD_p \bar{\nabla} p = qp\mu_p \bar{E}_p - qD_p \bar{\nabla} p \quad (4-8)$$

here  $\mu$  is the mobility and  $D$  the diffusivity;  $n$  and  $p$  indicate the electron and hole concentration, respectively. The mobility ( $\mu$ ) correlates with the diffusivity ( $D$ ) by the Einstein relationship based on Boltzmann statistics

$$D_n = \frac{kT}{q} \mu_n \quad (4-9)$$

$$D_p = \frac{kT}{q} \mu_p \quad (4-10)$$

where subscripts  $n$  and  $p$  indicate electron and hole, respectively. Because the PEDOT-PSS is a p-type polymer material, the model mainly focuses on the holes distribution during the simulation process.

#### 4.3 Device Simulation Results

The two-dimensional device structure is developed with the dimensions of the device were chosen to approximate those of the real devices. The Figure 4-1 presents the schematic structure of the developed device.

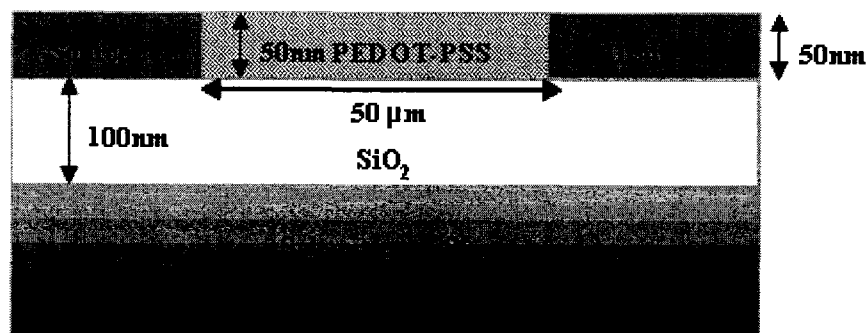


Figure 4-1 Schematic representation of the PEDOT-PSS OFET structure

The material parameters are shown in Table 4-1. Dielectric constant ( $\epsilon$ ) and effective density of states ( $N_V$ ) and ( $N_C$ ) of PEDOT-PSS are from Ref [166] and [167], and the electron affinity (equivalent to the LUMO level) and the energy bandgap are from Ref [168]. Mobility and doping concentration are obtained from the experimental results in Chapter Six. The S/D contacts are gold with a work function of 5.1 eV. The gate contact is  $n^+$ -Si with a work function of 4.2 eV. For the mobility, the experimentally determined value is used, which is  $\mu_p=0.0016\text{cm}^2/\text{Vs}$  at  $V_d=-30\text{V}$ . The simulation input commands can be found in Appendix A.

Table 4-1 Basic material parameters used in simulation

	PEDOT-PSS	Reference
$\epsilon$	3.5	[177]
$N_C, N_V$ ( $\text{cm}^{-3}$ )	$2 \times 10^{21}$	[178]
$N_A$ ( $\text{cm}^{-3}$ )	$1 \times 10^{17}$	[178]
$E_g$ (eV)	1.6	[179]
$\chi$ (eV)	3.6	[179]

Taurus simulator software [169, 170] was used during the simulation process. By solving Poisson's equation, the results of simulation present the energy level diagram of the OFET structure under thermal equilibrium, as shown in Figure 4-2. It is observed that  $E_C$  and  $E_V$  in PEDOT-PSS are equivalent to the LUMO level and the HOMO level, respectively.  $E_F$  is the Fermi level. Being highly doped,  $n^+$ -Si as the gate electrode has a Fermi level close to  $E_C$ . Its electric property is thus similar to a metal. Due to the difference of the work function between  $n^+$ -Si ( $\phi_m$ ) and PEDOT-PSS ( $\phi_s$ ) ( $\phi_m < \phi_s$ ), the Fermi levels align under thermal equilibrium, leading to a slight depletion (band bending down) of the PEDOT-PSS channel near the PEDOT-PSS/SiO<sub>2</sub> interface.

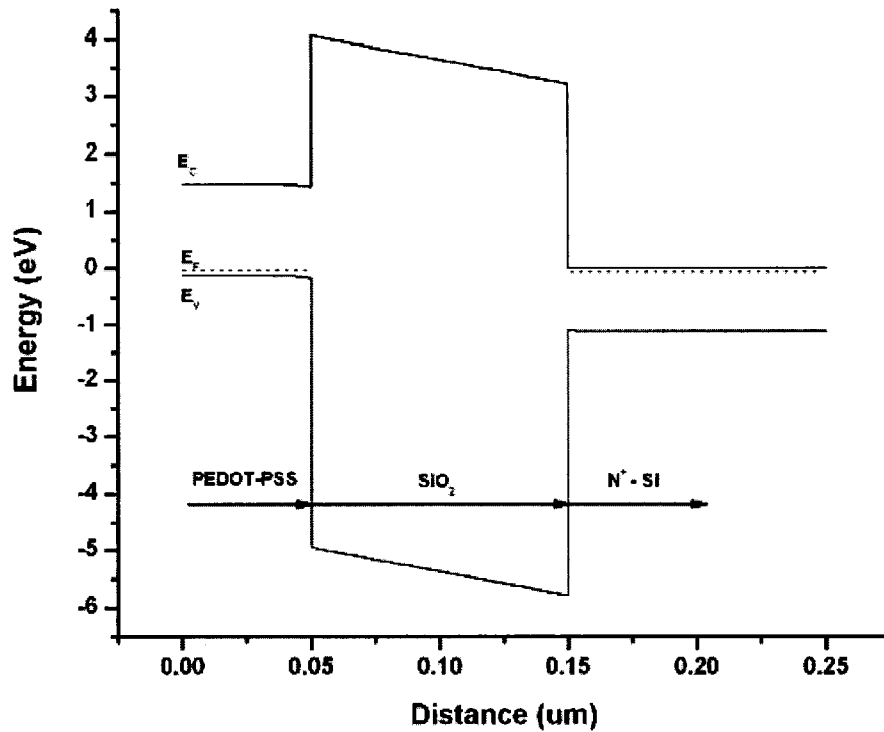


Figure 4-2 Energy level diagram of the OFET ( $n^+$ -Si-SiO<sub>2</sub>-PEDOT-PSS) structure under thermal equilibrium.

Figure 4-3 shows the calculated hole concentration profiles in the PEDOT-PSS layer, which is obtained from a cut-line at the middle of the channel starting from the PEDOT-PSS surface. The gate voltage is -10 V and both the source and drain voltages are 0 V. The background doping profile is also shown. The right y-axis in Figure 4-3 shows a linear scale for the hole concentration. One can see that the charge carriers are predominately located within 2 nm from the PEDOT-PSS/SiO<sub>2</sub> interface, where the carrier concentration reaches its maximum. This reveals the importance of the interface. Therefore, it is important to improve the interface in order to enhance the electrical characteristics of the resulting devices. It is also important to refine the mesh in this critical area, by which one can get accurate simulation results.

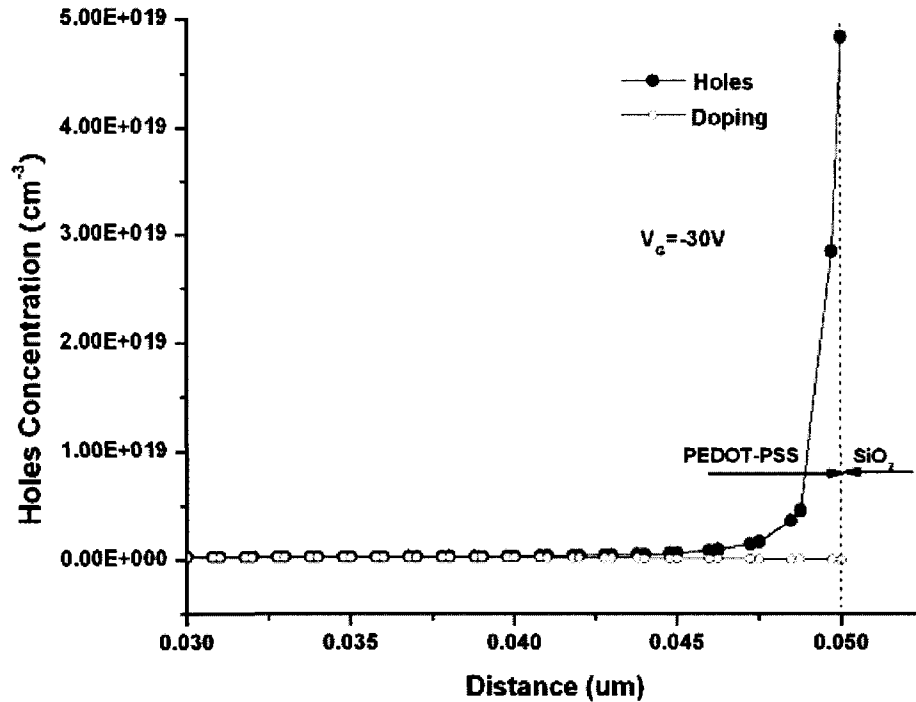


Figure 4-3 Hole concentration profile in the channel along the direction normal to PEDOT-PSS/SiO<sub>2</sub> interface.

The dependencies of the mobilities on concentration and field can be taken into account directly; however, there are other influences, such as, an exponential trap distribution, a Schottky contact or an Ohmic series resistance in a top-contact structure which will also result in significant deviations from Equation (3-2) and (3-3). Therefore, a Drift-Diffusion (DD) model with a constant mobility is preferred. From experimental results, the doping density of  $3 \times 10^{17} \text{ cm}^{-3}$  was estimated, according to the Equation (3-5). The detailed information and the input commands can be found in Appendix A.

Figure 4-4 shows the drain current as a function of drain-source voltage up to -20 V for various gate biases. The shape of the  $I_D$ - $V_D$  characteristics of the OFET is similar to those of field-effect transistors at the gate bias voltages ( $V_G$ ) higher than a threshold voltage ( $V_T$ ). At low drain-source bias ( $V_D \ll V_G$ ), there is a linear (or ohmic) region in

which the drain current is dependent on  $V_D$  and the saturation of  $I_D$  is observed at high drain biases ( $V_D > V_G$ ). The behavior of the OFET based on PEDOT-PSS are presented as Equations (3-2) and (3-3). Figure 4-5 shows the simulation gate transfer characteristics of the OFET based on PEDOT-PSS material. By linearly extrapolating the curve to the  $V_{GS}$  axis, the threshold voltage ( $V_T$ ) can be extracted to be 10 V. In Chapter Six, the comparison between experimental results and simulation results will be presented and the analysis of the resulting experimental data will demonstrate the advantage of combining the analytical estimates and the numerical simulation.

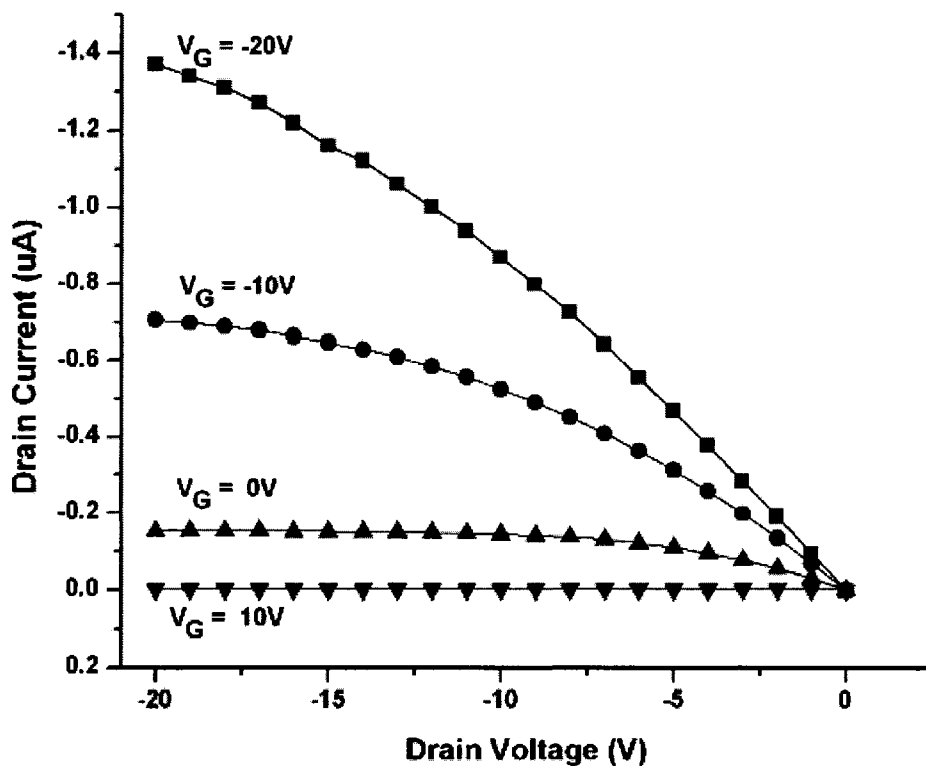


Figure 4-4 Simulation of output characteristics of OFETs based on PEDOT-PSS

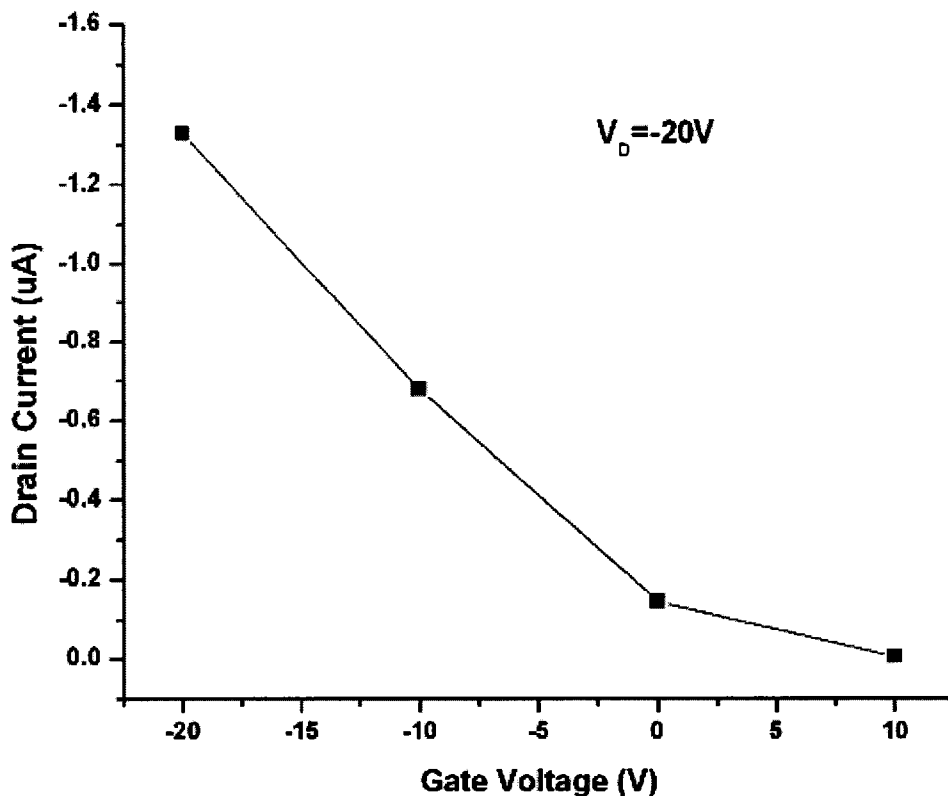


Figure 4-5 Simulation of transfer characteristics of OFET based on PEDOT-PSS

#### 4.4 Summary

Modeling and simulation are important for achieving an adequate understanding of the operation of the device. In this work, numerical simulation is carried out and the energy band diagram, hole distribution and electrical characteristics of the devices were produced by the Taurus simulator. Future more, numerical simulations realize the self contained task to clarify special effects as the possible occurrence of inversion and the influence of the type of the source/drain contacts on device mobility. The advantage of the simulations lies in the possibility to illuminate the mode of operation by inspecting the internal distributions of concentrations and fields and by relating them to the peculiarities of the device current characteristics.

## CHAPTER FIVE

### SOIL MOISTURE MONITORING SENSOR

#### BASED ON PEDOT-PSS RESISTOR

##### 5.1 Introduction

Recently, there has been a rapid growth in the development of microsensors for applications for relative humidity testing. For many years, “the influence of humidity has become the main concern in moisture sensitive areas, such as high voltage engineering systems, food processing, textile manufacturing, storage areas, computer rooms, hospitals, museums, libraries, and geological soil sample studies” [171]. Monitoring moisture content in soil has become a pre-requisite for a variety of processes, such as agriculture, areas prone to landslides, and laboratory testing. The application of microsensors in geologic and geotechnical engineering studies has emerged only recently owing to the complex boundary conditions that must be overcome in granular materials such as three phase solid-water-air void structures and heterogeneous particle distributions. Recent research in this area has focused on the measurement of suction and humidity in soils [172]. Measurement of moisture content has been guided by the agricultural industry resulting in improved time domain reflectometry devices (TDR) whose



dimensions are far too large for capturing microscale behavior. Determination of moisture and moisture migration during environmental and physical loading of soils are critical for model development. Direct observation at the microscale of these phenomena is difficult with the current technology, which requires a need for development of microsensors to capture this moisture response.

In Chapter One, we have introduced that organic polymers have been widely used for humidity sensor applications due to their reasonable characteristics. These humidity sensors detect either the absolute value of a physical quantity or a change in the value of electrical quantity and convert the measurement into useful input signals for an indicating or recording instrument. During the early stages of humidity sensor development, commercially available polymer electrolytes were directly used as the active sensing material. The use of PEDOT-PSS polymer material for humidity sensing applications using transistor phenomena was first reported by Nilsson, et al [173]. Polyamide fibers coated with PEDOT-PSS polymer material were also studied for humidity and temperature sensor applications [174]. In this paper, the use of PEDOT-PSS polymer material in the development of new microsensors for detecting gravimetric water content in soil samples will be demonstrated. A change in the resistance of the polymer film is monitored when it is exposed to different soil samples to compute the gravimetric water content present in the samples. When compared to sensors developed based on a transistor or capacitive structure, the sensors based on a resistive structure show the simplest structural design without complex fabrication processes. The simplicity and size of the developed sensor devices, as compared to other reported devices, enabled the measurement of the gravimetric water content present in the soil samples.

## 5.2 Experimental Details

PEDOT-PSS used in the following experiments was purchased from Baytron P. Bayer Corporation. The process steps involved in the fabrication of the moisture sensor are shown in Figure 5-1.

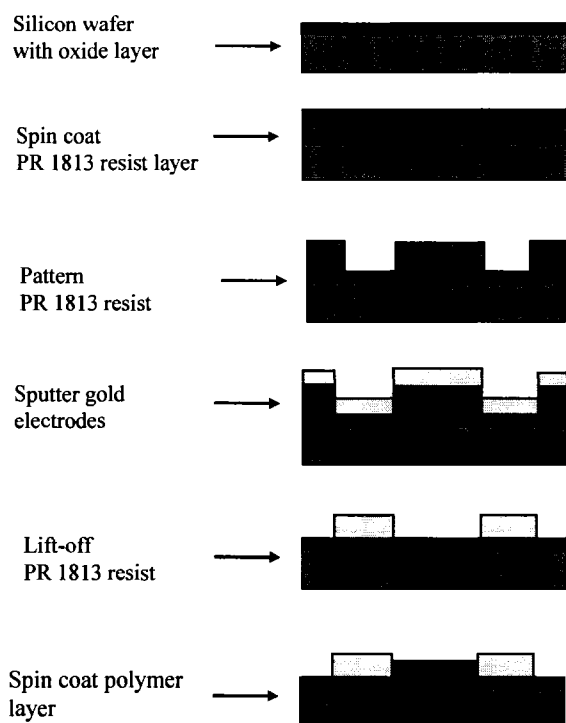


Figure 5-1 Schematic illustration of the fabrication process steps for the sensors

First, a mask was designed for fabricating the electrode patterns with different resistor lengths using L-Edit layout software. L-Edit layout software is a customized mask editor, which is a part of a complete integrated circuit design tool offered by Tanner Research Inc. A [100] silicon wafer with a 100 nm thick oxide layer was used as the base substrate for the fabrication of the sensor devices. The pattern transfer was performed by UV photolithographic process using commercially available PR 1813 positive photoresist (Sigma-Aldrich). Spin coating technique was used to fabricate the PEDOT-PSS film. A

typical spin coating process involves depositing a small amount of a fluid onto the center of a substrate, and then spinning the substrate at high speed depending on viscosity of the fluid. Centrifugal acceleration will cause most of the fluid to spread off the edge of the substrate, leaving a thin film of fluid on the surface. Final film thickness and other properties depend upon the fluid viscosity, drying rate, and surface tension used in the spin coating process. The individual sensor devices were then wire bonded to the external circuit for electrical measurements. The final microsensor device after wire bonding and packaging is shown in Figure 5-2. The total dimensions of the packaged sensor are 1.5 x 0.5 x 0.5 cm. A packaging cap from Sensirion Inc. was used to package the sensor presented. The filter in the cap is selective and will avoid the exposure of the sensor to any other environmental condition or soil granules, except humidity. The electrical characteristics of the sensor devices were first tested as a function of relative humidity (RH %). In order to study the incorporation of water in the PEDOT-PSS polymer material, attenuated total reflection-infrared (ATR-IR) was performed using a Thermo Nicolet Nexus 470 fourier transform infrared radiometer (FTIR) equipped with ZnSe ATR crystal. The FTIR spectroscopy provides a powerful tool to obtain both the chemical and spatial information of the sensing film [174-179].

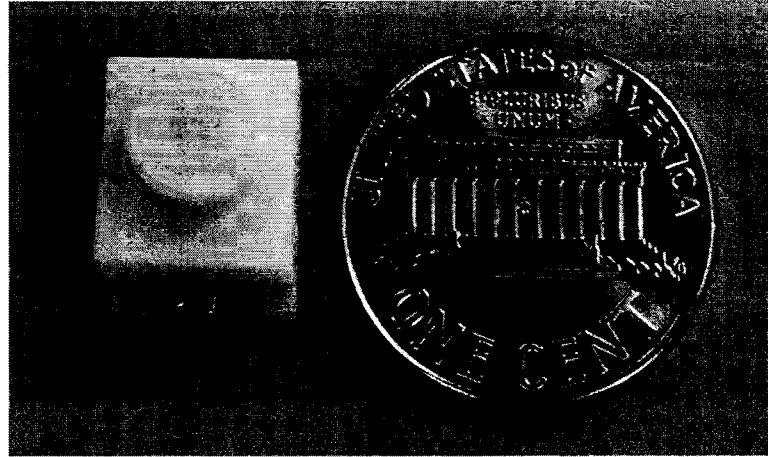


Figure 5-2 Final packaged microsensor device to measure gravimetric water content in soil samples.

After studying the device performance, the actual soil samples (Buckshot Clay, CH) containing different levels of gravimetric water content were investigated. The setup for testing soil sample consists of a glove box, as shown in Figure 5-3.

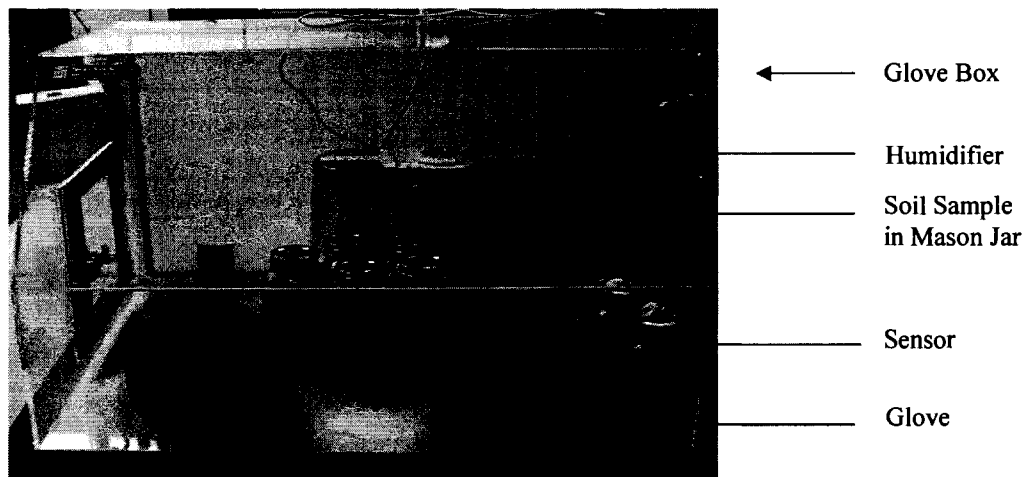


Figure 5-3 The soil sample testing setup system.

The soil samples were prepared in air tight mason jars and were placed inside the glove box to measure the gravimetric water content in the samples. The humidity inside

the glove box was controlled using a commercially available humidifier and nitrogen supply. The sensor is moved from one sample to another sample inside the glove box, and the change in the electrical characteristics of the sensor was monitored using a Keithley probe station.

### 5.3 Results and Discussions

The thickness of the spin-coated PEDOT-PSS film was measured to be 50 nm using a Tencor profilometer. The surface roughness profile of the film was measured using atomic force microscopy (AFM), as shown in Figure 5-4. It can be observed that the PEDOT-PSS film is relatively smooth with some rough peaks, probably due to the formation of PEDOT-PSS nanoclusters on the silicon substrate.

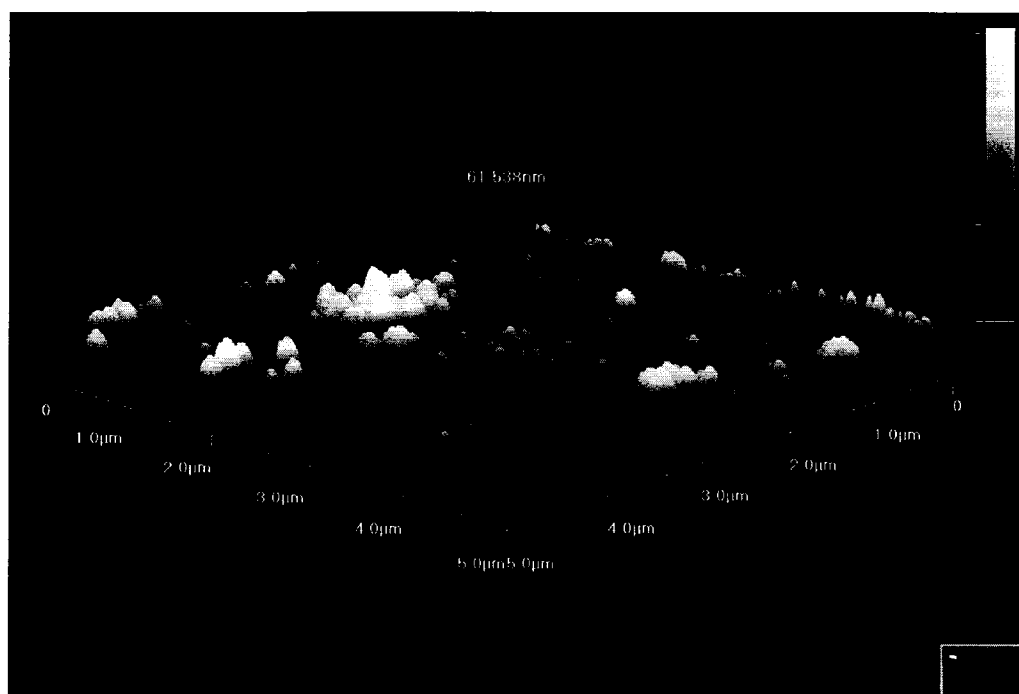


Figure 5-4 PEDOT-PSS surface measured using AFM.

The ATR-IR experiments were done to investigate the increase in absorption of water molecules in the PEDOT-PSS film when exposed to an increased moisture level (70% RH) relative to the ambient condition (45% RH). These experiments can provide evidence for the response of the PEDOT-PSS film (absorption of water molecules) in the moisture environment. The ATR-IR resultant curve for the spectrum between  $650\text{ cm}^{-1}$  and  $4000\text{ cm}^{-1}$  of the PEDOT-PSS film before (45% RH) and after exposure (70% RH) to moisture content is shown in Figure 5-5. The broader band between  $3000\text{ cm}^{-1}$  and  $3700\text{ cm}^{-1}$  corresponds to OH stretching and aromatic CH stretching between  $2850\text{ cm}^{-1}$  and  $2980\text{ cm}^{-1}$ . The unexposed film (45% RH) has a flattened peak centered at  $3420\text{ cm}^{-1}$ , whereas the exposed (70% RH) PEDOT-PSS film has a relatively sharp intense peak at  $3420\text{ cm}^{-1}$  in the spectrum indicating the absorption of OH molecules in the film. The small peaks at  $1750\text{ cm}^{-1}$  and  $1500\text{ cm}^{-1}$  in the spectrum appeared when the film was exposed to moisture content. These peaks indicate that the PEDOT-PSS molecular chain has been altered due to the presence of OH molecules.

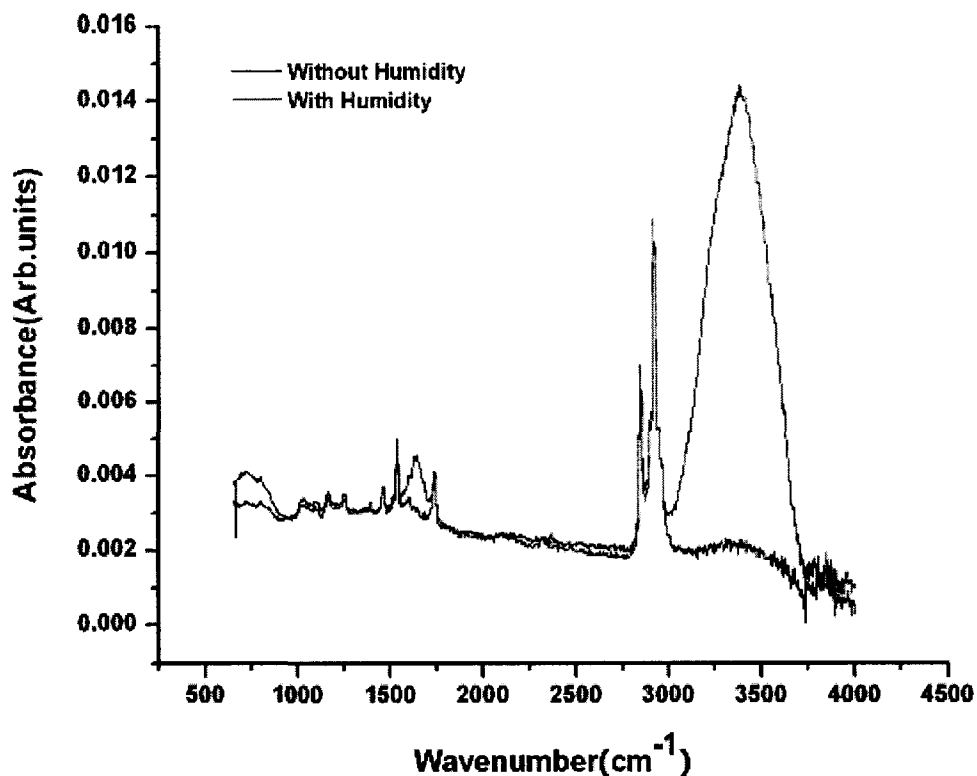


Figure 5-5 ATR-IR spectrum of PEDOT-PSS film without and with exposure to moisture content.

An analysis of the change in resistance, repeatability, and sensitivity of the PEDOT-PSS was done to study the sensor device performance. The results show that the resistance of the PEDOT-PSS polymer film increased when exposed to an increasing level of relative humidity. The output signal of the sensor device, in terms of percentage change in resistance with respect to change in relative humidity, is shown in Figure 5-6. The total percentage change in resistance of the PEDOT-PSS film was observed to be 45% for a 50 to 90 % change in relative humidity.

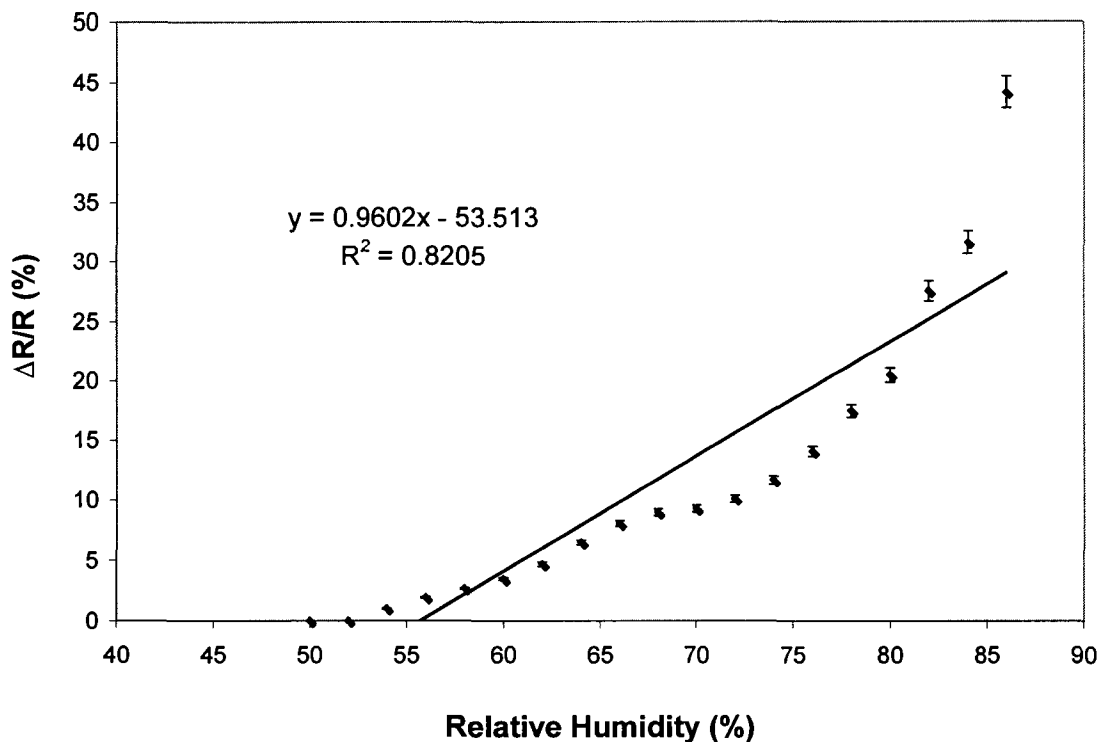


Figure 5-6 The change in sheet resistance of PEDOT-PSS moisture sensor vs. change in relative humidity

The humidity sensing mechanism can be explained on the basis of the dipole molecular effect on the polar polymers, such as PEDOT-PSS [181]. Experimental results obtained on molecularly doped polymers [181-183] indicate that the presence of dipoles initiate a decrease in effective carrier motilities. There is considerable evidence that the width of the density of states (DOS) can be influenced by the dipole moment of the dopant molecule. The width of the DOS increases with increasing dipole moment of the dopant molecule. An increase in the width of the DOS, with increasing inter-site distance, leads to an increase in charge carrier hopping distance which, in turn, decreases the conductivity of the polymer material. Since, the water molecules have larger dipole momentum they contribute to the decrease in the effective conductivity of the PEDOT-



PSS polymer material in the presence of humidity. On the other hand, PEDOT-PSS conductivity also depends on its component ratio (the ratio of PEDOT and PSS) [185]. Low conductivity indicated the presence of excess PSS in the film. In the polymer molecular structure, a single PSS chain interacts electrostatically over its length with many shorter PEDOT chains and the distance between adjacent PEDOT chains is small, and this favors the hopping of charges between PEDOT chains. But the higher density of insulating PSS material leads to increased hopping distance for the charge carriers and a resultant decrease in the electrical conductivity.

The developed moisture sensor devices were used to test the soil (Buckshot clay, CH) samples with different levels of gravimetric water content (15% to 35%). The electrical measurements were taken by imbedded microsensors in the soil samples. The average change in the resistance value of the sensor device, with respect to change in gravimetric water content measured at different time intervals, are shown in Figure 5-7. Measuring at different time intervals helped in determining the optimum time that the sensor takes to give a stabilized reading when placed in soil samples. The intent of the sensors is to measure the air saturation present within the interstitial pore spaces in the soil. No moisture movement is present in the compacted clay samples as no moisture is being allowed to enter or leave the sample during testing. The effect of internal moisture movement is minimized by allowing the samples sufficient time to equilibrate. Therefore, the effects of permeability resulting from differential grain size (in the same soil sample or different kinds of soil samples) does not influence the speed at which sensor data is taken, as moisture is in equilibrium throughout the specimen during the experiments. After the equilibration, any changes in moisture content due to environmental effects

such as drying or wetting, occur slowly with respect to the sensor response time. This is true even for very permeable soils, i.e. sands. Therefore, following an initial equilibrium state, the sensors will have sufficient time to react to this changing behavior independent of grain size.

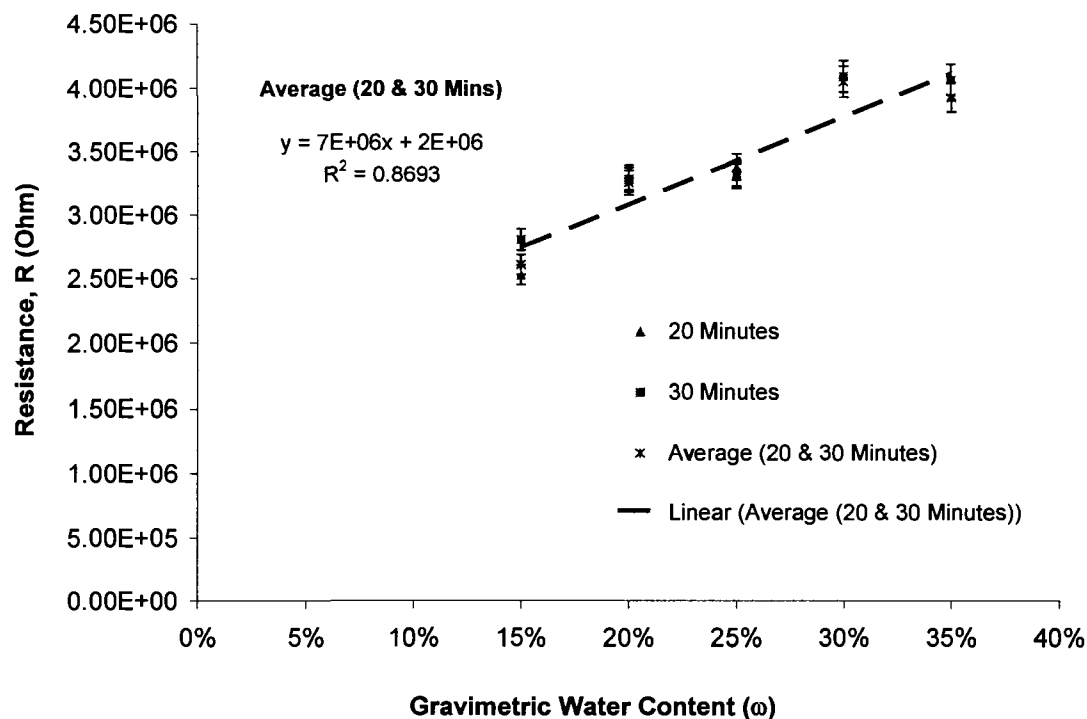


Figure 5-7 The change in sheet resistance of PEDOT-PSS moisture sensor vs. gravimetric water content in soil samples.

It can be observed from the plots in Figure 5-7 that the resistance values measured when the sensor device was placed in the soil sample for 20 and 30 minutes time intervals were mostly comparable. This indicates that any time between 20 to 30 minutes is adequate for the sensor to give a stabilized reading in any particular gravimetric water content level in soil samples. Hence, the resistance values of the sensor at 20 minutes and 30 minutes are averaged and plotted in Figure 5-7. The change in the output resistance of

the sensor device was observed to be from 2.5 M to 4.0 M ohm when exposed to soil samples (Buckshot clay, CH) with 15 – 35 % change in gravimetric water content. The results obtained show that the sensor devices, thus fabricated, can be applied to measure gravimetric water content in the soil samples which, therefore, can be used in geologic and geotechnical engineering.

Experiments were also conducted to see the effect of the sensor with and without using the Sensirion packaging cap. It was observed that when the sensor is unpackaged (i.e. not covered by the cap) and placed above the soil sample instead of imbedding it in the soil sample, the slope of the sensor response increases compared to the sensor which is packaged and embedded in the soil sample, as shown in Figure 5-8. From these results, it can be concluded that there is obviously some effect on the sensor due to the environment when the sensors are placed above the soil sample. More accurate readings can be generated by imbedding the packaged microsensors in the soil samples.

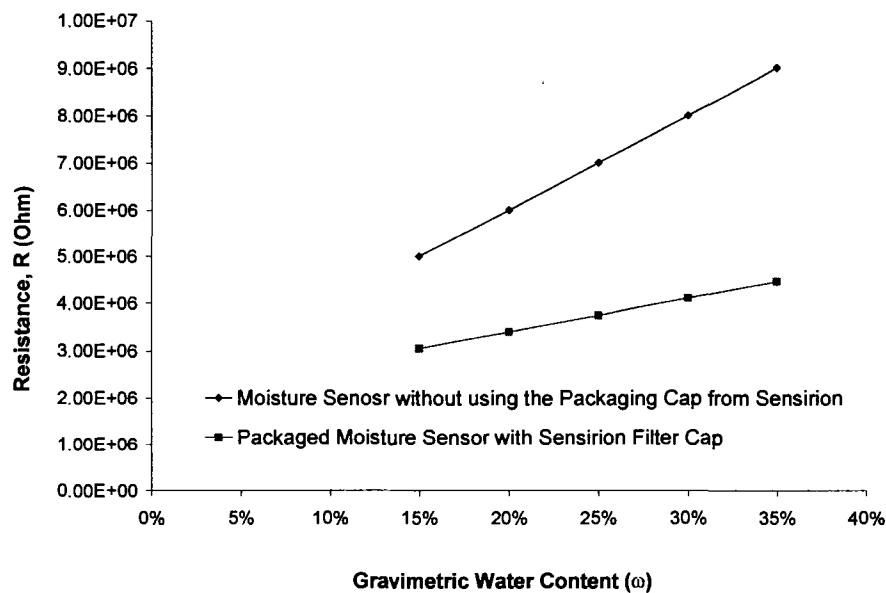


Figure 5-8 Resistance versus water content in CH soil samples measured using unpackaged and packaged sensor device.

In order to check the repeatability of the microsensors, experiments were performed to compare two different measurements performed at two different time period and also to compare the response of two different microsensors. As shown in Figure 5-9 and Figure 5-10, it can be observed that there is some offset from one device to the other or from one measurement to the other as in the case of other humidity sensors. There was some hysteresis (1%) observed during the experiments conducted using soil samples. However, this offset can be minimized by normalizing the results obtained by taking the value of the microsensor at 15% soil sample as the base line.

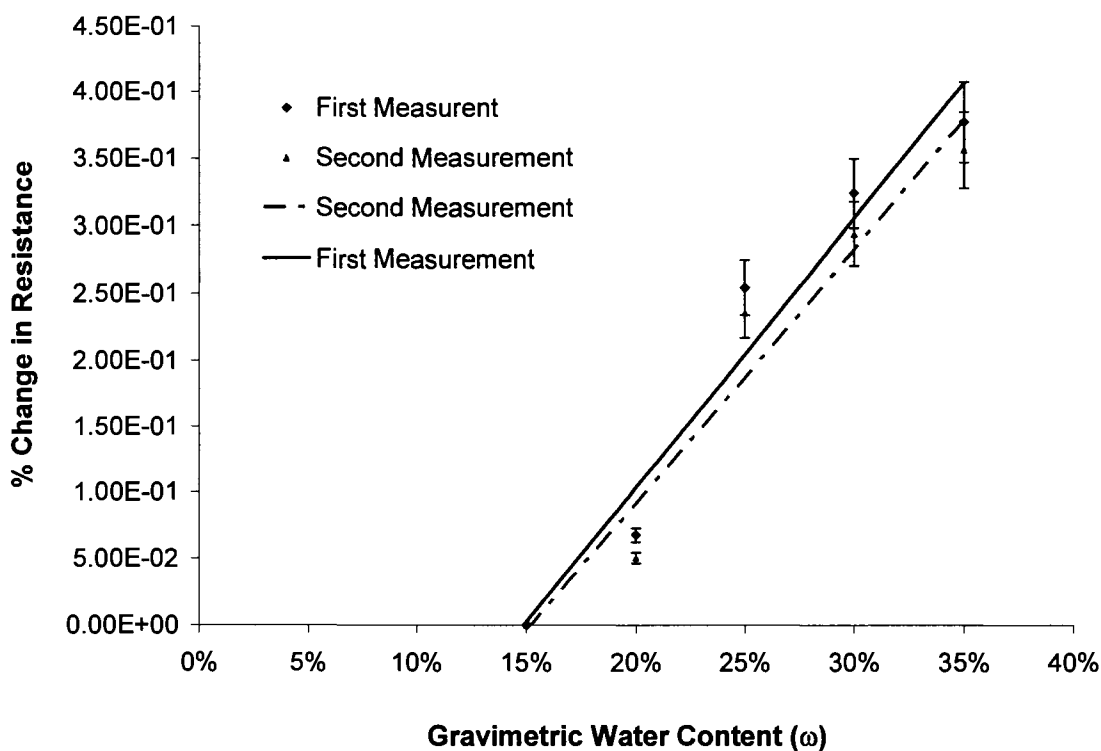


Figure 5-9 Percentage change in resistance value of the packaged sensor device for two different measurements to the change in water content of the CH soil samples.

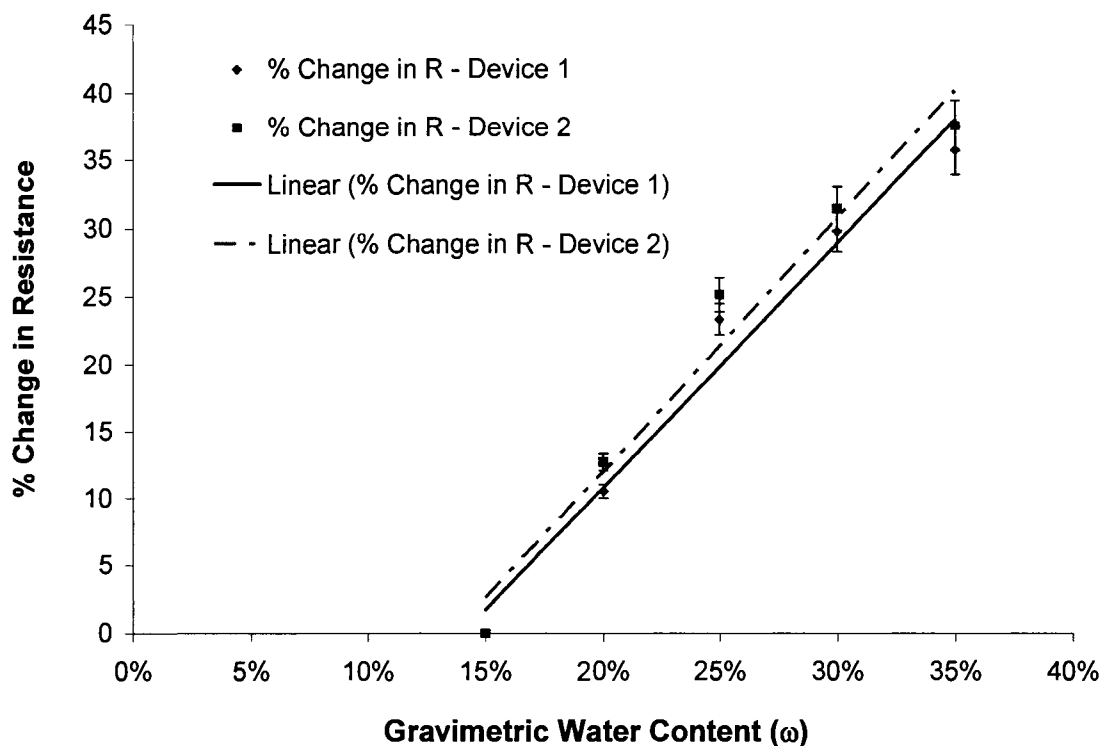


Figure 5-10 Percentage change in resistance value of the two different packaged microsensors to the change in water content of the CH soil samples.

#### 5.4 Conclusions

A moisture sensor based on poly(3,4-ethylenedioxythiophene-poly(styrene-sulfonate) (PEDOT-PSS) conductive polymer was successfully developed and presented in this paper. The sensors showed promising performance in terms of response time, sensitivity and repeatability. The PEDOT-PSS polymer sensors thus developed were successfully used to test the gravimetric water content in the soil samples. The change in the output resistance of the sensor device was observed to be from 2.5 M to 4.0 M ohm when exposed to soil samples with 15 – 35 % change in gravimetric water content. At present, it is intent that these sensors will need to be calibrated for a given soil for the purposes of research. Once a family of calibration curves has been developed for a range

of grain size distributions, then any soil of similar grain size could adopt a curve to approximate moisture content. The results obtained are promising for further development of the given sensors and their application as miniaturized and cost effective alternatives to commercially available sensors for geological and geotechnical studies.

## CHAPTER SIX

### FIELD EFFECT TRANSISTOR BASED

### ON PEDOT-PSS

#### 6.1 Introduction

It is known that semiconducting polymers provide reasonable properties. Since then, compared with the OFETs made of vacuum deposited small molecules, polymer FETs normally have significantly lower field effect mobility, thus reducing the possibility to use them for practical applications, such as drive circuits for organic displays. As previously introduced, the conductivity of conducting polymer, PEDOT-PSS, can be affected by an electric field. In an all-polymer field effect transistor (FET), some devices with doped conducting polymers as an active channel material have been reported [185]. Unlike the conventional organic field effect transistor (OFETs), such as, pentacene, thiophene oligomer, or undoped conjugated polymers, our devices show some promising features: (1) a simple structure configuration, easy to fabricate and low cost; (2) the source, channel, and drain are continuous without boundaries; (3) easy control of channel width. This OFET is a p-type device and operates in the accumulation mode by application of a negative gate voltage. A similar response was observed for the devices using poly(3-hexylthiophene) (P3HT) [186] and poly(p-phenylene vinylene)s (PPV) [187].

In their saturation mode of operation, polymer and organic based FETs obey a quadratic current-voltage (I-V) relationship similar to conventional FETs. Previously, some work based on flexible and transparent all-polymer FETs fabricated on one substrate has been reported [188]. It was observed that the device operated at lower voltages both in the depletion and enhancement modes in response to positive and negative gate voltages, respectively. However, the detailed mechanism is unclear since the application of conventional field effect theory yields surprisingly large carrier mobility ( $\mu$ ). Moreover, the device is unstable where the threshold voltage shifts and response becomes slower with time, which distinguishes the mechanism from conventional field effect.

The OFET devices resemble conventional thin film transistors and focuses on top-contact structures in which the source and drain contacts are defined on the gate insulator. The organic active layer is deposited and covers the source and drain contacts as well as filling the gap between them, where the conducting channel forms. Consequently, the charge carriers forming the conducting channel are injected from the contacts. In order to improve the devices stability, protective materials have been used to protect the devices from degradation.

## 6.2 Device Fabrication

A conducting polymer solution was prepared by diluting 1 mL of 1.3 wt.% PEDOT-PSS (from Sigma-Aldrich Corporation) in distilled water, to a final volume of 5 mL. A [100] silicon wafer with a 0.1  $\mu$ m thick silicon dioxide layer was used as the substrate for the fabrication of the sensor devices and also served as the gate region of the OFETs. First, a mask was designed using the L-Edit layout software for fabricating the source and drain gold electrode pair patterns, in between which the device channel region



is also defined. The pattern transfer was performed by the UV photolithographic process using the commercially available PR 1813 positive photoresist (Sigma-Aldrich).

Prior to the spin-coating of PEDOT-PSS, the substrate was subjected to O<sub>2</sub> plasma for 60 s to hydrophobize and clean the photoresist residue from the channel region of the patterned surface. After spin-coating PEDOT-PSS, the samples were annealed for 2 minutes at 75°C in air to improve the polymer film morphology and firmness. Next, for the protection of device, poly(4-vinylphenol) (PVP,  $M_w = 20000$ , Aldrich Inc.) or cellulose acetate solution (2.5% (w/v) of cellulose acetate in Tetrahydrofuran (THF) (60%) and acetone (40%) solution) was coated on different devices, respectively, by spin-coating.

### 6.3 Results and Discussion

The  $I_D$ - $V_D$  current characteristics of an OFET based on PEDOT-PSS are shown in Figure 6-1 (Symbol line-experimental results). This device behaves as a typical p-type OFET and the drain current  $I_D$  is controlled by the gate voltage  $V_{GS}$ . The negative gate voltage enhances the conduction of the channel, due to the formation of hole accumulation, while a positive gate voltage reduces the conduction of the channel. When a positive gate voltage is applied to the device, the device will be turned off. Figure 6-1 shows that  $I_D$  increases linearly with  $V_{DS}$  when  $V_{GS}$  is small. As  $V_{GS}$  increases to be more negative,  $I_D$  rises more steeply at the small  $V_{DS}$  and displays a tendency to saturate at relatively high  $V_{DS}$ .

According to the description in Chapter Three, the  $I_D$ - $V_D$  shows two working regions: a linear region and a saturation region. Drain current values in the saturation region and the linear region are obtained from Equations (3-2) and (3-3), respectively.

Figure 6-2 shows the measured gate transfer characteristics of the OFET based on PEDOT-PSS material. By linearly extrapolating the curve to the  $V_{GS}$  axis, the threshold voltage  $V_{TH}$  can be extracted to be 20 V. It indicates that the OFET is a normally on transistor, which could be due to the unintentional doping of PEDOT-PSS probably by oxygen and moisture in the area [189]. In the saturation region, a threshold voltage and mobility of 10 V and  $1.66e-3 \text{ cm}^2/\text{Vs}$  for the device can be deduced from Equation (3-7). The device channel (PEDOT-PSS) thickness is around 50nm which was measured by KLA Tencor Profilometer. The conductivity of the spin-coated film produced from the PEDOT-PSS solution, was measured to be  $2e-4 \text{ S/cm}$ , according to Equation (3-5).

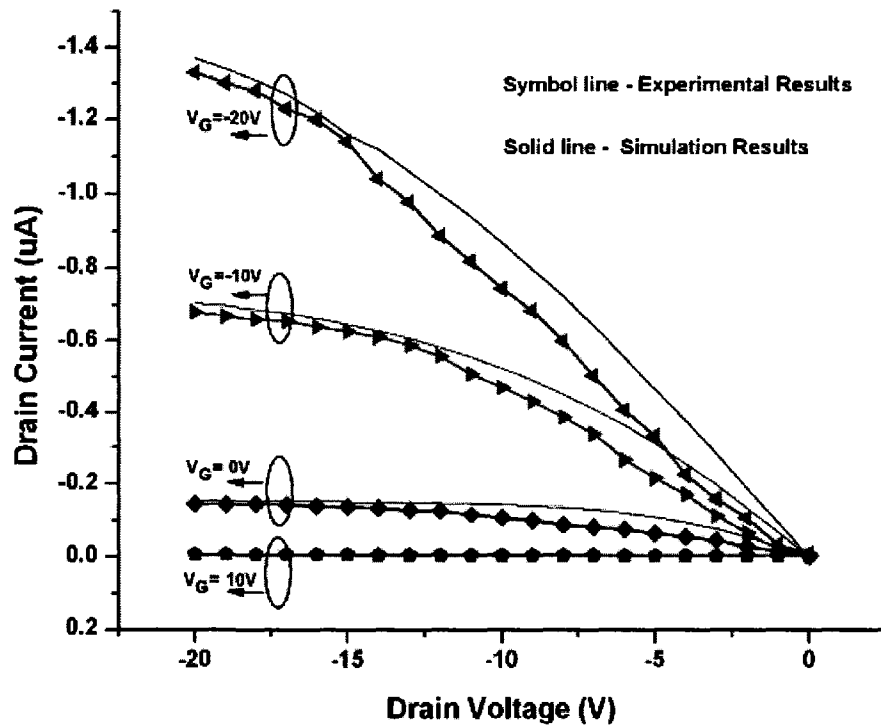


Figure 6-1 The comparison between experimental and simulation output characteristics of OFETs based on PEDOT-PSS

Figure 6-1 and Figure 6-2 also show the simulation results compared with the experimental data. A discrepancy between the simulation and experimental results is

observed. It can be seen that all calculated values are higher than the experimental values. This may not indicate an invalid assumption for the mobility and doping level. And the contact effect shows significant function during the real device measurement process. For the experimental device, the regions adjacent to the vertical contact sides are not filled with material that is the same as the rest of the PEDOT-PSS film. Therefore, the deposition along the edges of the contacts contributes to a structurally disordered material with very low mobility. However, in the simulation discussed here these regions are regarded as bulk material which has a constant carrier mobility. Continuing with the above simulation, the contact resistance in the model should be considered due to the significant effect on the electrical characteristics of the devices, as described in Chapter Three. A considerable voltage drop could be due to the contact resistance, resulting in the effective channel voltage being significantly lower than the total drain voltage [170].

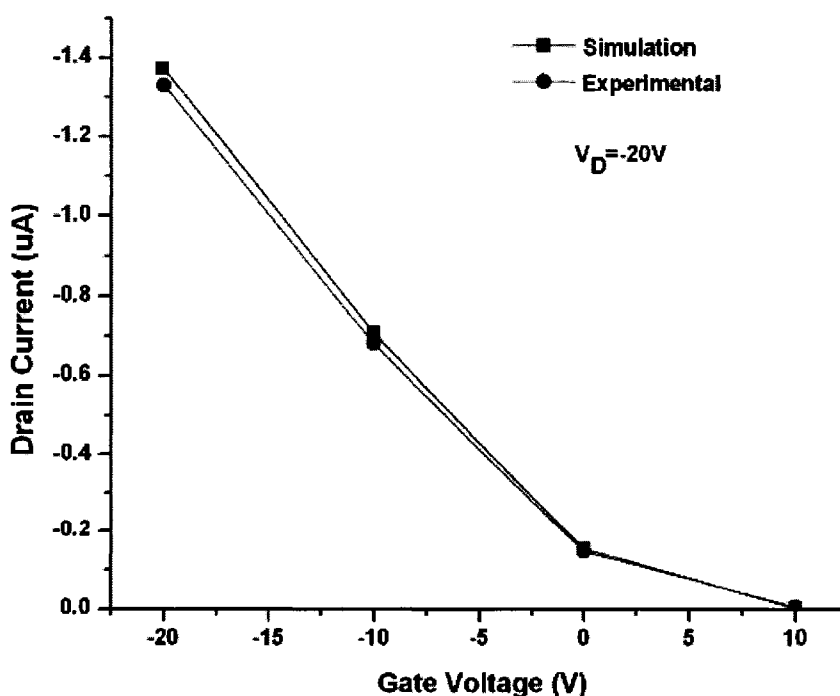


Figure 6-2 The comparison between simulation and experimental results for the transfer characteristics of OFET based on PEDOT-PSS

As described in Chapter 2, PEDOT-PSS is a sensitive material, thus, the degradation of the device occurs due to the polymer material used as the active channel. In order to protect the device from degradation, PVP and cellulose acetate are deposited on the device substrate to prevent the reaction between active layers and water and oxygen. The drain current decreased due to the device degradation in three days. After deposition of PVP and cellulose acetate on the device surface, the changes in drain current were negligible after three days when compared with the device without a protective layer shown in Figure 6-3 and threshold voltages are around +10V which is almost no change.

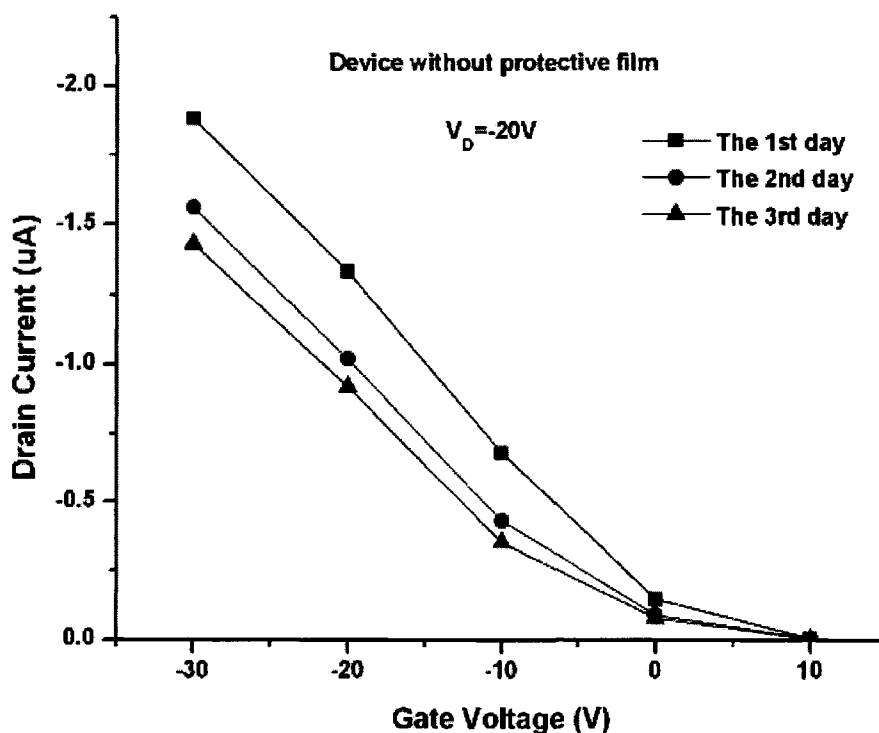


Figure 6-3 The comparison of the transfer characteristics of OFET based on PEDOT-PSS without a protective layer over three days

As shown in Figure 6-4 and 6-5, the device with cellulose acetate protective film presents negligible degradation over three days compared with the PVP as the protective

film. Another reason that affects the device performance is the membrane reaction to the various membrane damaging conditions, such as free chlorine, free oxygen, bacteria and pH level [191].

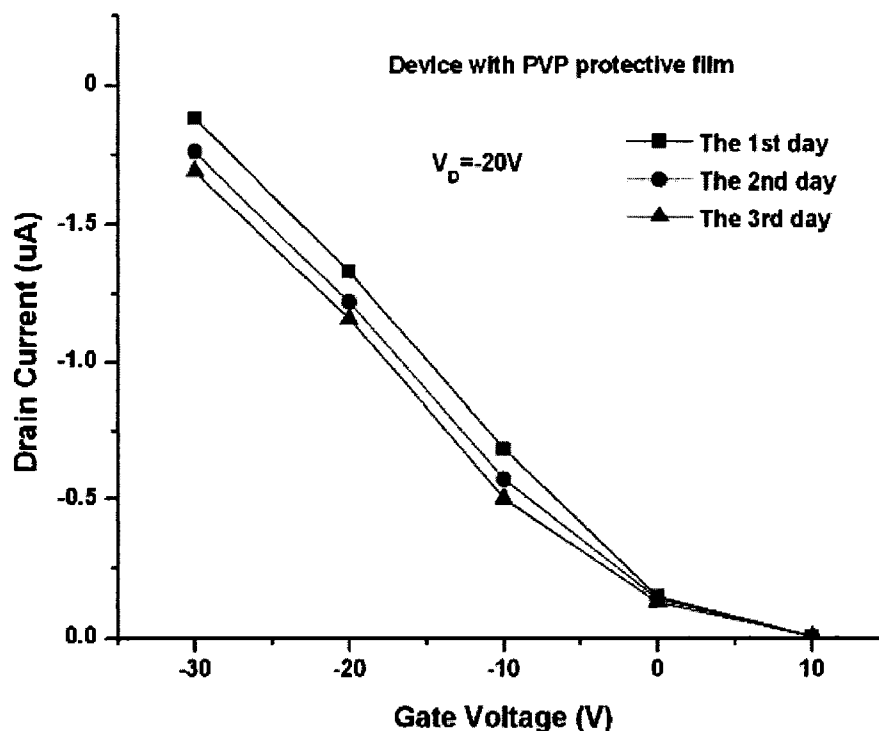


Figure 6-4 The comparison of the transfer characteristics of OFET based on PEDOT-PSS with a PVP protective layer over three days

Cellulose acetate membranes are advantageous for water desalination, despite their limits. Apart from their acceptable performance figures with respect to flux and selectivity, their main advantage is that they are highly chlorine resistant [190]. For oxygen, cellulose acetate is more resistant than PVP. According to the above description and the comparison between cellulose acetate and PVP, cellulose acetate is the more reasonable choice for use as the protective membrane for the glucose sensor devices which are discussed in Chapter Seven.

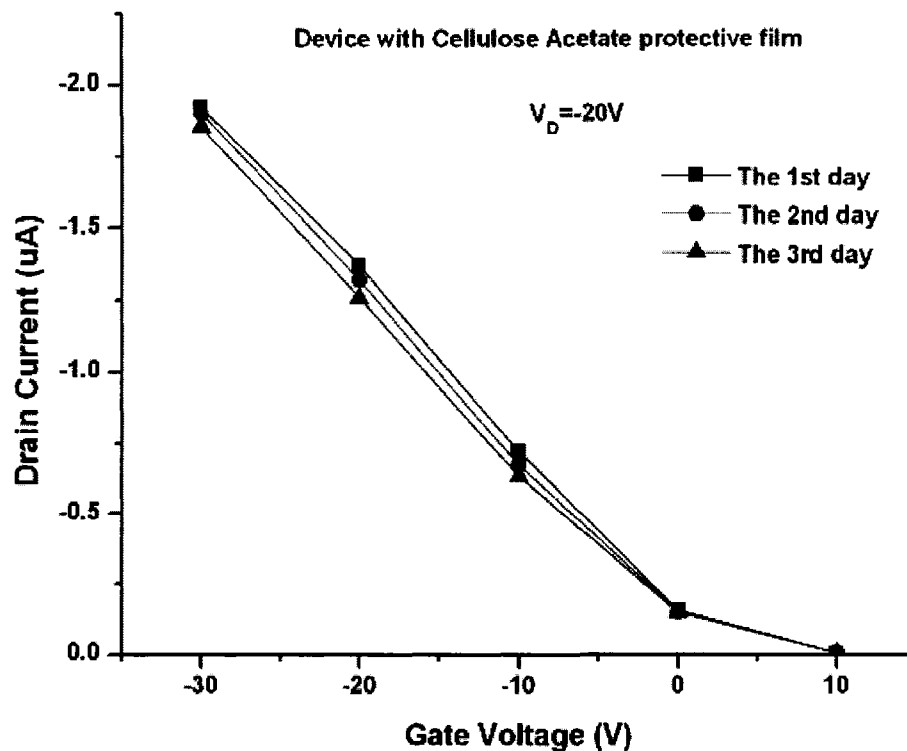


Figure 6-5 The comparison of the transfer characteristics of OFET based on PEDOT-PSS with a cellulose acetate protective layer over three days

#### 6.4 Summary

In conclusion, OFETs with the simplified structure have been fabricated based on PEDOT-PSS as the channel sensing material using easy and low cost spin-coating fabrication process. The fabricated OFETs were characterized in the atmosphere at room temperature, with the field-effect mobility being  $1.66e-3 \text{ cm}^2/Vs$  and the threshold voltage is 10V. The comparison between simulation and experimental results was presented. Due to the nonuniform film structure of the PEDOT-PSS material, there is a discrepancy between simulation and experimental results. Also, the performance of OFETs is related to the PEDOT-PSS degradation. PVP and cellulose acetate have proven to be promising protective layers against degradation for the OFET devices and,

furthermore, cellulose acetate will be used as the membrane for the developed glucose sensor based on PEDOT-PSS.

## CHAPTER SEVEN

### GLUCOSE SENSOR BASED ON PEDOT-PSS FIELD EFFECT TRANSISTOR

#### 7.1 Introduction

In recent years, various types of biosensors, some of which are already in practical use, have been developed [191-198]. Such sensors have been used for different applications, including health care, food and environmental monitoring. Organic thin film transistors (OTFT) and field effect transistors (OFET) present much promise for chemical and biological sensing applications [199-203], and biosensors based on ion-sensitive OFETs [199] have been developed. OFETs have a number of advantages over other types of biosensors. For example, the organic sensing materials can be fabricated into sensor devices using low-temperature processes and low-cost substrates. Moreover, “as OFETs are based on organic semiconductors, the molecular structure and morphology of these materials can be more easily tailored to enhance the sensitivity and selectivity of the resulting biosensors” [200].

In recent years, conducting polymer materials, such as polypyrrole (PPy) and polyaniline, have emerged as potential candidates for biosensor applications [204-205].



Researchers have used these polymers and their composites in OFETs as the charge-transfer reaction layer between an enzyme and electrode, via a ramified conducting polymer matrix network [201-203]. Traditional GO<sub>x</sub>-based biosensors, which rely on anodic peroxide detection, use H<sub>2</sub>O<sub>2</sub> permselective membrane. However, conducting polymer-based glucose sensors use a GO<sub>x</sub> membrane and are capable of precise and fast measurement, with sensing range extending up to 30 mM, as compared to that of traditional glucose sensors (~2 mM) [206].

Recently, there has been an increased interest in the application of PEDOT-PSS as a suitable matrix system for enzyme entrapment and charge-transfer media in glucose sensors. PEDOT-PSS also displays excellent electrochemical stability, reliability, and interesting redox properties, as compared to that of PPy [207-209]. It can be switched to a different oxidation state and conductivity by changing the applied potential or pH. For OFETs based on PEDOT-PSS, the applied gate voltage allows this material to switch between different redox states [210]. Within a potential range, the redox states can affect enzyme interactions with conducting polymers [211]. Therefore, GO<sub>x</sub> enzyme can interact directly with the conducting polymer (PEDOT-PSS) to form a biosensor.

As a continuation of our work on p-type conducting polymers (PEDOT-PSS) for a soil moisture sensing application [212], an OFET-based glucose sensor, with PEDOT-PSS and GO<sub>x</sub> as the channel materials to detect different levels of glucose concentration, is presented in this paper. The mechanism of operation of this biosensor device is fundamentally different from that of traditional potentiometric and amperometric sensors, where the conducting polymer is used as an electrode. The fabrication steps of the present glucose sensor are also simpler. Moreover, the glucose sensor presented has displayed a

reasonable level of sensitivity, repeatability, and stability. The evaluated range of glucose detection shows that the developed biosensor can be used to detect glucose concentration between normal and diabetic patients.

## 7.2 Experiment Details

A conducting polymer solution was prepared by diluting 1 mL of 1.3 wt.% PEDOT-PSS (from Sigma-Aldrich Corporation) in distilled water, to a final volume of 5 mL. GOx solution was prepared by dissolving 6 mg of GOx enzyme (250 KU) in 50 ml of 0.1 M phosphate buffer, pH 6.5, which contains 1.5 mM of ethylenediaminetetraacetic acid (EDTA) as antimicrobial agent and 10% (w/v) of glycerol as stabilizer. The glucose solution ranging from 0.2 to 3 mg/ml was prepared for the evaluation of the biosensor presented in this paper.

Figure 7-1 shows the schematic diagram of the device structure for the OFET-based glucose sensor. A [100] silicon wafer with a 0.1  $\mu$ m thick silicon dioxide layer was used as the substrate for the fabrication of the sensor devices and also serving as the gate region of the OFETs. First, a mask was designed using the L-Edit layout software for fabricating the source and drain gold electrode pair patterns, in between which the device channel region is also defined. The pattern transfer was performed by the UV photolithographic process using the commercially available PR 1813 positive photoresist (Sigma-Aldrich).

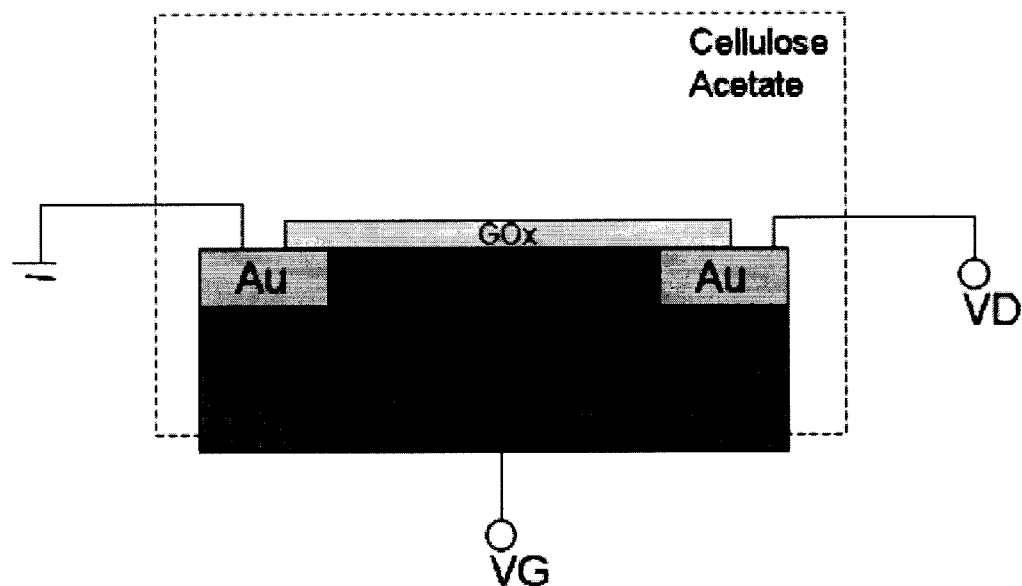
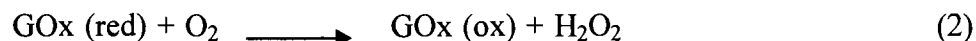
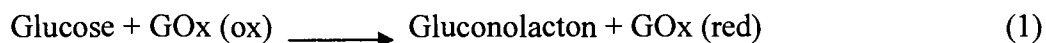


Figure 7-1 A schematic diagram of the device structure for the glucose sensor

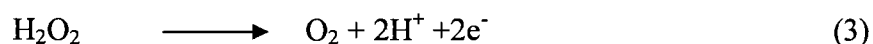
Prior to the spin-coating of PEDOT-PSS and GOx, the substrate was subjected to O<sub>2</sub> plasma for 60 s to hydrophobize and clean the photoresist residue from the channel region of the patterned surface. After spin-coating PEDOT-PSS, the samples were annealed for 2 minutes at 75°C in air, to improve the polymer film morphology and firmness. This step was followed by spin-coating of the GOx layer. The total film thickness was measured to be about 50 nm (using a Tencor Profilometer). Finally, the substrate was dip coated in a cellulose acetate solution, 2.5% (w/v) of cellulose acetate in Tetrahydrofuran (THF) (60%) and acetone (40%) solution, to form a protecting membrane that would allow glucose to pass while preventing water molecules from entering the substrate. The individual sensor devices were then wire bonded for electrical measurements.

### 7.3 Results and Discussion

In general, the reaction between GOx enzyme and glucose produces hydrogen peroxide ( $\text{H}_2\text{O}_2$ ) and Gluconolacton (gluconic acid), as described by Equations 1 and 2 [213].



GOx enzyme, used with a conductive material as sensing electrode, can be used to detect glucose through the measurement of electrons generated by oxidation of  $\text{H}_2\text{O}_2$  (Equation 3) formed during the reaction given in Equations 1 and 2 [213].



The working mechanism of the glucose sensor is based on the reduction/oxidation reactions, as shown in Figure 7-2. Due to the redox property of PEDOT-PSS and oxidation of hydrogen peroxide, the reaction between PEDOT-PSS and hydrogen peroxide can take place [214] and be detected electrically, as shown by the OFET-based glucose sensor reported in this work.

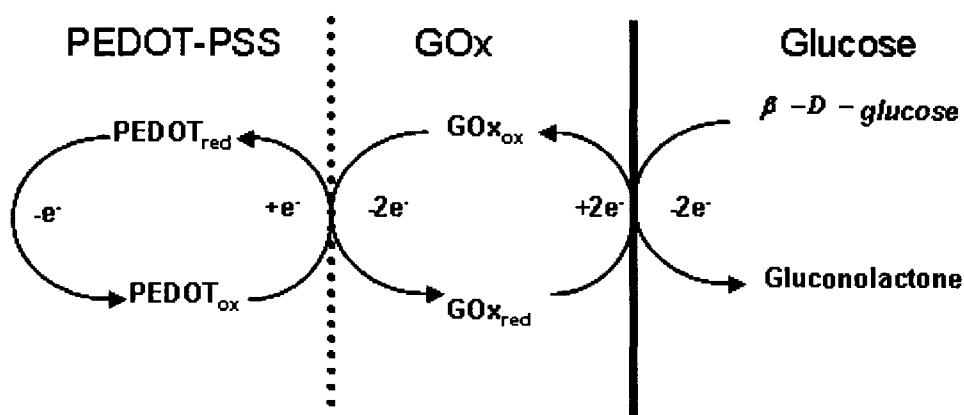


Figure 7-2 The working mechanism of the PEDOT-PSS based glucose sensor

A Keithley probe station was used to characterize the electrical behavior of the fabricated OFET-based glucose sensors. Figure 7-3 shows the OFET's drain current versus gate voltage characteristic ( $I_D - V_G$ ), measured at a drain voltage ( $V_D$ ) of  $-1.5$  V, with  $V_G$  swept between  $+10$  V and  $-30$  V, while being exposed to different concentrations of glucose solution. It can be noted that for the given conditions, the drain current increases when the device is exposed to higher concentrations of glucose solution. This is attributed to the increase in the charge carrier concentration occurring in the OFET's channel region, based on the concept schematically described by the diagram in Figure 7-2. Moreover, it can be observed that at a given glucose concentration, a negative gate voltage enhances the channel conduction while a positive gate voltage reduces it. This is consistent with the behavior expected for PEDOT-PSS based p-type OFETs.

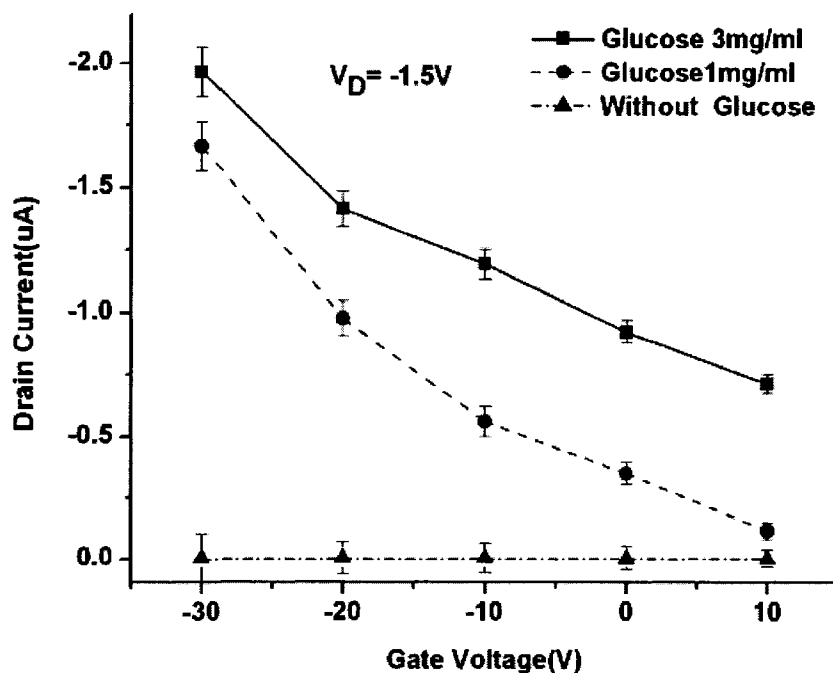


Figure 7-3 The drain current – gate voltage characteristic ( $I_D - V_G$ ) of the OFET-based glucose sensor when exposed to 0 mg/ml (normal device), 1 mg/ml, and 3 mg/ml of glucose concentration solution.

The output characteristic (drain current versus drain voltage) of the developed OFET-based glucose sensor is shown in Figure 7-4. The results confirm that the device behaves as a p-type field effect transistor. When a positive bias is applied to the gate electrode, the electrons produced from the reaction between  $GO_x$  and glucose are expected to move to the channel region (PEDOT-PSS). Cations ( $H^+$ ) produced during the reaction can easily transfer to the channel region [215] causing electrochemical dedoping (reduction) of  $PEDOT^+$  to the less conducting  $PEDOT^0$  (neutral) state [216], as shown by Equation 4.



The decrease in charge density is also accompanied by the reduction of hole mobility due to the presence of an increased number of ions in PEDOT-PSS [217]. Therefore, the decrease in conductivity of PEDOT-PSS in the channel region, due to electrochemical dedoping and reduction of hole mobility, can be the main cause for the decrease in drain current in the presence of glucose under positive gate bias, as shown in Figure 7-4.

When negative bias is applied to the gate electrode, holes accumulate in the channel region, as in the case of p-type field effect transistors. As mentioned above, the density of electrons increases when the device is exposed to higher concentrations of glucose, according to Figure 7-2 and Equations 1, 2, and 3. Due to the negative bias on the gate electrode, electrons produced during the reaction between  $GO_x$  and glucose will be pushed away from the channel region, thereby reducing the chances of reduction of PEDOT-PSS [216]. However, hydrogen peroxide, produced during the reaction according to Equation 2, has an impact on the device performance due to its strong

oxidation property. As a consequence, interaction between the hydrogen peroxide and PEDOT-PSS is directly possible by the reduction and oxidation reactions. Therefore, positively charged PEDOT-PSS will be oxidized in the presence of hydrogen peroxide and will have higher stability with higher concentration of free charge carriers [218]. This results in a high conductivity for PEDOT-PSS and a higher drain current in response to the increasing concentration of glucose solution under negative gate bias, as shown in Figure 7-4.

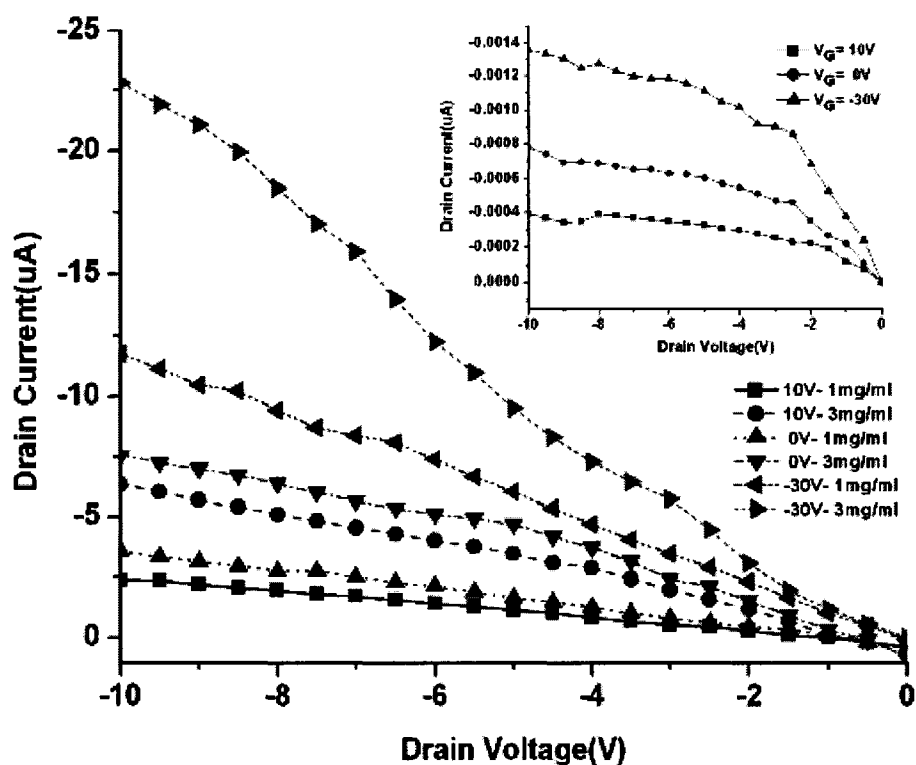


Figure 7-4 The output characteristic ( $I_D$ - $V_D$ ) of the OFET-based glucose sensor for 1mg/ml, and 3mg/ml of glucose concentration solution. Insert:  $I_D$ - $V_D$  of the device in the absence of glucose solution.

Figure 7-5 shows the change in drain current versus time when the glucose sensor device is exposed to different concentration of glucose solution (1 mg/ml, 2 mg/ml and 3

mg/ml). The potential on the drain and gate electrodes was set at -1.5 V and 0 V, respectively. In Figure 7-5, it is shown that after a 10-20 seconds response time, the output current of the sensor reached a stable state and exhibited a relatively steady level during the exposure of glucose solution on the device. During the 10-20 seconds, the response curve showed two different linear slopes and it was also observed that the first slope is bigger than second one. This phenomenon occurs because when the exact amount of glucose solution was dropped on the device surface initially, there was a bigger slope due to the larger amount of glucose in the solution. With the glucose reacting with GOx and polymer, a lesser amount of glucose was left in the solution. After 10-20 seconds, the glucose quantity became constant and the response current also reached a stable state. From Figure 7-5, it is also observed that the measured drain current reached steady state more rapidly at higher concentrations of glucose. Moreover, the steady state value of the drain current is higher for larger values of glucose concentration. With the assumption that the enzyme was uniformly distributed throughout the film, the reaction is expected to take place faster on the surface of the film at higher concentrations of glucose solution, as compared to lower values [219]. When glucose solutions are absorbed away from the surface of the sensor device, the response current gradually decreased to zero. The results in Figure 7-5 also show that the device response is repeatable over time.



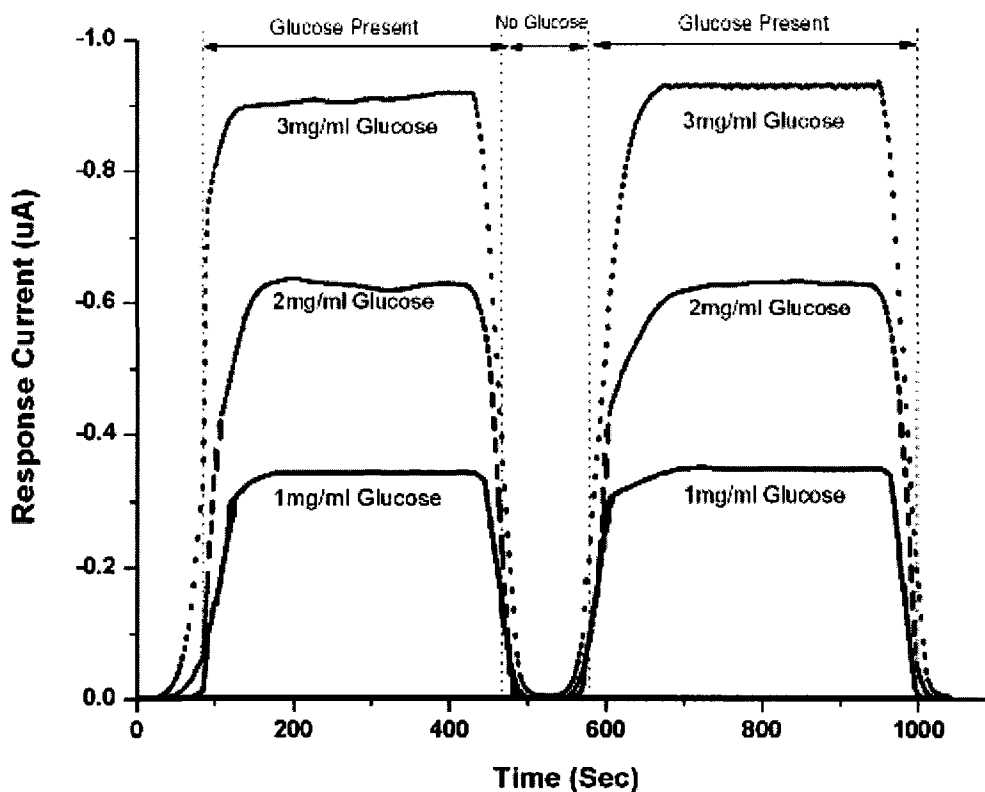


Figure 7-5 Drain current versus time, at  $V_D = -1.5$  V and  $V_G = 0$  V, measured at different glucose concentration values.

Figure 7-6 shows the change in drain current when the glucose sensor was exposed to different concentrations of glucose over a period of time. The drain and gate potentials were maintained at -1.5 V and 0 V, respectively. When the concentration of glucose was changed from 0.2 mg/ml to less than 0.2 mg/ml (by adding DI water), the current decreased. Then, when the concentration of glucose was changed from less than 0.2 mg/ml to more than 0.2 mg/ml (by adding 2 mg/ml glucose), a sharp increase in the measured current was observed. From the results in Figures 7-5 and 7-6, it is observed that for the developed PEDOT-PSS OFET-based biosensor, a relatively rapid response of 10-20 seconds was detected at each glucose concentration value. Similarly with Figure 7-

5, during the first 10-20 seconds, the response curve showed two different slopes. The reason is also the same as the description for Figure 7-5.

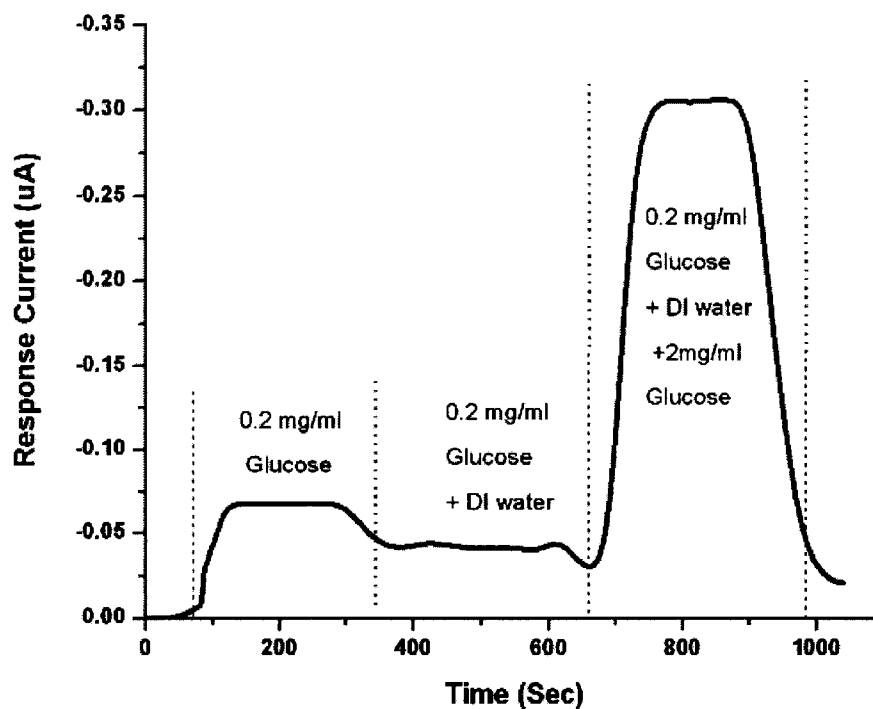


Figure 7-6 Drain current versus time, at  $V_D = -1.5$  V and  $V_G = 0$  V, measured at different glucose concentration values, illustrating the effect of change in glucose concentration from 0.2mg/ml to 2mg/ml by adding DI water and subsequently adding 2mg/ml glucose solution.

The relationship between the sensor response current (i.e. drain current) and glucose concentration is shown in Figure 7-7 when the gate and drain potentials are set at 0 V and -1.5 V, respectively. It can be clearly observed that the drain current increases due to the increase in glucose concentration. The sensitivity of the developed OFET-based glucose sensor was measured to be  $0.3 \mu\text{A}$  per 1 mg/ml of glucose concentration. The observed rise in drain current due to the increase in glucose concentration is attributed to the redox property of PEDOT-PSS. The reduction-oxidation can occur between hydrogen peroxide and the PEDOT-PSS film in the OFET channel region.

Therefore, the more hydrogen peroxide that is produced, the more PEDOT-PSS gets oxidized, resulting in higher conductivity and increase in drain current.

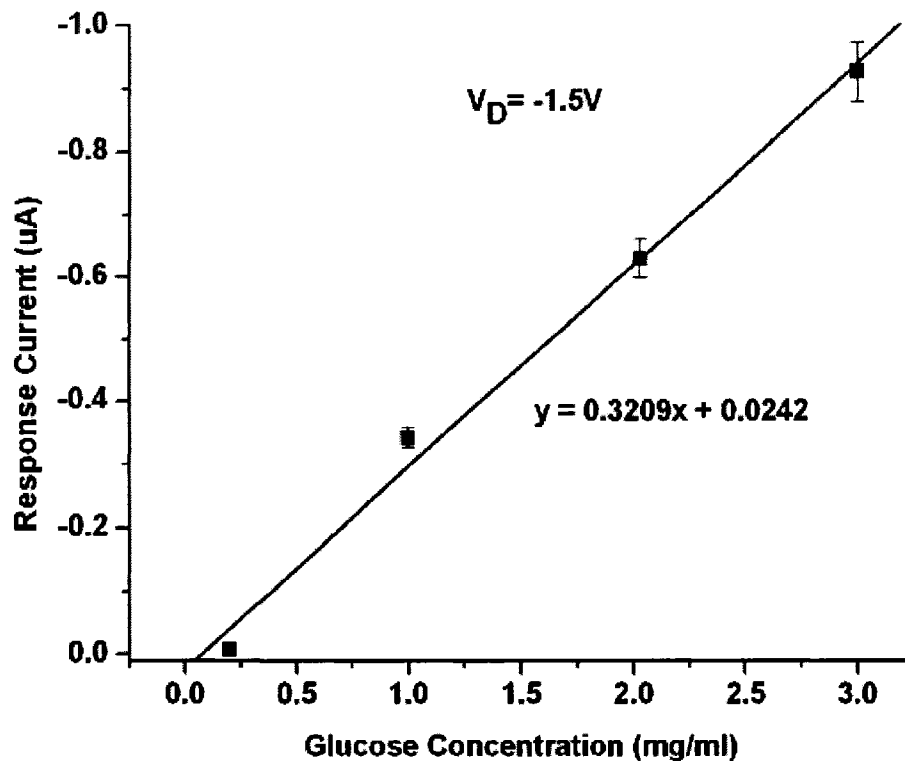


Figure 7-7 Drain current versus glucose concentration, at  $V_D = -1.5$  V and  $V_G = 0$  V. The solid line is the linear fit of the displayed data points.

Since we know that GOx catalyses the reaction of glucose to produce hydrogen peroxide and gluconic acid and that the latter changes the pH of the solution, the modulation in  $I_D$  was measured in standard buffer solutions with pH in the range from 4 to 10, as shown in Figure 7-8. It is observed that with increasing pH, a decrease in the current occurred. This observation indicates that the device based on PEDOT-PSS OFET can be used as a sensor over a wide range of pH environments. But, the value change is not noticeable as compared with the response current under glucose sensing. Then it has been proven that the response of the OFET to glucose is not identically depending on the

production of hydrogen peroxide, which adjusted the pH environment of polymer/GOx. The main factor affecting the current response to the glucose is the redox property of the PEDOT-PSS and the reduction-oxidation between the polymer material and hydrogen peroxide.

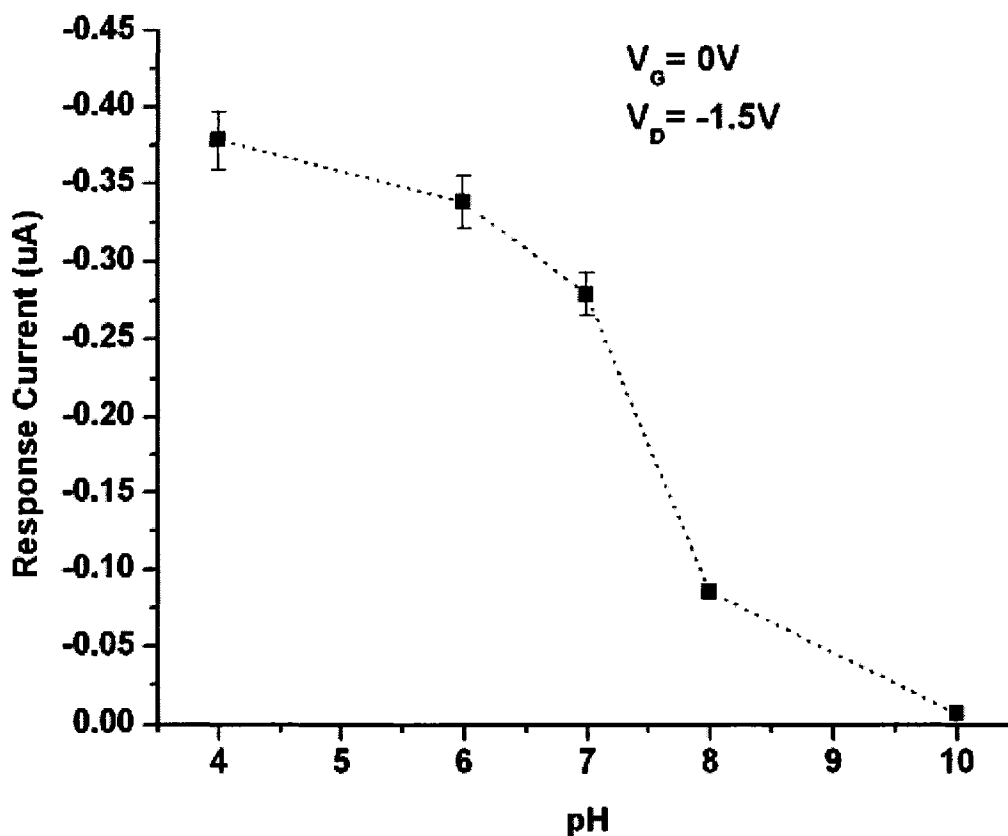


Figure 7-8 Drain current  $I_D$  of the OFET based on PEDOT-PSS as a function of PH. The gate voltage  $V_G$  is set to 0 V and the drain voltage  $V_D$  is set to 1.5V.

#### 7.4 Summary

As reported here, PEDOT-PSS conductive polymer-based OFET has been successfully developed and demonstrated as glucose sensor. A simple spin-coating technique has been used to immobilize GOx enzyme on PEDOT-PSS polymer film to form the channel region of the device. A linear relationship between the drain current

response and glucose concentration (0.2 mg/ml to 3 mg/ml) has been determined. The reported OFET-based glucose sensor has displayed good performance detecting glucose in the concentration range of 0.2 mg/ml to 3 mg/ml. This range covers the human body blood glucose level of 0.7 mg/ml to 1.5 mg/ml. The sensitivity of the developed OFET-based glucose sensor has been measured to be  $0.3 \mu\text{A}/(\text{mg/ml})$ . The modulation of drain current measurement in standard buffer solutions with pH in the range from 4 to 10 has proven that the response of the OFET device to glucose is not identically dependent on the pH environment change due to the production of hydrogen peroxide, but is dependent on the reduction-oxidation between PEDOT-PSS and hydrogen peroxide.

## CHAPTER EIGHT

### CONCLUSIONS AND FUTURE WORK

#### 8.1 Conclusions

In this dissertation, organic electronic devices based on PEDOT-PSS as the active layer have been fabricated and analyzed. Fundamental applications that are useful, such as soil moisture monitoring sensors, and glucose sensors were investigated and presented. For OFETs, the device mobility was measured and discussed based on the developed model.

2-D numerical simulation based on Taurus simulator was set up in order to get more adequate understanding of device operation and theory. The Taurus simulator is built on the fundamentals of the self-consistently solved Poisson's equation and current continuity equations. The simulations were implemented by taking into consideration the important parameters of the devices, resulting in the simulation results being in good agreement with the experimental data.

According to the theoretical and experimental results analysis on the key issues, corresponding improvements have been made to the device performance. First, the commercial poly(3,4-ethylenedioxythiophene)-polystyrene sulfonate (PEDOT-PSS) was studied. The modified PEDOT-PSS was utilized as the active layer of the organic resistors and OFETs, giving the promising conductivity. After the modification of

polymer material, the device characteristics were improved. Secondly, an improvement of the semiconductor-insulator interface has been developed, which was done by a simple annealing of the SiO<sub>2</sub> surface prior to the deposition of the PEDOT-PSS layer. Thirdly, the device degradation was investigated as the polymer material shows sensitivity to the environment. Protective coating, such as PVP and cellulose acetate were used to protect the devices from degradation. Finally, polymer based resistors and OFETs using PEDOT-PSS were investigated and successfully developed for soil moisture and glucose sensing, respectively. The developed moisture sensor showed promising performance in terms of response time, sensitivity and repeatability, and can be used to test the gravimetric water content in the soil samples. The resistance of the sensor device was changed from 2.5 M to 4.0 M ohm when exposed to soil samples with 15 – 35 % change in gravimetric water content. It has been demonstrated that moisture sensors, based on PEDOT-PSS, are promising for geological and geotechnical applications. The glucose sensor based on PEDOT-PSS was also investigated and developed. It shows reasonable characteristics for detecting glucose in the concentration range of 0.2 mg/ml to 3 mg/ml which covers the human body blood glucose level of 0.7 mg/ml to 1.5 mg/ml. The sensitivity of the developed OFET-based glucose sensor has been tested to be 0.3  $\mu\text{A}/(\text{mg}/\text{ml})$ . Because of low cost and better performance, this approach for an OFET based glucose sensor can provide an economical method for the development of organic bioelectronic devices.

The observed characteristics of the devices and calculated results have proved that PEDOT-PSS has a promising conductivity which enables this polymer to be used in many significant organic electronic devices.

## 8.2 Future Work

### 8.2.1 Glucose Sensors Based on Layer-by-Layer Self-Assembly

The electronic sensor devices based on PEDOT-PSS were developed successfully. However, the main issue of polymer sensors is sensitivity of the deposited polymer, which is determined by the thickness of the sensing film, sensing area and surface roughness. Thus, the deposition of the sensing film on the devices during the fabrication process is important for controlling the device characteristics. Layer-by-Layer (LbL) self-assembly is a unique technique for the deposition of composite and polymeric films with controlled thickness in the nanometer range [220]. The attractive feature of this approach is its ability to assemble complicated structures from components, and integrate them into self-assembling constructions for wide range of applications [221]. The LbL process involves alternating immersion of a substrate into aqueous solutions of oppositely charged polycation and polyanion polymers which are the basic component units used to form a multilayer. Structural stability is another promising feature of the LbL self assembly system. One important additional feature of self-assembly is hierarchy, where primary building blocks associate into more complex secondary structures that are integrated into the next size-level in the hierarchy. Due to these attractive characteristics, LbL self-assembly is investigated for deposition of an ultrathin PEDOT-PSS film for sensor applications.

An LbL application is the realization of ultra-thin films of conductive polymers, as nanoengineered active regions in polymer-based devices. The schematic cross-section of polymer sensors fabricated by LbL self-assembly is shown in Figure 8-1, where  $n$  bilayers of PEDOT-(PSS/PAH) $n$  ( $n$  is dependent on the active layer thickness) are



deposited on the precursor layer (PSS/PAH)<sub>n</sub>. The structure is fabricated on n<sup>+</sup>-Silicon wafer with high quality thermal oxide. The structure of such a sensor devices is illustrated in Figure 8-1. The same layer used for the sensing part would be the active film for p-type OFETs.

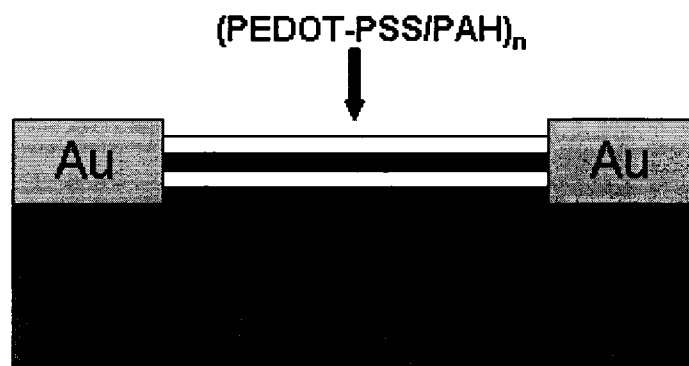


Figure 8-1 A schematic cross section of Layer-by-Layer self-assembly PEDOT-PSS sensor

Figure 8-2 shows the relationship between the response current of the sensor using the LbL self-assembly technique and glucose concentration when the gate and drain potentials are set at 0 V and -1.5 V, respectively. It can be clearly observed that the drain current increases due to an increase in glucose concentration. The sensitivity of the developed OFET-based glucose sensor was measured to be 1.05  $\mu\text{A}$  per 1mg/ml of glucose concentration which shows a higher sensitivity than the glucose sensor fabricated by the spin-coating technique, which achieves 0.3  $\mu\text{A}$  per 1mg/ml of glucose concentration. Therefore, the LbL self-assembly technique opens an alternative way for the fabrication of a wide range of polymer sensors due to low cost and light weight.

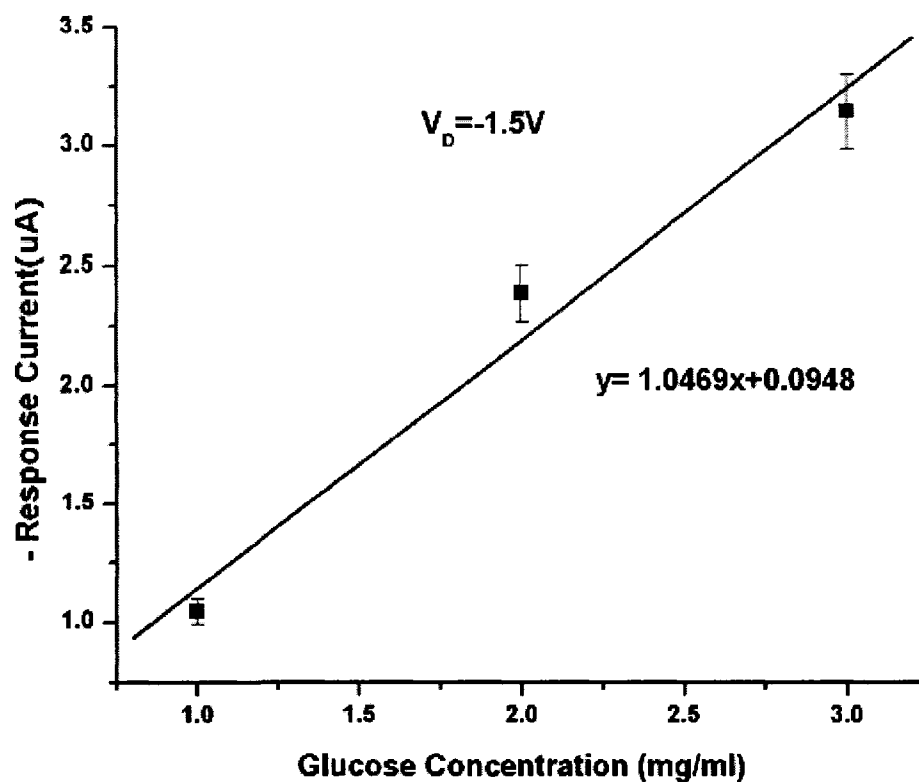


Figure 8-2 Drain current for the glucose sensor fabricated by the LBL self-assembly technique versus glucose concentration, at  $V_D = -1.5$  V and  $V_G = 0$  V. The solid line is the linear fit of the displayed data points

### 8.2.2 Heterostructure Organic Semiconductor Devices

Heterostructures are the main building parts of many of the most advanced organic semiconductor devices presently being developed and produced. They are essential elements for the highest-performance in high-speed and high-frequency digital and analog devices [222]. The advantage of heterostructures is that they offer precise control over the states and motions of charge carriers in organic semiconductors. Heterostructures can improve the performance of organic semiconductor devices, such as OFETs, because they permit the device designer to locally modify the energy-band structure of the organic material and thereby control the motion of the charge carriers

[223]. Polymer based heterostructure is studied in conventional metal-oxide-semiconductor field effect transistors to increase charge carrier mobility in the transistors [223]. High mobility results in the high speed of the transistors. Currently available polymer charge carrier mobility is at least 4 orders of magnitude lower than that for silicon.

Figure 8-3 shows the schematic diagram of the heterostructure device. The heavily n-doped silicon substrate acts as the gate electrode. The gate dielectric insulator is 1000 Å thick thermal silicon dioxide. A layer of 500 Å Au/30 Å Ti is sputter deposited on the SiO<sub>2</sub> as the source/drain electrodes, and patterned by a lift-off process. Between the source and drain electrode there is a 50nm channel. The P-type semiconductor polymer, PPy, PEDOT-PSS, and P3HT can be chosen to be used as the active material for heterostructure devices with alternative film thicknesses.

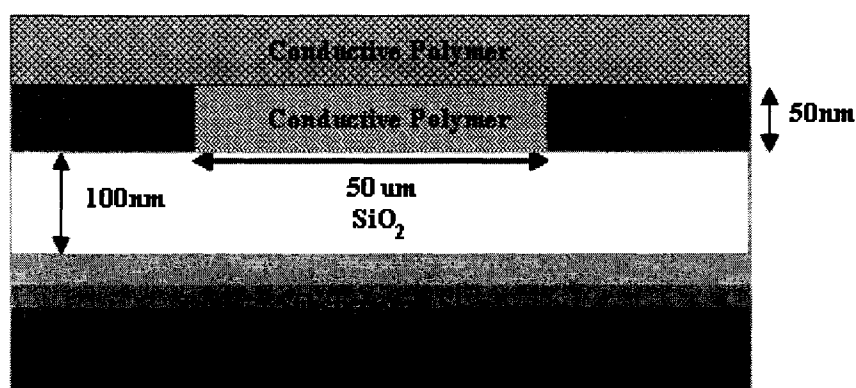


Figure 8-3 A schematic cross section of heterostructure sensor devices

Among a number of conducting polymers, polypyrrole (PPy) offers reasonably high conductivity and has fairly good environmental stability. It has been decided to concentrate on PPy for the humidity sensor [224] based on past literature reviews which have suggested it would be the easiest to fabricate and have high sensitivity to humidity.

There are three types of conductivities affected by doping conjugated polymers: intrachain, intermolecular, and ionic conductivities [225]. This observation makes response prediction even more difficult, as the dopant can have more than one effect on the conductivity of the conjugated polymer. PEDOT-PSS is highly stable in its doped state because of low band gap (ca. 1.6-1.7 V) and reaches conductivities as high as  $200 \text{ S cm}^{-1}$ . “Due to its interesting electronic properties, it has been considered for applications as antistatic coatings, hole-injecting layers for organic light-emitting diodes, sensors, photodiodes, and electrochromic windows” [226]. The PEDOT-PS has a high electrochemical stability, as can be seen by the reversibility with successive potential cycling of the polymer film in monomer free electrolyte solution. P3HT has self organizing properties to form a microcrystalline structure in films. Self-organization in P3HT results in a lamellar structure with two-dimensional conjugated sheets formed by interchain stacking [227]. The lamellae can adopt by two different orientations: “parallel and perpendicular to the substrate, the mobilities of which differ by more than a factor of 100. In samples with high regioregularity (96%) and low molecular weight, the preferential orientation of ordered domains is with the (100)-axis normal to the film and the (010)-axis in the plane of the film [228]. Another property of P3HT is that it can be dissolved in a variety of solvents, such as chloroform, chlorobenzene, tetrahydrofuran, p-xylene and toluene, etc. Previous research has noted that the field-effect mobility can vary significantly with different solvents [229]. Low boiling point and rapid evaporation time for crystallization during spin coating results in lower field effect mobility. The deposition methods for P3HT are drop casting, contact printing, Langmuir-Blodgett, dip coating, spin coating, and inkjet printing.

With the fabrication of a polymer based heterostructure FET, the modeling and simulation of devices by Taurus can be developed to modify the reasonable results. In the simulation, the contact resistance and field-effect mobility effect can be included because these two effects are important for device performance.

### 8.3 General Considerations

The applications of organic electronics present several advantages, such as low cost for the materials and simple processing, like spin-coating. In combination with sensor elements built the same way out of similar substances, this technology will lead to new devices with unique features. The use of flexible substrates for organic materials will enable entrance to new fields of applications. The techniques for device fabrication are low cost and easy to access. Together, this will reduce development and fabrication costs and new markets will be accessed with low cost organic electronic sensor devices.

But, some disadvantages are observed due to their organic nature as well. For example, the long term stability of devices must be improved to make devices more attractive. Oxygen and moisture are the main reasons for organic electronic device degradation. Thus, packaging should be considered and given much attention in order to overcome these obstacles on the way introducing the organic electronic devices into the market place.

Until now, organic electronic devices have not had a crucial role in many sensor applications. Invariably, electronically active organic materials are successfully used in displays. Very likely, the field of organic electronics will further grow and find many applications.

## APPENDIX A

### TAURUS-DEVICE INPUT SIMULATION COMMAND

```
Taurus {device}
DefineDevice (
name=devicemesh
minX=0.0 maxX=15
minY=-50nm maxY=200nm
region(material=silicon, name=channel1),
region(material=aluminum,name=source1),
region(material=aluminum,name=drain1),
region(material=oxide, name=oxide1)
region(material=polysilicon, name=polysilicon1)
x=0.0 dx=500nm
x=15 dx=500nm
y=-50nm dy=1nm
y=-5nm dy=2.5nm
y=0 dy=5nm
y=200nm dy=10nm
)
Defineboundary(
region=polysilicon1,
polygon2d(
point(x=0,y=200nm),          point(x=15,y=200nm),          point(x=15,y=100nm),
point(x=0,y=100nm)))
Defineboundary(
```

```
region=oxide1,  
polygon2d(  
point(x=0, y=0nm), point(x=15,y=0nm), point(x=15,y=100nm), point(x=0,y=100nm)))  
DefineBoundary(  
region=source1,  
polygon2d(  
point(x=0,y=-50nm), point(x=5,y=-50nm),point(x=5,y=0nm),point(x=0,y=0nm)))  
DefineBoundary(  
region=drain1,  
polygon2d(  
point(x=10,y=-50nm), point(x=15,y=-50nm),point(x=15,y=0nm),point(x=10,y=0nm)))  
DefineBoundary(  
region=channell1,  
polygon2d(  
point(x=5,y=0nm), point(x=5,y=-50nm),point(x=10,y=-50nm),point(x=10,y=0nm)))  
Regrid (  
MinX=0, MaxX=15, MinY=-50nm, MaxY=200nm,  
MaxDeltaY=10nm,  
Criterion (Name=AllInterfaces) )  
save (meshfile=FET1.tdf)  
# Flat contact  
Definecontact (name=source, X (min=0, max=5.05) Y(min=-50nm, max=0nm))  
Definecontact (name=drain, X (min=10 max=15) Y(min=-50nm, max=0nm))
```



```

Definecontact (name=gate, X (min=0 max=15) Y(min=199nm, max=200nm))

contact(name=gate, workfunction=5.0)

contact(name=source, workfunction=5.1)

contact(name=drain, workfunction=5.1)

# Doping

profile (name=pptype, region=channel1, uniform(value=3e17))

profile (name=ntype, region=polysilicon1, uniform(value=2e19))

Regrid ( region=channel1,
        MaxDeltaY=2nm)

save (meshfile=FET2.tdf)

#Device characteristics

Taurus {device}

DefineDevice(Name=tft, meshfile=FET2.tdf, areafactor=500)

# Define aluminum properties

Physics(
Aluminum(
global (workfunction=5.1)))

# Define PEDOT-PSS properties

Physics(silicon(holecontinuity(mobility(constant=true,mup0=0.0016))))

Physics(Silicon(global(global(conductionDensityOfStates(AtRoomTemperature=1e21),
ValenceDensityOfStates(AtRoomTemperature=1e21))))))

Physics(Silicon(Global
(Permittivity=3.5, ElectronAffinity=3.6, Bandgap (Eg300=1.6))))

```

```

# Set equilibrium bias on contacts
SetBias (value=0.0) {Contact (name=source, type=voltage)}
SetBias (value=0.0) {Contact (name=gate, type=voltage)}
SetBias (value=0.0) {Contact (name=drain, type=voltage)}
# Specify zero-carrier solution
Symbolic (carriers=0)
numerics (iterations=100, relativeerror=5e-3)
# Initialization that only solve poisson's equation
# Do Solve
Solve {couple {Poissons}}
Symbolic (
  Couple (iterations=100 linearSolver=direct relativeError=5e-3)
    {Poissons holeContinuity}
)
Solve {}
Save (meshfile=initial.tdf add(valenceband conductionband bandgap electronPotential
holePotential))
# Specify one-carrier solution with holes
Symbolic (carriers=1,holes)
ramp(
voltage(electrode=gate,endvalue=-30,nsteps=30)
)
Ramp (logfile=Id21E.data

```

```
Voltage (electrode=drain, startvalue=0,endValue=-20, nSteps=20)
```

```
)
```

```
Save (meshfile=gate21.tdf add(valenceband conductionband bandgap))
```

```
Ramp (logfile=Idno.data
```

```
Voltage (electrode=drain, endValue=0, nSteps=10)
```

```
)
```

```
ramp(
```

```
voltage(electrode=gate,endvalue=-20,nsteps=20)
```

```
)
```

```
Ramp (logfile=Id22E.data
```

```
Voltage (electrode=drain, startvalue=0,endValue=-20, nSteps=20)
```

```
)
```

```
Save (meshfile=gate22.tdf add(valenceband conductionband bandgap))
```

```
Ramp (logfile=Idno.data
```

```
Voltage (electrode=drain, endValue=0, nSteps=10)
```

```
)
```

```
ramp(
```

```
voltage(electrode=gate,endvalue=-10,nsteps=10)
```

```
)
```

```
Ramp (logfile=Id23E.data
```

```
Voltage (electrode=drain, startvalue=0,endValue=-20, nSteps=20)
```

```
)
```

```
Save (meshfile=gate23.tdf add(valenceband conductionband bandgap))
```

```
Ramp (logfile=Idno.data
Voltage (electrode=drain, endValue=0, nSteps=10)
)
ramp(
voltage(electrode=gate,endvalue=0,nsteps=10)
)
Ramp (logfile=Id24E.data
Voltage (electrode=drain, startvalue=0,endValue=-20, nSteps=20)
)
Save (meshfile=gate24.tdf add(valenceband conductionband bandgap))
Ramp (logfile=Idno.data
Voltage (electrode=drain, endValue=0, nSteps=10)
)
ramp(
voltage(electrode=gate,endvalue=10,nsteps=5)
)
Ramp (logfile=Id25E.data
Voltage (electrode=drain, startvalue=0,endValue=-20, nSteps=20)
)
#solve {}
Save (meshfile=gate25.tdf add(valenceband conductionband bandgap))
Ramp (logfile=Idno.data
Voltage (electrode=drain, endValue=0, nSteps=10)
```

```
)  
ramp(  
voltage(electrode=gate,endvalue=20,nsteps=10)  
)  
Ramp (logfile=Id26E.data  
Voltage (electrode=drain, startvalue=0,endValue=-20, nSteps=20)  
)  
#solve {}  
Save (meshfile=gate26.tdf add(valenceband conductionband bandgap))
```

## REFERENCES

- [1] H. Shirakawa, E. J. Louis, A. G. MacDiarmid, C. K. Chiang, and A. J. Heeger. "Synthesis of Electrically-Conducting Organic Polymers: Halogen Derivatives of Polyacetylene, (CH)<sub>n</sub>X". *Journal Chemical Society: Chemical Communication*, Vol.16, (1977) 578-580.
- [2] A. Tsumura, H. Koezuka and T. Ando. "Macromolecular electronic device: field-effect transistor with a polythiophene thin film". *Applied Physics Letters*, Vol. 49, (1986) 1210-1212.
- [3] S. Hoshino, M. Yoshida, S. Uemura, T. Kodzasa, N. Takada, T. Kamata and K. Yase. "Influence of moisture on device characteristics of polythiophene-based field-effect transistors". *Journal of Applied Physics*, Vol. 95, (2004) 5088-5093.
- [4] Y. Miyahara, T. Moriizumi and K. Ichimura. "Integrated enzyme FETS for simultaneous detections of urea and glucose". *Sensors and Actuators*, Vol.7, (1985) 1-10.
- [5] S. D. Senturia. "Microsystem Design, chapter 18.2.". Boston / Dordrecht / London: *Kluwer Academic Publishers*, (2001) 470-474.
- [6] G.L. David, M. Voigt, C. Giebeler, A. Buckley, J. Wright, K. Böhlen, J. Fieret and R. Allott. "Laser-assisted patterning of conjugated polymer light emitting diodes". *Organic Electronics*, Vol.6, (2005) 221-228
- [7] F. Jiang, Y.C. Tai, K. Walsh, T. Tsao, G.-B. Lee and C.-M. Ho. "A flexible MEMS technology and its first application to shear stress sensor skin". *Proceedings of the IEEE International Conference on MEMS*, (1997) 465-470.
- [8] R. Nohria, Y. Su, R.K. Khillan, R. Dikshit, Y. Lvov and K. Varshramyan. "Development of humidity sensors using layer-by-layer nanoassembly of polypyrrole". *Micro- and Nanosystems- Materials and Devices. Symposium (Materials Research Society Symposium Proceedings)*, Vol.872, (2005) 329-335.
- [9] R. Keyes. "Miniaturization of electronics and its limits". *IBM Journal of Research and Development archive*, Vol.32, (1988) 24-28.
- [10] Celebrating the year 2000 Nobel Prize in Chemistry to Alan Heeger, Alan MacDiarmid and Hideki Shirakawa for the Discovery and Development of Conductive Polymers, *Synthetic Metals*, Vol.125, (2001).

- [11] J. M. Shaw and P. F. Seidler. "Organic electronics: Introduction". *IBM Journal of Research and Development*, Vol. 45, (2001) 3-8.
- [12] W. Xue, J. Engel and L.Chang . "Liquid crystal polymer (LCP) for MEMS: processes and applications", *Journal of Micromechanics and Microengineering*, Vol.13, (2003) 628-633.
- [13] T. M. Schweizer. "Electrical characterization and investigation of the piezoresistive effect of PEDOT: PSS thin films". *Dissertation*, (2005) 5.
- [14] A. L. Baseman. "What's new in plasticizers". *Plastics Technology*, Vol. 9, (1963) 45-56.
- [15] L. Pietronero and E. Cappelluti. "Low carrier density organic conductors: Unconventional electron-phonon coupling and superconductivity". *Proceedings - Electrochemical Society, Fullerenes and Nanotubes: Materials for the New Chemical Frontier - Proceedings of the International Symposium on Fullerenes, Nanotubes, and Carbon Nanoclusters*, (2004) 184-196.
- [16] S. E. Gledhill, B.Scott and B. A. Gregg. "Organic and nano-structured composite photovoltaics: An overview". *Journal of Materials Research*, Vol. 20, (2005) 3167-3169.
- [17] A. Tsumura, H. Koezuka and T. Ando. "Macromolecular electronic device: field-effect transistor with a polythiophene thin film". *Applied Physics Letters*, Vol. 49, (1986) 1210-1212.
- [18] J. H. Burroughes, C.A. Jones and R.H. Friend. "New semiconductor device physics in polymer diodes and transistors". *Nature*, Vol. 335, (1988) 137-141.
- [19] T.W. Kelley, P. F. Baude, C. Gerlach, D.E. Ender, D. Muyres, M. A. Haase, D.E. Vogel and S. D. Theiss. "Recent progress in organic electronics: materials, devices, and processes". *Chemistry of Materials*, Vol. 16, (2004) 4413-4422.
- [20] H. E. Katz, A.J. Lovinger, Hong, X., Dodabalapur, A., Johnson, J., Wang, B. and Raghavachari, K.. "Design of organic transistor semiconductors for logic elements, displays, and sensors". *Proceedings of the SPIE - The International Society for Optical Engineering*, Vol. 4466, (2001) 20-30.
- [21] R. D. Yang, J. Park, N. Corneliu, I. K. Schuller, C.W. Trogler and A. C. Kummel. "Ultralow drift in organic thin-film transistor chemical sensors by pulsed gating". *Journal of Applied Physics*, Vol.102, (2007) 034515
- [22] B. Singh, N. Marjanovic, N.S. Sariciftci, R. Schwodiauer and S. Bauer. "Electrical characteristics of metal-insulator-semiconductor diodes and transistors with space charge electret insulators: towards nonvolatile organic memories". *IEEE Transactions on Dielectrics and Electrical Insulation*, Vol.13, (2006) 1082-1086.

- [23] S. C. J. Meskers, J. K. J. Duren and R. A. J. Janssen. "Non-linearity in the I-V characteristic of poly(3,4-ethylenedioxythiophene):poly(styrenesulfonic acid) (PEDOT:PSS) due to Joule heating". *Organic Electronics*, Vol. 5, (2004) 207-211.
- [24] F. Kannari. "Deposition of functional organic thin films by laser ablation using UV and VUV lasers". *Pacific Rim Conference on Lasers and Electro-Optics, CLEO - Technical Digest*, Vol. 3, (1999) 686-687.
- [25] K.S. Jang, S. S. Han, J. S. Suh and E. J. Oh. "Synthesis and characterization of alcohol soluble polypyrrole", *Synthetic Metals*, Vol. 119, (2001) 107-108.
- [26] J. C. Scott, J. H. Kaufman, P.J. Brock, R. DiPietro, J. Salem and J. A. Goitia. "Degradation and failure of MEH-PPV light-emitting diodes". *Journal of Applied Physics*, Vol. 79, (1996) 2745-2751.
- [27] X. J. Yan, H. Wang, D. Yan. "An investigation on air stability of copper phthalocyanine-based organic thin-film transistors and device encapsulation". *Thin Solid Films*, Vol. 515, (2006) 2655-2658.
- [28] G. D. Hutchison. "Forty years of Moore's law: Ever smaller transistors and ever larger wafers". *ECS Transactions, Silicon Materials Science and Technology X*, Vol. 2, (2006) 3-9.
- [29] K. Flamm. "Moore's law and the economics of semiconductor price trends". *International Journal of Technology, Policy and Management*, Vol. 3, (2003) 127-141.
- [30] Y. Lvov, K. Ariga, M. Ond, I. Ichinose and T. Kunitake. "Alternate assembly of ordered multilayers of SiO<sub>2</sub> and other nanoparticles and polyions". *Langmuir*, Vol. 13, (1997) 6195-6203.
- [31] J.E. Wong, A.K. Gaharwar, D. Muller-Schulte, D. Bahadur and W. Richtering. "Layer-by-layer assembly of a magnetic nanoparticle shell on a thermoresponsive microgel core". *Journal of Magnetism and Magnetic Materials*, Vol. 311, (2007) 219-223.
- [32] C.Q. Sun, W.W. Yang, J.X. Wang, S. Zhao and Y.Y. Sun. "Multilayered construction of glucose oxidase and gold nanoparticles on Au electrodes based on layer-by-layer covalent attachment". *Electrochemistry Communications*, Vol. 8, (2006) 665-672.
- [33] H. Sirringhaus, T. Kawase and R.H. Friend. "High-resolution ink-jet printing of all-polymer transistor circuits". *MRS Bulletin*, Vol. 26, (2001) 539-543.
- [34] D.J. Hayes, W.R. Cox and M.E. Grove. "Low-cost display assembly and interconnect using ink-jet printing technology". *1999 Display Manufacturing Technology Conference. Digest of Technical Papers*, (1999) 13-16.



- [35] M. Plotner, T. Wegener, S. Richter, S. Howitz and W. J. Fischer, . “Investigation of ink-jet printing of poly-3-octylthiophene for organic field-effect transistors from different solutions”. *Synthetic Metals*, Vol. 147, (2004) 299-303.
- [36] D. B. Wallace and D. J. Hayes. “Solder Jet - Optics Jet - AromaJet - Reagent Jet - Tooth Jet and other Applications of Ink-Jet Printing Technology”. *International Conference on Digital Printing Technologies*, (2002) 228-235.
- [37] N. A. Fox, M. J. Youh, W. N. Wang, J. W. Steeds, H.-F. Cheng and I.-N. Lin. “Properties of electron field emitters prepared by selected area deposition of CVD diamond carbon films”. *Diamond and Related Materials*, Vol. 9, (2000) 1263-1269.
- [38] J. Steiger, S. Heun and N. Tallant. “Polymer light emitting diodes made by ink jet printing”. *Journal of Imaging Science and Technology*, Vol. 47, (2003) 473-478.
- [39] W.T. Pimbley. “Drop formation from a liquid jet: a linear one-dimensional analysis considered as a boundary value problem”. *IBM Journal of Research and Development*, Vol. 20, (1976) 148-156.
- [40] R. Uematsu, T. Ushioda, M. Takahashi and H. Fukuchi. “Higher harmonic excitation method for ultra-high resolution printing”. *1986 SID International Symposium. Digest of Technical Papers. First Edition*, (1986) 190-192.
- [41] S. Y. Chou, P. R. Krauss and P. J. Renstrom. “Imprint of sub-25 nm vias and trenches in polymers”. *Applied Physics Letters*, Vol. 67, (1995) 3114-3116.
- [42] C. C. Ceden, J. Seekamp, A. P. Kam, T. Hoffmann, S. Zankovych, C. Menozzi, M. Cavallini, M. Murgia, G. Ruani, F. Biscarini, M. Behl, R. Zentel and J. Ahopelto. “Nanoimprint lithography for organic electronics”. *Microelectronic Engineering*, Vol. 61-62, (2002) 25-31.
- [43] W. Jian and S. Y. Chou, . “Direct nanoimprint of submicron organic light-emitting structures”. *Applied Physics Letters*, Vol. 75, (1999) 2767-2769.
- [44] I. Fratoddi, P. Altamura, A. Bearzotti, A. Furlani and Russo, M.V.. “Electrical and morphological characterization of poly(monosubstituted) acetylene based membranes: Application as humidity and organic vapors sensors”. *Thin Solid Films*, Vol. 458, (2004) 292-298.
- [45] J.V. Haftfield, P. Neaves, P.J. Hicks, K. Persaud, K. and P. Travers. “Towards an integrated electronic nose using conducting polymer sensors”. *Sensors and Actuators, B: Chemical*, Vol. 18, (1994) 221-228.
- [46] K. I. Arshak, E.G. Moore, C. Cuniffe and L.M. Cavanagh. “ Using design of experiment to investigate the effects of conducting polymer composite sensor composition on the response to a homologous series of alcohols”. *25th International Conference on Microelectronics (IEEE Cat. No. 06TH8868)*, (2006) 4.

- [47] Y. Li, M. J. Yang and Y. She. "Humidity sensitive properties of crosslinked and quaternized poly(4-vinylpyridine-co-butyl methacrylate)". *Sensors and Actuators, B: Chemical*, Vol. 107, (2005) 252-257.
- [48] Albareda-Sirvent M., Merkoci, A. and Alegret, S.. "Configurations used in the design of screen-printed enzymatic biosensors. A review". *Sensors and Actuators B: Chemical*, Vol. 69, (2000) 153-163.
- [49] J. Engel, J. Chen, F. Zhifang and L. Chang. "Polymer micromachined multimodal tactile sensors". *Sensors and Actuators A (Physical)*, Vol. 117, (2005) 50-61.
- [50] A. Kros, S. V. Hovel, R.J.M.Nolte and N. A. Sommerdijk. "A printable glucose sensor based on a poly(pyrrole)-latex hybrid material". *Sensors and Actuators, B: Chemical*, Vol. 80, (2001) 229-233.
- [51] V. K. Varadan. "Three dimensional polymer MEMS with functionalized carbon nanotubes and modified organic electronics". *2003 Third IEEE Conference on Nanotechnology. IEEE-NANO 2003. Proceedings*, Vol. 2, (2003) 212-215.
- [52] H. He, M.A. Mortellaro, S. T. Young, R. J. Fraatz and J. K. Tusa. "A fluorescent chemosensor for sodium based on photoinduced electron transfer". *Analytical Chemistry*, Vol. 75, (2003) 549-555.
- [53] H. Q. Yan and C.C. Liu. "Humidity effects on the stability of a solid polymer electrolyte oxygen sensor". *Sensors and Actuators, B: Chemical*, Vol.B10, (1993) 133-136.
- [54] Y. Li, Y. Chen, C. Zhang, T. Xue and M. Yang. "A humidity sensor based on interpenetrating polymer network prepared from poly(dimethylaminoethyl methacrylate) and poly(glycidyl methacrylate)". *Sensors and Actuators, B: Chemical*, Vol. 125, (2007) 131-137.
- [55] Y. Sakai, M. Matsuguchi and N. Yonesato. "Humidity sensor based on alkali salts of poly(2-acrylamido-2-methylpropane sulfonic acid)". *Electrochimica. Acta.*, Vol. 46, (2001) 1509-1514.
- [56] G. Harsanyi. "Polymer films in sensor application: A review of present uses and future possibilities". *Sensor review*, Vol. 20, (2000) 98-105.
- [57] M. Matsuguchi, Y. Takahashi, T. Kuroiwa, T. Ogura, S. Obara and Y. Sakai. "Effect of sensing film thickness on drift phenomenon of capacitive-type humidity sensors". *Journal of the Electrochemical Society*, Vol.150, (2003)192-195.
- [58] J. Y. Ouyang, Q. F. Xu, C.W. Chu, Y. Yang, G.Li and J. Shinar. "On the mechanism of conductivity enhancement in poly(3,4-ethylene dioxythiophene):poly(styrene sulfonate) film through solvent treatment". *Polymer*, Vol.45, (2004) 8443-8450.

- [59] D. Nilsson, T. Kugler, P. Svensson and M. Berggen. "An all-organic sensor-transistor based on a novel electrochemical transducer concept printed electrochemical sensors on paper". *Sensors and Actuators B Chemical*, Vol.86, (2002) 193-197.
- [60] W. A. Daoud , J. H. Xin and Y. S.Szeto. "Polyethylenedioxythiophene coatings for humidity, temperature and strain sensing polyamide fibers". *Sensors and Actuators B Chemical*, Vol.109, (2005) 329-333.
- [61] C. Werkhoven. "Time-domain reflectometry for detecting soil moisture content". *Computers in Agriculture 1994. Proceedings of the 5th International Conference*, (1994) 853-857
- [62] Y. Liu, A. G. Erdman and T. Cui. "Acetylcholine biosensors based on layer-by-layer self-assembled polymer/nanoparticle ion-sensitive field-effect transistors". *Sensors and Actuators A: Physical*, Vol.136, (2007) 540-545.
- [63] A. Loi, I. Manunza and A. Bonfiglio. "Flexible, organic, ion-sensitive field-effect transistor". *Applied Physics Letters*, Vol.86, (2005) 103512.
- [64] D. Niwa, T. Homma and T. Osaka. "Fabrication of Organic Monolayer Modified Ion-Sensitive Field Effect Transistors with High Chemical Durability". *Japanese Journal of Applied Physics, Part 2: Letters*, Vol.43, (2004) L105-L107.
- [65] S. B. Adeloju and G. G. Wallace. "Electroimmobilisation of sulphite oxidase into a polypyrrole film and its utilisation for flow amperometric detection of sulphitelyst". *Analytica Chimica Acta*, Vol.332, (1996) 145-153.
- [66] W.J. Sung and Y.H. Bae. "A glucose oxidase electrode based on electropolymerized conducting polymer with polyanion-enzyme conjugated dopant". *Analytical Chemistry*, Vol.72, (2000) 2177-2181.
- [67] Y. Hanazato, M. Nakako, S. Shiono and M. Maeda. "Integrated multi-biosensors based on an ion-sensitive field-effect transistor using photolithographic techniques". *IEEE Transactions on Electron Devices*, Vol.36, (1989) 1303-1310.
- [68] Adam K. Wanekaya, W. Chen, Nosang V. Myung and A. Mulchandani. "FET based conducting polymer coated carbon nanotube bio/chemical sensor". *AIChE Annual Meeting, Conference Proceedings, 05AIChE: 2005 AIChE Annual Meeting and Fall Showcase, Conference Proceedings*, (2005) 14151.
- [69] R.W. Scheller, F. Schubert, B. Neumann, D. Pfeiffer, R. Hintsche, I. Dransfeld, U. Wollenberger, R. Renneberg and A. Warsinke. "Second generation biosensors". *Biosensors & Bioelectronics*, Vol.6, (1991) 245-253.
- [70] M.Chen. "Printed Electrochemical Devices Using Conducting Polymers as Active Materials on Flexible Substrates". *Proceedings of the IEEE*, Vol.93, (2005) 1339-1347.

- [71] A. Ernst, O. Makowski, B. Kowalewska, K. Miecznikowski and P. J. Kulesza. "Hybrid bioelectrocatalyst for hydrogen peroxide reduction: Immobilization of enzyme within organic-inorganic film of structured Prussian Blue and PEDOT". *Bioelectrochemistry*, Vol.71, (2007) 23-28.
- [72] B. Zhou, J. Gao, Z. B. Hu. "Robust polymer gel opals - An easy approach by inter-sphere cross-linking gel nanoparticle assembly in acetone". *Polymer*, Vol.48, (2007) 2874-2881
- [73] D.M.Taylor and D.J.Morris. "Engineering challenges for polymer electronics". *IEE Japan and IEEE Dielectrics and Electrical Insulation Society, Proc ISEIM*, (2001) 537-540.
- [74] L. Li, X. Zhu, R. J. Jeng, Y. M. Chen and J. Kumar. "Stable Second-Order Optical Nonlinearity in Novel Photocrosslinkable Polymers". *Report: TR-1148-92-12*, (1992) 9p.
- [75] Marina Mastragostino, Catia Arbizzani and Francesca Soavia. "Conducting polymers as electrode materials in supercapacitors". *Solid State Ionics*, Vol.148, (2002) 493-498.
- [76] X.D.Wang, K. Ogino, K. Tanaka and H. Usui. "Novel polyimine as electroluminescent material prepared by vapor deposition polymerization". *Thin Solid Films*, Vol.438-439, (2003) 75-79.
- [77] A. M. Rahman, P. Kumar, D. S. Park and Y. B. Shim. "Electrochemical Sensors Based on Organic Conjugated Polymers". *Sensors*, Vol.8, (2008) 118-141.
- [78] A. Kassim, H.N.M. Ekarmul Mahmud, L. M. Yee and Nurain Hanipah. "Electrochemical Preparation and Characterization of Polypyrrole-Polyethylene Glycol Conducting Polymer Composite Films". *The Pacific Journal of Science and Technology*, Vol. 7, (2006) 103-107.
- [79] A. Sionkowska. "The influence of UV light on collagen/poly(ethylene glycol) blends". *Polymer Degradation and Stability*, Vol.91, (2006) 305-312.
- [80] Sung Y. Hong. "Molecular Design of Novel Conjugated Polymers for Blue-Light-Emitting Devices". *Bull. Korean Chemical Society*, Vol.24, (2003) 961.
- [81] J. Roncali. "Conjugated poly(thiophenes): synthesis, functionalization, and applications". *Chemical Review*, Vol.92, (1992) 711-738.
- [82] T. Blythe and D. Bloor. "Electrical properties of polymer, Second edition". *Cambridge university press*, (2005) 5-7.
- [83] A. Ajayaghosh. "Donor-acceptor type low band gap polymers: polysquaraines and related systems". *Chemical Society Review*, Vol.32, (2003) 181-191.

- [84] S. Kalapala and A. J. Easteal. "Novel poly(methyl methacrylate)-based semi-interpenetrating polyelectrolyte gels for rechargeable lithium batteries". *Journal of Power Sources*, Vol.147, (2005) 256-259.
- [85] O. Hilt, J. A. Reeduk, H. C. F. Martens, H. B. Brom and M. A. J. Michels. "Dopant effect on the charge transport in conjugated polymers". *Physica Status Solidi B*, v 218, (2000) 279-282
- [86] A. G. MacDiarmid. "Synthetic metals: a novel role for organic polymers". *Synthetic Metals*, Vol.125, (2001) 11-22.
- [87] R. A. Khalkhali. "Electrochemical Synthesis and Characterization of Electroactive Conducting Polypyrrole Polymers". *Russian Journal of Electrochemistry*, Vol.41, (2005) 950-955.
- [88] Alan G. MacDiarmid. "Synthetic metals: a novel role for organic polymers". *Synthetic Metals* , Vol.125, (2001) 11-22
- [89] C. K. Chiang, S. C. Gau, C. R. Fincher, Y. W. Park and A. G. MacDiarmid. "Polyacetylene, (CH) sub x:n-Type and p-Type Doping and Compensation". *Report: LRSM-TR-78-4*, (1978) 18
- [90] J. L. Bredas, B. Themans, J. M. Andre, R. R. Chance and R. Silbey. "The role of mobile organic radicals and ions (solitons, polarons and bipolarons) in the transport properties of doped conjugated polymers". *Synthetic Metals*, Vol.9, (1984) 265-274.
- [91] Y. Furukawa, A. Sakamoto, H. Ohta and M. Tasumi. "Raman characterization of polarons, bipolarons and solitons in conducting polymers". *Synthetic Metals*, Vol. 49, (1992) 335-340.
- [92] W. R. Salaneck and I. Lundstrom. "Electrically Conducting Organic Polymers: Connections Between Geometric and Electronic Structure". *Physica Scripta*. Vol. 25, (1989) 9-16.
- [93] Y. Qiu, Z. An and C. Q. Wu. "Dynamics of polaron formation in a polymer/metal structure". *Synthetic Metals*, Vol.135-136, (2003) 503-504.
- [94] A. J. Heeger. "Semiconducting and metallic polymers: the fourth generation of polymeric materials". *MRS Bulletin*, Vol. 26, (2001) 900-904.
- [95] K. Kojima and M. Terao. "Investigation into recording on electrochromic information layers of multi-information-layer optical disk using electrical layer selection". *Japanese Journal of Applied Physics, Part 1 (Regular Papers, Short Notes & Review Papers)*, Vol.43, (2004) 7058-7064.
- [96] Christopher A. Thomas. "Donor-acceptor methods for band gap reduction in conjugated polymers: the role of electron rich donor heterocycles". *Dissertation*, (2002) 78.

- [97] D. Bott. "Electrically conducting polymers". *Physics in Technology*, Vol.16, (1985) 121-126.
- [98] D. Moses, A. Denenstien, J. Chen, A. J. Heeger, P. McAndrew, T. Woerner, A. G. MacDiarmid and Y.W. Park. "Effect of nonuniform doping on electrical transport in trans-(CH)<sub>x</sub>: studies of the semiconductor-metal transition". *Physical Review B (Condensed Matter)*, Vol.25, (1982) 7652-7660.
- [99] E. M. Conwell. "Impurity band conduction in germanium and silicon". *Physical Review*, v 103, (1956) 51-61.
- [100] N. F. Mott. "On the transition to metallic conduction in semiconductors". *Canadian Journal of Physics*, Vol.34, (1956) 1356-1368.
- [101] N.F. Mott and E. A. Davis. "Electronic Processes in Noncrystalline Materials". *Clarendon Press, Oxford*, (1971) 327.
- [102] M.A. Abkowitz, H.A. Mizes and J. S. Facci. "Emission limited injection by thermally assisted tunneling into a trap-free transport polymer". *Applied Physics Letters*, Vol.66, (1995) 1288-1290.
- [103] R. Schmechel. "Gaussian disorder model for high carrier densities: theoretical aspects and application to experiments". *Physical Review B (Condensed Matter and Materials Physics)*, Vol.66, (2002) 235206-1-6.
- [104] S Capaccioliyz, M Lucchesiy, P.A. Rollay and G Ruggerix. "Dielectric response analysis of a conducting polymerdominated by the hopping charge transport". *Journal of Physics: Condensed Matter* , Vol.10, (1998) 5595-5617.
- [105] K.L. Ngai, T.R. Gopalakrishnan and M. Beiner. "Relaxation in poly(alkyl methacrylate)s: Change of intermolecular coupling with molecular structure, tacticity, molecular weight, copolymerization, crosslinking, and nanoconfinement". *Polymer*, Vol.47, (2006) 7222-7230.
- [106] J. Bernholc, D. Brenner, M. Buongiorno Nardelli, V. Meunier, and C. Roland. "Mechanical and electrical properties of nanotubes". *Annu. Rev. Mater. Res.*, Vol.32, (2002) 347-375.
- [107] V. I. Arkhipov, J. Reynaert, Y. D. Jin, P. Heremans, E. V. Emelianova, G. J. Adriaenssens and H. Bässler. "The effect of deep traps on carrier hopping in disordered organic materials". *Synthetic Metals* , Vol.138, (2003) 209-212.
- [108] I. Vladimir, H.B. Arkhipov and E. V. Emelianova. "Charge Carrier Injection Into A Disordered Organic Dielectric". *Materials Research Society Symposium - Proceedings*, Vol. 734, (2003) 139-148.
- [109] V. I. Arkhipov and P. Heremans. "Charge carrier mobility in doped semiconducting polymers". *Applied Physics Letters*, Vol. 82, (2003) 3245-3247.

- [110] C.K. Chiang, C. R. Fincher, Y. W. Park, A. J. Heeger, H. Shirakawa, E.J. Louis, S. C. Gau and A.G. MacDiarmid. "Electrical conductivity in doped polyacetylene". *Physical Review Letters*, Vol. 39, (1977) 1098-1101.
- [111] V. I. Arkhipov, P. Heremans, E. V. Emelianova, G. J. Adriaenssens and H. Bässler. "Charge carrier mobility in doped disordered organic semiconductors". *Journal of Non-Crystalline Solids*, Vol.338-340, (2004) 603-606.
- [112] M.E.J. Newman and R. B. Stinchcombe. "Hopping conductivity of the Fibonacci-chain quasicrystal". *Physical Review B (Condensed Matter)*, Vol.43, (1991) 1183-1186.
- [113] O. Rubel, S.D. Baranovskii, K. Hantke, B. Kunert, W.W. Ruhle, P. Thomas, K. Volz and W. Stolz. "Kinetic effects in recombination of optical excitations in disordered quantum heterostructures: Theory and experiment". *Journal of Luminescence*, Vol.127, (2007) 285-290.
- [114] Y. Shen, K. Diest, M. H. Wong, B. R. Hsieh, D. H. Dunlap and G. G. Malliaras, "Charge transport in doped organic semiconductors", *Physical Review B (Condensed Matter and Materials Physics)*, Vol.68, (2003) 81204-1-4.
- [115] Y. Kanemitsu, H. Funada and Y. Masumoto. "Electric-field dependence of the hole drift mobility in molecularly doped polymers: importance of the disorder of hopping sites". *Journal of Applied Physics*, Vol.71, (1992) 300-303.
- [116] M. Koehler, J. R. de Lima, M. G. E. Luz and I. A. Hümmelgen. "Charge Injection into Thin Conjugated Polymer Films". *physica status solidi*, Vol.173, (1999) 29-39.
- [117] A. L. Pettersson, F. Carlsson, O. Inganäs and H. Arwin. "Spectroscopic ellipsometry studies of the optical properties of doped poly(3,4-ethylenedioxythiophene): An anisotropic metal". *Thin Solid Films*, Vol.313-314, (1998) 356-361.
- [118] G. Zotti, P. H. Aubert, S. M. Waybright, J. R. Reynolds and L. Groenendaal. "Electrochemistry of poly(3,4-alkylenedioxythiophene) derivatives". *Advanced Materials*, Vol.15, (2003) 855-879.
- [119] S.K. M. Jönsson, W. R. Salaneck and M. Fahlman. "Spectroscopy of ethylenedioxythiophene-derived systems: from gas phase to surfaces and interfaces found in organic electronics". *Journal of Electron Spectroscopy and Related Phenomena*, Vol.137-140, (2004) 805-809.
- [120] H. Okuzaki, S. Ashizawa, Y. Shinohara, H. Shindo and Y. Watanabe. "Polymer FET with a conducting channel". *Synthetic Metals*, Vol.153, (2005) 41-44.
- [121] J. O. Ouyang, C. W. Chu, F.C. Chen, Q. F. Xu and Y. Yang. "High-conductivity poly(3,4-ethylenedioxythiophene):poly(styrene sulfonate) film and its application in polymer optoelectronic devices". *Advanced Functional Materials*, Vol.15, (2005) 203-208.

- [122] M. Cecchi, D. Braun, H. Smith, L. Vanasupa. "Statistical method to optimize the efficiency of multi-layer polymer LEDs". *Materials Research Society Symposium - Proceedings*, Vol. 665, (2001)93-98.
- [123] M.M. De Kok, M. Buechel, S.I.E. Vulto, C.H.L. Weijtens and V. Van Elsbergen. "Modification of PEDOT:PSS as hole injection layer in polymer LEDs". *Physica Status Solidi (A) Applied Research*, v 201, (2004) 1342-1359.
- [124] S.H. Park, J.U. Kim, J.K. Lee and M. R. Kim, . "Photovoltaic properties of dye-sensitized solar cells with thermal treated PEDOT:PSS as counter electrodes". *Molecular Crystals and Liquid Crystals*, Vol. 471, (2007) 113-112.
- [125] M.M.De Kok, M. Buechel, S.I.E. Vulto, P. Weijer, E. A. Meulenkaamp, S.H.P.M. de Winter, A.J.G. Mank, H.J.M. Vorstenbosch, C.H.L. Weijtens and V. van Elsbergen. "Modification of PEDOT:PSS as hole injection layer in polymer LEDs". *Physica Status Solidi A*, Vol. 201, (2004) 1342-1359.
- [126] C.H.L. Weijtens, V. Van Elsbergen, M.M. de Kok and S.H.P.M. Winter. "Effect of the alkali metal content on the electronic properties of PEDOT: PSS". *Organic Electronics*, v 6, (2005) 97-104.
- [127] J. Hwang, F. Amy and A. Kahn. "Spectroscopic study on sputtered PEDOT · PSS: Role of surface PSS layer". *Organic Electronics: physics, materials, applications*, Vol. 7, (2006) 387-396.
- [128] Y. J. Lin, F. M. Yang, C. Y. Huang, W. Y. Chou, J. Chang and Y. C. Lien. "Increasing the work function of poly(3,4-ethylenedioxythiophene) doped with poly(4-styrenesulfonate) by ultraviolet irradiation". *Applied Physics Letters*, Vol. 91, (2007) 092127.
- [129] D. Zielke, A.C. Hubler, U. Hahn, N. Brandt, M. Bartzsch, U. Fugmann, T. Fischer, J. Veres and S. Ogier. "Polymer-based organic field-effect transistor using offset printed source/drain structures". *Applied Physics Letters*, Vol.87, (2005) 123508-1-3.
- [130] P. Cosseddu and A. Bonfiglio. "A comparison between bottom contact and top contact all organic field effect transistors assembled by soft lithography". *Thin Solid Films*, Vol.515, (2007) 7551-7555.
- [131] C. Santato, F. Cicoira, P. Cosseddu, A. Bonfiglio, P. Bellutti, M. Muccini, R. Zamboni, F. Rosei, A. Mantoux and P. Doppelt. "Organic light-emitting transistors using concentric source/drain electrodes on a molecular adhesion layer". *Applied Physics Letters*, Vol. 88, (2006)163511-1-3.
- [132] F.L. Xue, Y.Su and K. Varahramyan. "fied PEDOT-PSS conducting polymer as S/D electrodes for device performance enhancement of P3HT TFTs". *IEEE Transactions on Electron Devices*, Vol. 52, (2005) 1982-1987.



- [133] K. Ryu, L. Kymissis, V. Bulovic and C.G. Sodini. "Direct extraction of mobility in pentacene OFETs using C-V and I-V measurements". *IEEE Electron Device Letters*, Vol. 26, (2005) 716-718.
- [134] S. Janietz, U. Assawapirm and D. Sainova. "New concepts for the development of active functional polymers for p and n-type OFET- applications". *Materials Research Society Symposium Proceedings*, Vol. 965, (2006) 386-391.
- [135] C.B. Liu, Y.H. Tang and S. Nie. "Synthesis and electronic properties of pentacene derivatives as promising n-type semiconductor candidates". *Central European Journal of Chemistry*, Vol. 4, (2006) 723-731.
- [136] D. M. de. Leeuw, P. W. M. Blom, C. M. Hart, C. M. J. Mutsaers, C. J. Dury, M. Matters and H. Termeer. "Polymeric integrated circuits and light-emitting diodes". *IEDM Technical Digest*, (1997) 331-336.
- [137] C. Tanase, P.W.M. Blom, E.J. Meijer and D.M. De Leeuw. "Charge transport in disordered organic field-effect transistors". *Organic and Polymeric Materials and Devices - Optical, Electrical and Optoelectronic Properties. Symposium (Mater. Res. Soc. Symposium Proceedings*, Vol. 725, (2002) 125-129.
- [138] T.H .Cui, G. Liang and K. Varahramyan. "An organic poly(3,4 ethylenedioxythiophene) field-effect transistor fabricated by spin coating and reactive ion etching". *IEEE Transactions on Electron Devices*, Vol.50, (2003) 1419-1422.
- [139] O. Marinov, M.J. Deen and B. Iniguez. "Charge transport in organic and polymer thin-film transistors: recent issues". *IEE Proceedings-Circuits, Devices and Systems*, Vol.152, (2005) 189-209.
- [140] V. Podzorov, E. Menard, J.A. Rogers and M.E. Gershenson. "Hall effect in the accumulation layers on the surface of organic semiconductors". *Physical Review Letters*, Vol. 95, (2005) 226601.
- [141] M. Roth, M. Rehahn, M. Ahles, R. Marcus, R. Schemmel and H. Von Seggern. "A general synthetic approach to novel bis(tetracenyl) aromatics for OFET application". *Materials Research Society Symposium Proceedings*, Vol.871, (2005) 226-231.
- [142] R.A. Street and A. Salleo. "Contact effects in polymer transistors". *Applied Physics Letters*, Vol. 81, (2002) 2887-2889.
- [143] L. Burgi, T.J. Richards, R.H. Friend and H. Sirringhaus. "Close look at charge carrier injection in polymer field-effect transistors". *Journal of Applied Physics*, Vol. 94, (2003) 6129-6137.
- [144] I. Torres, D. Taylor and E. Itoh. "Interface states and depletion-induced threshold voltage instability in organic metal-insulator-semiconductor structures". *Applied Physics Letters*, Vol. 85, (2004) 314-316.

- [145] O. Marinov, M.J. Deen, G. Vamvounis, J. Yu, S. Holdcroft and W. Woods. "Instability of the noise level in polymer field-effect transistors with non-stationary electrical characteristics". *Unsolved Problems of Noise (UPoN 2002)*, September 2002, AIP Conf. Proc., Vol.665, (2003) 488–495.
- [146] M. Zhu, G. R. Liang, T. H. Cui and K. Varahramyan. "Temperature and field dependent mobility in pentacene-based thin film transistors". *Solid-State Electronics*, Vol.49, (2005) 884-888.
- [147] A. Iribarren, R. Castro-Rodriguez, V. Sosa and J. L. Pena. "Modeling of the disorder contribution to the band-tail parameter in semiconductor materials". *Physical Review B (Condensed Matter)*, Vol.60, (1999) 4758-4762.
- [148] M. Abkowitz, A. Lakatos and H. Scher. "AC conductivity and AC photoconductivity in amorphous and crystalline insulators", *Physical Review B (Solid State)*, Vol. 9, (1974) 1813-1822.
- [149] W. P. Hu, Y. O. Liu, Y. Xu, S. G. Liu, S. Q. Zhou and D.B. Zhu. "The application of Langmuir-Blodgett films of a new asymmetrically substituted phthalocyanine, amino-tri-tert-butyl-phthalocyanine, in diodes and in all organic field-effect-transistors". *Synthetic Metals*, Vol.104, (1999) 19-26.
- [150] M.T. Viciosa, and M. Dionisio. "Molecular mobility and fragility in n-ethylene glycol dimethacrylate monomers". *Journal of Non-Crystalline Solids*, Vol.341, (2004) 60-67.
- [151] W. Bantikassegn and O. Inganäs. "Electronic properties of junctions between aluminum and neutral or doped poly[3-(4-octylphenyl)-2,2'-bimioophene]". *Synthetic Metals*, Vol.87, (1997) 5-10.
- [152] D. Cahen, A. Kahn and E. Umbach. "Energetics of molecular interfaces". *Materials Today*, Vol.8, (2005) 32-41.
- [153] R. Hattori and J. Kanicki. "Contact resistance in Schottky contact gated-four-probe a-Si thin-film transistor". *Japanese Journal of Applied Physics, Part 2 (Letters)*, Vol.42, (2003) 907-909.
- [154] L. Burgi, T.J. Richards, R.H. Friend and H. Sirringhaus. "Close look at charge carrier injection in polymer field-effect transistors". *Journal of Applied Physics*, v 94, (2003) 6129-6137.
- [155] A. Dziedzic. "Carbon/polyesterimide thick-film resistive composites - Experimental characterization and theoretical analysis of physicochemical, electrical and stability properties". *Microelectronics Reliability*, Vol. 47, (2007) 354-362.
- [156] A. Dziedzic and A. Kolek. "1/f noise in polymer thick-film resistors". *Journal of Physics D (Applied Physics)*, Vol.31, (1998) 2091-2097.

- [157] S. L. Fu. "Electrical characteristics of polymer thick film resistors. II. Phenomenological explanation". *IEEE Transactions on Components, Hybrids, and Manufacturing Technology*, Vol. CHMT-4, (1981) 289-293.
- [158] T. Anderson and S. Roth. "Conducting Polymers: Electrical Transport and Current Applications". *Brazilian Journal of Physics*, Vol.24, (1994) 746-754.
- [159] W. Bantikassegn and O. Inganäs. "Electronic properties of junctions between aluminum and neutral or doped poly[3-(4-octylphenyl)-2,2'-bimioophene]". *Synthetic Metals*, Vol.87, (1997) 5-10.
- [160] K.H. Baik, Y.W. Heo, D.P. Norton, S.J. Pearton, J.R. aRoche, B. Luo, F. Ren, and J.M. Zavada. "Annealing temperature dependence of contact resistance and stability for Ti/Al/Pt/Au ohmic contacts to bulk n-ZnO". *Journal of Vacuum Science & Technology B (Microelectronics and Nanometer Structures)*, Vol. 21, (2003) 2378-2381.
- [161] S. Oussalah, B. Djeddar and R. Jerisian. "A comparative study of different contact resistance test structures dedicated to the power process technology". *Solid-State Electronics*, Vol. 49, (2005) 1617-1622.
- [162] R.W. Dutton and A.J. Strojwas. "Perspectives on technology and technology-driven CAD". *IEEE Transactions on Computer-Aided Design of Integrated Circuits and Systems*, Vol.19, (2000) 1544-1560.
- [163] B. Iniguez, T.A. Fjeldly, F. Danneville and M.J. Deen. "Compact-modeling solutions for nanoscale double-gate and gate-all-around MOSFETs". *IEEE Transactions on Electron Devices*, Vol. 53, (2006) 2128-2142.
- [164] A. El Ayyadi and A. Jungel. "Semiconductor simulations using a coupled quantum drift-diffusion schrodinger-poisson model". *SIAM Journal on Applied Mathematics*, Vol.66, (2006) 554-572.
- [165] Y. Li, S. M. Yu and J.W. Lee. "Quantum mechanical corrected simulation program with integrated circuit emphasis model for simulation of ultrathin oxide metal-oxide-semiconductor field effect transistor gate tunneling current". *Japanese Journal of Applied Physics, Part 1 (Regular Papers, Short Notes & Review Papers)*, Vol. 44, (2005) 2132-2136.
- [166] T. Kawase, P.K.H.Ho, R.H. Friend and T. Shimoda. "Low voltage operation of polymer light-emitting device with conducting polymer distributed Bragg reflector". *Electrical, Optical, and Magnetic Properties of Organic Solid-State Materials V. Symposium (Materials Research Society Proceedings)*, Vol. 598 (2000) BB11.49.1-6.
- [167] D.J.Pinner and N. Tessler. "Transient electroluminescence of polymer light emitting diodes using electrical pulses". *Journal of Applied Physics*, Vol.86, (1999) 5116-5130.

- [168] G. Liang, T. H. Cui and K. Varahramyan. "Electrical characteristics of diodes fabricated with organic semiconductors". *Microelectronic Engineering*, Vol.65, (2003) 279-284.
- [169] Synopsys, inc, *TCAD Business Unit*. "Taurus process & Device Manual". (2002).
- [170] Mohan V. Dunga, Chung-Hsun Lin, Xuemei (Jane) Xi, Darsen D. Lu, Ali M. Niknejad and Chenming Hu. "Modeling Advanced FET Technology in a Compact Model". *IEEE Transactions on electron devices*, Vol. 53, (2006) 1971-1978.
- [171] S. Jain, S. Chakane, A.B. Samui, V.N. Krishnamurthy and S.V. Bhoraskar. "Humidity sensing with weak acid-doped polyaniline and its composites". *Sensors and Actuators B: Chemical*, Vol. 96, (2003) 124-129.
- [172] Albrecht, B. A., Benson, C. H. and Beuermann, S.. "Polymer Capacitance Sensors for Measuring Soil Gas Humidity in Drier Soils". *Geotech Test J*, Vol.26, (2003) 3-11.
- [173] D. Nilsson, T. Kugler, P. Svensson and M. Berggen, "An all-organic sensor-transistor based on a novel electrochemical transducer concept printed electrochemical sensors on paper". *Sensors and Actuators B*, Vol.86, (2002) 193-197.
- [174] John Coates Encyclopedia of analytical chemistry © John Wiley and Sons Ltd, Chicester, (2000).
- [175] L.H. Kidder, A.S. Haka and E.N. Lewis. "Instrumentation for FT-IR imaging, in: J.M. Chalmers, P.R. Griffiths (Eds.)". *Handbook of Vibrational Spectroscopy*, Vol. 2, (2002) 386.
- [176] S.G. Kazarian and J.S. Higgins. "New Opportunities in Micro- and Macro-Attenuated Total Reflection Infrared Spectroscopic Imaging: Spatial Resolution and Sampling Versatility". *Applied Spectroscopy*, Vol. 57, (2003) 381-389.
- [177] J.L. Koenig, S.Q. Wang and R. Bhargava. "FTIR images". *Analytical Chemistry*, Vol. 73, (2001) 360A-369A.
- [178] J.M. Chalmers, N.J. Overall, M.D. Schaeberle, I.W. Levin, E.N. Lewis, L.H. Kidder, J. Wilson and R. Crocombe. "FT-IR imaging of polymers: An industrial appraisal". *Vibrational Spectroscopy*, Vol. 30, (2002) 43-52.
- [179] K.L.A. Chan and S.G. Kazarian. "New opportunities in micro- and macro-attenuated total reflection infrared spectroscopic imaging: Spatial resolution and sampling versatility". *Applied Spectroscopy*, Vol.57, (2003) 381-389.
- [180] P. M. Borsenberger and H. Bässler. "Concerning the role of dipolar disorder on charge transport in molecularly doped polymers". *Journal of Chemical Physics*, Vol. 95, (1991) 5327-5331.

- [181] H. Bassler. "Localized States and Electronic Transport in Single Component Organic Solids with Diagonal Disorder". *Physica Status Solidi (b)*, v 107, (1981) 9-54.
- [182] H. Bassler. "Charge Transport in Disordered Organic Photoconductors. A Monte Carlo Simulation Study". *Physica Status Solidi (b)*, Vol. 175, (1993) 15-56.
- [183] P. M. Borsenberger, E. H. Magin, M. van der Auveraer and E C. de Schryver. "The Role of Disorder on Charge Transport in Molecularly Doped Polymers and Related Materials". *Physica Status Solidi (a)*, Vol. 40, (1993) 9-47.
- [184] X. Crispin, S. Marciniak, W. Osikowicz, G. Zotti, A. W. Denier Vander Gon, F. Louwet, M. Fahlman, L. Groenendaal, F. Deschryver and W. R. Salaneck. "Conductivity, Morphology, Interfacial Chemistry, and Stability of Poly(3,4-ethylene dioxythiophene)-Poly(styrenesulfonate): A Photoelectron Spectroscopy Study". *Journal of Polymer Science: Part B: Polymer Physics*, Vol. 41, (2003) 2561-2583.
- [185] H. Koezuka, A. Tsumura and T. Ando. "Field-effect Transistor with polythiophene thin film". *Synthetic Metals*, Vol.18, (1986) 699-704.
- [186] V. Singh, M. Yano, W. Takashima and K. Kaneto. "Study of gate induced channel in organic field effect transistors using poly(3-hexylthiophene) films". *Japanese Journal of Applied Physics, Part 1 (Regular Papers, Short Notes & Review Papers)*, Vol. 45, (2006) 534-537.
- [187] A. J. Van Breemen, P. T. Herwig, Ceciel H.T. Chlon, F. M. Herman, E. M. Benito, D. Leeuw, M. Dago and W. M. Paul. "High-performance solution-processable poly(p-phenylene vinylene)s for air-stable organic field-effect transistors". *Advanced Functional Materials*, Vol. 15, 2005 (872-876).
- [188] P. Cosseddu and A. Bonfiglio. "A comparison between bottom contact and top contact all organic field effect transistors assembled by soft lithography". *Thin Solid Films*, Vol. 515, (2007) 7551-7555.
- [189] X.C. Liu, A. P. Chakraborty, G. Parthasarathi and C. Luo. "Generation of conducting polymer-based heterojunctions, diodes and capacitors using an intermediate-layer lithography method". *Proceedings of SPIE - The International Society for Optical Engineering*, Vol. 6556, (2007) 65560Z.
- [190] Iftikhar Ahmad, Mohamed Nuri Rahuma and Mohamed Gebril A. Elarafi. "Effective Management System for Protection of Desalination Plants Against Corrosion and Scaling". *Jowfe Oil Technology Benghazi (Libya)*.
- [191] M. Mehrvar and M. Abdi. "Recent Developments, Characteristics, and Potential Applications of Electrochemical Biosensors". *Analytical Sciences*, Vol. 20, (2004) 1113-1126.

- [192] S. K. Arya, P. R. Solanki, R. P. Singh, M. K. Pandey, M. Datta and B. D. Malhotra. "Application of octadecanethiol self-assembled monolayer to cholesterol biosensor based on surface plasmon resonance technique". *Talanta*, Vol.69, (2006) 918-926.
- [193] G. Moschopoulou and S. Kintzios. "Application of "membrane-engineering" to bioelectric recognition cell sensors for the ultra-sensitive detection of superoxide radical: A novel biosensor principle". *Analytica Chimica Acta*, Vol. 573-574, (2006) 90-96.
- [194] W. J. Ho, C. J. Yuan and O. Reikobm. "Application of SiO<sub>2</sub>-poly(dimethylsiloxane) hybrid material in the fabrication of amperometric biosensor". *Analytica Chimica Acta*, Vol. 572, (2006) 248-252.
- [195] D. A. Healy, C. J. Haye, P. Leonard, L. McKenna and R. O'Kennedy. "Biosensor developments: application to prostate-specific antigen detection". *Trends in Biotechnology*, Vol. 25, (2007) 125-131.
- [196] W. Haasnoot, M. Bienenmann-Ploum, U. Lamminmäki, M. Swanenburg and H. Rhijn. "Application of a multi-sulfonamide biosensor immunoassay for the detection of sulfadiazine and sulfamethoxazole residues in broiler serum and its use as a predictor of the levels in edible tissue". *Analytica Chimica Acta*, Vol.552, (2005) 87-95.
- [197] H. Muramatsu, M. Suda and T. Ataka. "Piezoelectric resonator as a chemical and biochemical sensing device". *Sensors and Actuators, A: Physical*, Vol. 21, (1990) 362-368.
- [198] B. A. Mazzeo and A. J. Flewitt. "Observation of protein-protein interaction by dielectric relaxation spectroscopy of protein solutions for biosensor application". *Applied Physics Letters*, Vol. 90, (2007) 123901-123903.
- [199] D. Niwa, T. Homma and T. Osaka. "Fabrication of Organic Monolayer Modified Ion-Sensitive Field Effect Transistors with High Chemical Durability". *Japanese Journal of Applied Physics, Part 2: Letters*, Vol. 43, (2004) L105-L107.
- [200] A. Loi, I. Manunza and A. Bonfiglio. "Flexible, organic, ion-sensitive field-effect transistor". *Applied Physics Letters*, Vol. 86, (2005) 103512.
- [201] Y. Liu, A. G. Erdman and T. Cui. "Acetylcholine biosensors based on layer-by-layer self-assembled polymer/nanoparticle ion-sensitive field-effect transistors". *Sensors and Actuators A: Physical*, Vol.136, (2007) 540-545.
- [202] Y. Hanazato, M. Nakako, S. Shiono and M. Maeda. "Integrated multi-biosensors based on an ion-sensitive field-effect transistor using photolithographic techniques". *IEEE Transactions on Electron Devices*, Vol. 36, (1989) 1303-1310.

- [203] Adam K. Wanekaya, W. Chen and A. Mulchandani. "FET based conducting polymer coated carbon nanotube bio/chemical sensor". *AICHE Annual Meeting, Conference Proceedings*, 05AICH: 2005 AICHE Annual Meeting and Fall Showcase, Conference Proceedings, (2005) 14151.
- [204] S. B. Adeloju and G. G. Wallace. "Electroimmobilisation of sulphite oxidase into a polypyrrole film and its utilisation for flow amperometric detection of sulphite". *Analytica Chimica Acta*, v 332, (1996) 145-153.
- [205] W.J. Sung and Y.H. Bae. "A glucose oxidase electrode based on electropolymerized conducting polymer with polyanion-enzyme conjugated dopant". *Analytical Chemistry*, Vol.72, (2000) 2177-2181.
- [206] R.W. Scheller, F. Schubert, B. Neumann, D. Pfeiffer, R. Hintsche, I. Dransfeld, U. Wollenberger, R. Renneberg and A. Warsinke. "Second generation biosensors". *Biosensors & Bioelectronics*, Vol. 6, (1991) 245-253.
- [207] A. Kros, Nico A.J.M. Sommerdijk and J.M.Nolte. "Poly(pyrrole) versus poly(3,4-ethylenedioxythiophene): Implications for biosensor applications". *Sensors and Actuators, B: Chemical*, Vol. 106, (2005) 289-295.
- [208] Z. T. Zhu, J. T. Mabeck, C.C. Zhu, N. C. Cady, C. A. Batt and G. G. Malliaras. "A simple poly(3,4-ethylene dioxythiophene)/poly(styrene sulfonic acid) transistor for glucose sensing at neutral pH". *Chemical communications*, Vol. 13, (2004) 1556-1579.
- [209] A. Michalska, A. G. uszkiewicz, M. Ogonowska, M. Ocypa and K. Maksymiuk. "PEDOT films: multifunctional membranes for electrochemical ion sensing". *Journal of Solid State Electrochemistry*, Vol. 8, (2004) 381-389.
- [210] M.Chen. "Printed Electrochemical Devices Using Conducting Polymers as Active Materials on Flexible Substrates". *Proceedings of the IEEE*, Vol. 93, (2005) 1339-1347.
- [211] A. Ernst, O. Makowski, B. Kowalewska, K. Miecznikowski and P. J. Kulesza. "Hybrid bioelectrocatalyst for hydrogen peroxide reduction: Immobilization of enzyme within organic-inorganic film of structured Prussian Blue and PEDOT". *Bioelectrochemistry*, Vol. 71, (2007) 23-28.
- [212] J. Liu, M. Agarwal, and K. Varahramyan. "Polymer-based Microsensor for Soil Moisture Measurement". *Sensor and Actuators: B Chemical*, Vol.129, (2008) 599-604.
- [213] V.K. Gade, D.J. Shirale, P.D. Gaikwad, P.A. Savale, K.P. Kakde, H.J. Kharat and M.D. Shirsat. "Immobilization of GOD on electrochemically synthesized Ppy – PVS composite film by cross-linking via glutaraldehyde for determination of glucose". *Reactive & Functional Polymers*, Vol. 66 (2006)1420-1426.

- [214] V. Syritski, K. Idla and A. Öpik. “Synthesis and redox behavior of PEDOT/PSS and PPy/DBS structures”. *Synthetic Metals*, Vol. 144, (2004) 235–239.
- [215] H. Randriamahazaka, C. Plesse, D. Teyssie and C. Chevrot. “Ions transfer mechanisms during the electrochemical oxidation of poly(3,4-ethylenedioxythiophene) in 1-ethyl-3-methylimidazoliumbis((trifluoromethyl)sulfonyl)amide ionic liquid”. *Electrochemistry Communications*, Vol. 6, (2004) 299–305.
- [216] D. J. Macaya, M. Nikolou, S. Takamatsu, J. T. Mabeck, R. M. Owensb and G. G. Malliaras. “Simple glucose sensors with micromolar sensitivity based on organic electrochemical transistors”. *Sensors and Actuators B*, Vol. 123, (2007) 374–378.
- [217] E. L. Kupila, J. Lukkari and J. Kankare. “Redox processes in thick films of polypyrrole/dodecylsulfate in the presence of alkali and tetramethylammonium chlorides”. *Synthetic Metals*, Vol. 74, (1995) 207-215.
- [218] A.J. Epstein, F.C. Hsu, N.R. Chiou and V.N. Prigodin. “Electric-field induced ion-leveraged metal–insulator transition in conducting polymer-based field effect devices”. *Current Applied Physics*, Vol.2, (2002) 339–343.
- [219] D. D. Borole, U. R. Kapadi, P. P. Mahulikar and D. G. Hundiwale. “Glucose Oxidase Electrodes of Poly(o-anisidine), Poly(otoluidine), and Their Copolymer as Biosensors: A Comparative Study”. *Journal of Applied Polymer Science*, Vol. 94, (2004) 1877–1884.
- [220] P. Paul, T. Zhiyong, S. Bong Sup and K. Nicholas. “Counterintuitive effect of molecular strength and role of molecular rigidity on mechanical properties of layer-by-layer assembled nanocomposites”. *Nano Letters*, Vol. 7, (2007) 1224-1231.
- [221] Khillan, R.K., Ghan, R., Dasaka, R., Su, Y., Lvov, Y. and Varahramyan, K.. “Layer- by-layer nanoarchitecture of ultrathin films assembled of PEDOT-PSS and PPy to act as hole transport layer in polymer light emitting diodes and polymer transistors”. *2004 4th IEEE International Conference on Polymers and Adhesives in Microelectronics and Photonics, 2004 4th IEEE International Conference on Polymers and Adhesives in Microelectronics and Photonics*, (2004) 225-229.
- [222] Akinwande, A.I., Ruden, P.P., Vold, P.J., Han, C.-J., Grider, D.E., Narum, D.H., Nohava, T.E., Nohava, J.C. and Arch, D.K.. “A self-aligned gate III-V heterostructure FET process for ultrahigh-speed digital and mixed analog/digital LSI/VLSI circuits”. *IEEE Transactions on Electron Devices*, Vol.36, (1989) 2204-2216.
- [223] R. William. “Development of an interactive design environment for heterostructure and quantum-well devices”. *IEEE Transactions on Electron Devices*, Vol.38, (1991) 2704-2705.



- [224] R. Nohria, R. K. Khillan, Y. Su, Y. Lvov and K. Varahramyan. "Layer-by-layer nano-assembled polypyrrole humidity sensor". *2005 NSTI Nanotechnology Conference and Trade Show. NSTI Nanotech*, Vol.2, (2005) 422-425.
- [225] K. Arshak, E. Moore, G. M. Lyons, F. Harris and S. Clifford. "A review of gas sensors employed in electronic nose applications". *Sensor Review*, Vol. 24 (2004) 181-198.
- [226] C. Xia and R. C. Advincula. "In Situ Investigations of the Electrodeposition and Electrochromic Properties of Poly(3,4-ethylenedioxythiophene) Ultrathin Films by Electrochemical-Surface Plasmon Spectroscopy". *Langmuir*, Vol.18, (2002) 3555 - 3560.
- [227] H. Sirringhaus, P. J. Brown, R. H. Friend, M. M. Nielsen, K. Bechgaard, B. M. W.Langeveld-Voss, A. J. H. Spiering, R. A. J. Janssen, E. W. Meijer, P. Herwig and D. M. de Leeuw. "Two-dimensional charge transport in self-organized, highmobility conjugated polymers". *Nature*, Vol.401, (1999) 685-688.
- [228] H. Li, Y. Xu, S. Bao, P. He, H. J. Qian and F. Q. Liu. "Synchrotron radiation photoemission spectrum study on  $K_3C_{60}$  film". *Science in China, Series A (Mathematics, Physics, Astronomy)*, Vol. 43, (2000) 1189-1194.
- [229] Z. Bao, A. Dodabalapur and A. J. Lovinger. "Soluble and processable regioregular poly (3-hexylthiophene) for thin film field-effect transistor applications with high mobility". *Applied Physics Letters*, Vol. 69, (1996) 4108-4110.